

1989

Sorption and transport of atrazine, alachlor and fluorescent dyes in alluvial aquifer sands

David Alan Sabatini
Iowa State University

Follow this and additional works at: <https://lib.dr.iastate.edu/rtd>



Part of the [Civil Engineering Commons](#)

Recommended Citation

Sabatini, David Alan, "Sorption and transport of atrazine, alachlor and fluorescent dyes in alluvial aquifer sands " (1989). *Retrospective Theses and Dissertations*. 9237.

<https://lib.dr.iastate.edu/rtd/9237>

This Dissertation is brought to you for free and open access by the Iowa State University Capstones, Theses and Dissertations at Iowa State University Digital Repository. It has been accepted for inclusion in Retrospective Theses and Dissertations by an authorized administrator of Iowa State University Digital Repository. For more information, please contact digirep@iastate.edu.

INFORMATION TO USERS

The most advanced technology has been used to photograph and reproduce this manuscript from the microfilm master. UMI films the text directly from the original or copy submitted. Thus, some thesis and dissertation copies are in typewriter face, while others may be from any type of computer printer.

The quality of this reproduction is dependent upon the quality of the copy submitted. Broken or indistinct print, colored or poor quality illustrations and photographs, print bleedthrough, substandard margins, and improper alignment can adversely affect reproduction.

In the unlikely event that the author did not send UMI a complete manuscript and there are missing pages, these will be noted. Also, if unauthorized copyright material had to be removed, a note will indicate the deletion.

Oversize materials (e.g., maps, drawings, charts) are reproduced by sectioning the original, beginning at the upper left-hand corner and continuing from left to right in equal sections with small overlaps. Each original is also photographed in one exposure and is included in reduced form at the back of the book. These are also available as one exposure on a standard 35mm slide or as a 17" x 23" black and white photographic print for an additional charge.

Photographs included in the original manuscript have been reproduced xerographically in this copy. Higher quality 6" x 9" black and white photographic prints are available for any photographs or illustrations appearing in this copy for an additional charge. Contact UMI directly to order.

U·M·I

University Microfilms International
A Bell & Howell Information Company
300 North Zeeb Road, Ann Arbor, MI 48106-1346 USA
313/761-4700 800/521-0600

Order Number 8920182

**Sorption and transport of atrazine, alachlor and fluorescent dyes
in alluvial aquifer sands**

Sabatini, David Alan, Ph.D.

Iowa State University, 1989

U·M·I
300 N. Zeeb Rd.
Ann Arbor, MI 48106

Sorption and transport of atrazine, alachlor
and fluorescent dyes in alluvial aquifer sands

by

David Alan Sabatini

A Dissertation Submitted to the
Graduate Faculty in Partial Fulfillment of the
Requirements for the Degree of
DOCTOR OF PHILOSOPHY

Department: Civil and Construction Engineering
Major: Water Resources

Approved:

Signature was redacted for privacy.

In Charge of Major Work

Signature was redacted for privacy.

For the Major Department

Signature was redacted for privacy.

For the Graduate College

Iowa State University
Ames, Iowa

1989

TABLE OF CONTENTS

	Page
NOMENCLATURE	ix
INTRODUCTION	1
LITERATURE REVIEW	4
Cases of Pesticides in Groundwater	4
Nonpoint sources	4
Point sources	6
Pesticide transport prediction	7
Fundamentals of Solute Transport in Groundwater	7
Advection and dispersion	8
Adsorption and desorption	9
Other interactions	10
Fundamentals of Adsorption and Desorption	10
Intermolecular forces	11
Adsorption	12
Adsorption motivation and types	14
Factors affecting pesticide adsorption in soils	19
Batch and column adsorption techniques	23
Modeling of Solute Transport with Adsorption	23
Types of modeling approaches	23
One-dimensional solute transport	24
Equilibrium versus nonequilibrium adsorption	30
Equilibrium Adsorption and Desorption Expressions	30
Linear equilibrium adsorption expression	32
Freundlich equilibrium adsorption expression	38
Other equilibrium adsorption expressions	41
Estimating adsorption of pesticides on soils	42
Desorption and hysteresis of desorption	46
Nonequilibrium Adsorption and Desorption Expressions	50
Chemical versus physical nonequilibrium	50
Chemical nonequilibrium expressions	53
Physical nonequilibrium expressions	57
Equivalence of nonequilibrium expressions	65

	Page
Adsorption Studies with Atrazine and Alachlor	67
Batch results - atrazine	67
Batch results - alachlor	70
Column results - atrazine	70
Column results - alachlor	72
Fluorescent Dyes as Groundwater Tracers	72
Fluorescent dyes	72
Fluorescent dyes as water tracers	73
MATERIALS AND METHODS	75
Aquifer Materials	75
Chemicals	77
Batch Methods	82
Column Methods	84
BATCH STUDIES	88
Pesticides	88
Adsorption of atrazine and alachlor	88
Estimated linear partition coefficient	91
Competitive adsorption	93
Fluorescent Dyes	96
Adsorption of rhodamine WT and fluorescein	96
Estimated linear adsorption parameter	101
Effect of aquifer material	102
Effect of background ions	102
COLUMN STUDIES	113
Pesticides	113
Breakthrough curves for atrazine and alachlor	115
Effect of pore water velocity	120

	Page
Fluorescent Dyes	126
Breakthrough curves for rhodamine WT and fluorescein	126
Effect of background ions	133
Effect of aquifer material	136
Effect of size fractions and organic content	136
Effects of pore water velocity / concentration	146
MODELING RESULTS	150
Equilibrium Adsorption Modeling	150
Atrazine	151
Alachlor	155
Nonequilibrium Adsorption Modeling	158
Model sensitivity analyses	160
Atrazine	164
Alachlor	167
CONCLUSIONS AND RECOMMENDATIONS	172
Conclusions	172
Recommendations for Future Research	178
REFERENCES	179
ACKNOWLEDGEMENTS	189
APPENDIX A: BATCH DATA	190
APPENDIX B: COLUMN DATA	198

LIST OF FIGURES

	Page
Figure 1: Breakthrough curve - effect of Pe and adsorption	29
Figure 2: Linear adsorption isotherm	34
Figure 3: Linear versus nonlinear isotherm	39
Figure 4: Hysteresis of desorption - isotherms	48
Figure 5: Hysteresis of desorption - breakthrough curves	49
Figure 6: Adsorption conceptualization	51
Figure 7: Equilibrium versus nonequilibrium breakthrough curves	52
Figure 8: Chemical structures of pesticides (atrazine and alachlor) and dyes (rhodamine WT and fluorescein)	78
Figure 9: Schematic of column apparatus	85
Figure 10: Atrazine adsorption isotherm	89
Figure 11: Alachlor adsorption isotherm	90
Figure 12: Atrazine adsorption isotherm - single versus binary solutes	94
Figure 13: Alachlor adsorption isotherm - single versus binary solutes	95
Figure 14: Rhodamine WT adsorption isotherm (South Ames, 0 - 4500 $\mu\text{g/L}$)	97
Figure 15: Fluorescein adsorption isotherm (South Ames)	98
Figure 16: Rhodamine WT adsorption isotherm (South Ames, 0 - 1000 $\mu\text{g/L}$)	99
Figure 17: Rhodamine WT adsorption isotherm (Halletts)	104
Figure 18: Effects of background ions on rhodamine WT adsorption - preliminary batch tests	107
Figure 19: Effects of background ions on rhodamine WT adsorption - batch tests with replicates	108
Figure 20: Rhodamine WT adsorption isotherm (South Ames, CaCl_2)	110

	Page
Figure 21: Rhodamine WT adsorption isotherm with and without CaCl_2 (South Ames)	111
Figure 22: Atrazine and alachlor breakthrough curves (10.6 cm/h)	116
Figure 23: Atrazine breakthrough curves at three pore water velocities	121
Figure 24: Alachlor breakthrough curves at three pore water velocities	122
Figure 25: Atrazine elution curves at three pore water velocities (normalized such that $V/V_0 = 0.0$ corresponds to initiation of desorption)	123
Figure 26: Alachlor elution curves at three pore water velocities (normalized such that $V/V_0 = 0.0$ corresponds to initiation of desorption)	124
Figure 27: Rhodamine WT breakthrough curve (South Ames, NaCl , 11.7 cm/h, 201 $\mu\text{g/L}$)	128
Figure 28: Fluorescein breakthrough curve	129
Figure 29: Comparison of rhodamine WT and fluorescein column results	131
Figure 30: Rhodamine WT breakthrough curve (South Ames, CaCl_2 , 11.3 cm/h, 195 $\mu\text{g/L}$)	134
Figure 31: Rhodamine WT breakthrough curves - CaCl_2 versus NaCl	135
Figure 32: Rhodamine WT breakthrough curve (Halletts, CaCl_2 , 30.0 cm/h, 200 $\mu\text{g/L}$)	137
Figure 33: Rhodamine WT column runs with treated soils (0 - 400 pore volumes)	139
Figure 34: Rhodamine WT column runs with treated soils (0 - 70 pore volumes)	140
Figure 35: Rhodamine WT column runs with treated soils and glass beads	143
Figure 36: Rhodamine WT breakthrough as function of sand size fractions	145

	Page
Figure 37: Rhodamine WT breakthrough - effects of pore water velocity and concentration (0 - 200 pore volumes)	147
Figure 38: Rhodamine WT breakthrough - effects of pore water velocity and concentration (0 - 60 pore volumes)	148
Figure 39: Atrazine equilibrium modeling (10.6 cm/h)	152
Figure 40: Atrazine equilibrium modeling (30.3 cm/h)	153
Figure 41: Alachlor equilibrium modeling (10.6 cm/h)	156
Figure 42: Alachlor equilibrium modeling (30.3 cm/h)	157
Figure 43: Nonequilibrium model sensitivity analysis - radius of aggregate (r_{ag} , cm)	163
Figure 44: Nonequilibrium model sensitivity analysis - D_p (cm^2/s)	165
Figure 45: Atrazine nonequilibrium modeling (10.6 cm/h)	166
Figure 46: Atrazine nonequilibrium modeling (30.3 cm/h)	168
Figure 47: Alachlor nonequilibrium modeling (10.6 cm/h)	170
Figure 48: Alachlor nonequilibrium modeling (30.3 cm/h)	171

LIST OF TABLES

	Page
Table 1. Log K_{ow} values for various pesticides	44
Table 2. K_{oc} values for pesticides (atrazine and alachlor) and fluorescent dyes (rhodamine WT and fluorescein)	68
Table 3. Soil parameters for alluvial aquifer materials	76
Table 4. Physical and chemical properties of atrazine and alachlor	79
Table 5. Physical and chemical properties of rhodamine WT and fluorescein	81
Table 6. Batch adsorption parameters for atrazine and alachlor	92
Table 7. Measured and estimated K_{oc} values for atrazine and alachlor	92
Table 8. Batch adsorption parameters for rhodamine WT and fluorescein	100
Table 9. Measured and predicted K_{oc} values for rhodamine WT and fluorescein	103
Table 10. Effect of background ions on rhodamine WT adsorption	106
Table 11. Column parameters for atrazine and alachlor column runs	114
Table 12. Column adsorption parameters from column run CPA10 for atrazine and alachlor	118
Table 13. Column parameters for rhodamine WT and fluorescein column runs	127
Table 14. Column adsorption results for rhodamine WT and fluorescein column runs	132
Table 15. Column adsorption results for rhodamine WT and treated materials	141
Table 16. Dispersion coefficients - hydrodynamic and fitted	154
Table 17. Input parameters for nonequilibrium model runs	161

NOMENCLATURE

- b = surface stress coefficient (M/M)
- BALA = batch,alachlor, South Ames
- BATA = batch, atrazine, South Ames
- BFA = batch, fluorescein, South Ames
- BRA = batch, RWT, South Ames
- BRACA = batch, RWT, South Ames, calcium chloride
- BRH = batch, RWT, Halleys
- BW = column, RWT, South Ames, backwashed ($> 75 \mu\text{m}$)
- BW-HT/550 = column, RWT, South Ames, backwashed and heated @ 550°C
- BW-HT/850 = column, RWT, South Ames, backwashed and heated @ 850°C
- C = liquid phase solute concentration (M/L^3)
- C_e = liquid phase equilibrium concentration (M/L^3)
- CFA = column, fluorescein, RWT
- CO = initial concentration (M/L^3)
- CPA5 = column, pesticides, South Ames, 5 cm/h
- CPA10 = column, pesticides, South Ames, 10 cm/h
- CPA30 = column, pesticides, South Ames, 30 cm/h
- CRA = column, RWT, South Ames
- CRACA = column, RWT, South Ames, calcium chloride
- CRAHC = column, RWT, South Ames, high CO
- CRAHP = column, RWT, South Ames, high PWV
- CRH = column, RWT, South Ames

- C_s = equilibrium pesticide concentration at exterior of particle
(M/L³)
- D_l = free solution liquid diffusion coefficient (L²/t)
- D_m = molecular diffusion coefficient in pore water (L²/t)
- D_p = intraaggregate diffusion coefficient (L²/t)
- D_s = intraparticle diffusion coefficient (L²/t)
- D_x = hydrodynamic dispersion coefficient (L²/t)
- $D_{x, \text{fitted}}$ = hydrodynamic and nonequilibrium dispersion coefficient
(L²/t)
- d_{50} = median grain size diameter (L)
- erfc = complementary error function
- f = fraction adsorption sites in dynamic region
- f_{oc} = fraction organic carbon content (M/M)
- GLBDS = column, RWT, glass beads
- HT/850 = column, RWT, South Ames, heated @ 850 °C
- k_d = first order desorption rate constant (1/t)
- k_f = external film transfer coefficient (L/t)
- K_{fr} = Freundlich partition coefficient ((L³/M)^N)
- K_{oc} = linear partition coefficient normalized by fraction organic
carbon content (L³/M)
- K_{ow} = octanol/water partition coefficient
- K_p = linear equilibrium partition coefficient (L³/M)
- k_s = first order adsorption rate constant (1/t)
- L = column length (L)
- N = Freundlich exponent

- N_{ads} = Freundlich adsorption exponent
- N_{des} = Freundlich desorption exponent
- P_e = Peclet number
- $P_{e,eff}$ = P_e determined using $D_{x,fitted}$
- PWV = pore water velocity (L/t)
- q = ratio of solute on solid phase versus in liquid phase (M/M)
- R = radius of particle (L)
- r = radial dimension for particle (L)
- r_{ag} = radius of aggregate (L)
- r_f = retardation factor
- RWT = rhodamine WT
- t = time (t)
- V_0 = soil pore volume (L^3)
- v_x = pore water velocity (L/t)
- WS = column, RWT, South Ames, wet sieved ($> 300 \mu m$)
- x = dimension of solute transport (L)
- α' = first order mass transfer coefficient (1/t)
- α_x = soil dispersivity (L)
- η = pore water fraction (L^3/L^3)
- θ_m = mobile phase water content (L^3/L^3)
- θ_{im} = immobile phase water content (L^3/L^3)
- ρ_b = bulk soil density (M/L^3)
- ρ_s = solid phase particle density (M/L^3)
- τ_p = tortuosity factor

INTRODUCTION

Pesticides have been detected in groundwater formations serving as sources for rural and municipal water supplies. These contamination episodes may be from point or nonpoint sources. Atrazine (Aatrex) and alachlor (Lasso) are two of the most widely used pesticides in Iowa (Wintersteen, 1987) and are also two of the most commonly detected pesticides in Iowa groundwater formations serving as rural and municipal water supplies (Kelley, 1985; Kelley and Wnuk, 1986). These herbicides are widely used throughout the midwest (USDA, 1987) and have been detected in groundwater in other parts of the United States with reported concentrations in the range of 10^{-1} to 10^2 $\mu\text{g/L}$ (Holden, 1986). In an effort to respond to the identification of such contamination episodes, it is necessary to understand and be able to predict the movement of pesticides in the aquifer matrix.

Adsorption and desorption are major mechanisms affecting the rate of movement of pesticides in the subsurface. By retarding the movement of pesticides, adsorption and desorption influence the rate and degree of other mechanisms active in the subsurface (e.g., degradation, hydrolysis, etc.). A thorough understanding of adsorption and desorption of pesticides in aquifer materials is necessary to predict the rate of movement of these pesticides through aquifer materials. This will help to predict the fate of pesticides in the groundwater, to predict the time of appearance of pesticides down gradient (e.g., at a well) and to predict the time necessary for "pump and treat" remediation of pesticide

contaminated groundwater.

Much effort has been expended in developing models to predict the shapes of pesticide breakthrough curves experimentally observed. The simplest modeling approach considers equilibrium adsorption conditions. The more sophisticated models consider nonequilibrium due to physical or chemical limitations. Most generally, the actual adsorption step is not considered to be rate limiting and it is the transport of the pesticide to the adsorption site which is considered to be rate limiting. The ability of these models to predict pesticide transport without calibration to the data needs further investigation. The ability of batch studies and estimation techniques to predict the results observed in columns also needs further evaluation.

Due to the expense and health implications of conducting field scale research with pesticides, some researchers have used fluorescent dyes as surrogates for the pesticides. The majority of the use of fluorescent dyes has been as conservative tracers for determining the rate of surface water or groundwater flow. The ability of these fluorescent dyes to serve as nonconservative tracers for predicting the transport of sorbing pesticides needs to be investigated.

The purposes of this research were to investigate the transport of pesticides in a low organic content aquifer material, to evaluate the ability of several existing models to predict the observed results and to evaluate the ability of two fluorescent dyes (rhodamine WT and fluorescein) to serve as sorbing tracers for atrazine and alachlor.

In this research, laboratory batch tests, column runs and computer

modeling were conducted to investigate the following specific research objectives:

1. Evaluate the adsorption of alachlor and atrazine on a low organic carbon content alluvial aquifer material.
2. Determine the competitive adsorption (if any) when atrazine and alachlor are present jointly.
3. Investigate the use of rhodamine WT and fluorescein as adsorbing groundwater tracers with a low organic carbon content aquifer material.
4. Evaluate the ability of rhodamine WT and fluorescein to serve as adsorbing (nonconservative) tracers for atrazine and alachlor with a low organic carbon content aquifer material.
5. Evaluate the ability of batch studies and estimation techniques to predict the level of adsorption experienced in column studies for both the pesticides and the dyes.
6. Compare the ability of two existing models (a simple equilibrium model and a more sophisticated physical nonequilibrium model) to describe and predict the atrazine and alachlor breakthrough results experimentally observed.

LITERATURE REVIEW

Cases of Pesticides in Groundwater

Pesticides have been detected in groundwater from both point sources and nonpoint sources. A point source is defined as a source that can be traced to a discrete location (e.g., a pesticide formulator, a landfill, a spill). A nonpoint source is defined as a source that is not discrete in nature (e.g., fields receiving agricultural application). Several cases of groundwater contamination from point and nonpoint sources are reviewed.

Nonpoint sources

A major nonpoint source of pesticides in groundwater is the agricultural application of pesticides to fields. Historically, the loss of pesticides with surface runoff water or sediments into surface waters was the pathway of concern for pesticide movement. More recently, appearance of pesticides in groundwater due to agricultural application has become a major concern.

Kelley (1985) reported on a sampling survey of 128 wells in Iowa (representing 58 public water supplies) for synthetic organic contaminants (SOC) and pesticides. The wells that were sampled were selected based on evidence that organic contaminants may have been present. Fifty seven wells serving 33 water supplies were found to be contaminated with one or more organic contaminant. Pesticides detected and their maximum detected levels ($\mu\text{g/L}$) were as follows: alachlor,

16.6; atrazine, 10.0; cyanazine, 1.2; metolachlor, 0.6; metribuzin, 4.4 and fonofos, 0.1. Atrazine was the most commonly detected contaminant.

Hallberg (1985b) summarized pesticide concentrations detected in the groundwater from the Big Spring Basin in northeastern Iowa. The Big Spring Basin is a unique watershed in that the groundwater recharged from the basin flows into the Big Spring. This basin thus allows the investigation of the impacts of agricultural practices on groundwater in a closed system. Pesticides detected in the groundwater over the four year study and ranges of maximum concentrations ($\mu\text{g/L}$) were as follows: alachlor, 0.2 to 5.0; atrazine, 2.5 to 10.0; cyanazine, 0.7 to 4.6; metolachlor, 0.6 to 4.6; metribuzin, 3.6; 2,4-D, 0.2 and fonofos, 0.1 to 0.35.

Kelley and Wnuk (1986) discussed the sampling of municipal wells along the Little Sioux River in Iowa. Twenty-five wells serving twelve public drinking water supplies were sampled. The wells were located in alluvial, Pleistocene or bedrock formations. The samples were analyzed for the presence of 64 SOC and 35 pesticides. Nine of the 25 wells sampled, serving 6 public water supplies, were found to have one or more contaminant(s) present. Pesticides were the most frequently detected contaminants. Some of the pesticides detected and their maximum concentration ($\mu\text{g/L}$) were as follows: alachlor, 0.2; atrazine, 4.4; cyanazine, 0.7; metolachlor, 7.3; metribuzin, 1.1 and terbufos, 12.0. Wells in the Little Sioux alluvial system appeared to be the most susceptible to contamination. These wells ranged in depth from 26 to 65 feet while the other formations ranged from 50 to 380 feet in depth.

Holden (1986) discussed pesticides and groundwater quality in four states, including California, New York and Wisconsin. Pesticides detected in California groundwater and maximum concentrations ($\mu\text{g/L}$) included the following: aldicarb, 47.0; aldrin, 18.0; chlordane, 22.0; lindane, 46.0; simazine, 0.5 and 2,4-D, 4.0. In New York the most commonly detected pesticide was aldicarb. The average concentration of aldicarb, when detected, was 23.5 $\mu\text{g/L}$ (2,056 samples). Aldicarb has also been detected in Wisconsin groundwater with the maximum reported concentration being 110 $\mu\text{g/L}$. Alachlor and atrazine have been detected in Wisconsin groundwater at levels in excess of 10 $\mu\text{g/L}$.

Point sources

Pesticides may also enter groundwater from point sources. Examples of point sources that may contaminate groundwater include farm-chemical supply dealerships, accidental spills and landfills.

Hallberg (1985a) summarized data of contaminated groundwater in the vicinity of farm-chemical supply dealerships in the State of Iowa. Pesticides detected in wells or seeps and their concentrations ($\mu\text{g/L}$) were as follows: alachlor, 145.0; atrazine, 65.0; cyanazine, 36.0; metolachlor, 50.0; metribuzin, 8.0; trifluraline, 0.2 and fonofos, 1.3.

Holden (1986) indicated that Wisconsin has reported point source contamination of groundwater by several pesticides. The type of point source was not indicated. The pesticides detected and maximum concentration ($\mu\text{g/L}$) were as follows: alachlor, 88; atrazine, 140 and metolachlor, 55.

Shuckrow et al. (1981) summarized the quality of hazardous waste landfill leachates in the United States and discussed treatment technologies for these leachates. Among the chemicals commonly found in the landfill leachates were pesticides. Some of the pesticides commonly detected were DDT, aldrin, dieldrin and endrin. The concentrations at which these pesticides were detected ranged from 2.0 to 23.0 $\mu\text{g/L}$.

Pesticide transport prediction

It has been shown that pesticides are entering groundwater supplies from both point and nonpoint sources. The appearance of these pesticides in groundwater is particularly alarming due to the facts that a large percentage of the population of the United States (75% of the population of Iowa) relies on groundwater as a drinking water source (Murray and Reeves, 1977) and that many of the pesticides appearing in groundwater may have health impacts. This has resulted in USEPA proposing drinking standard limits for several of these pesticides (AWWA, 1988). These concerns make it vital to be able to predict the transport and fate of these pesticides once they have entered the groundwater. The movement of pesticides in groundwater is also referred to as solute transport (miscible displacement) in porous media.

Fundamentals of Solute Transport in Groundwater

The movement of pesticides in the subsurface is dependent in part on properties of the soil and the pesticide. At the simplest level, the movement of pesticides is concomitant to the flow of the groundwater. It

thus becomes necessary to describe the hydrodynamics of groundwater flow. Groundwater flow is assumed to consist of advection and dispersion components. Often, however, the flow of the pesticides in the soil differs from the flow of the groundwater due to interactions between the pesticides and the soil. Examples of such interactions are adsorption, biological decay, etc.

Advection and dispersion

The hydrodynamics of groundwater flow is described by advection and dispersion components. Advection (plug flow) is the idealized condition that assumes all groundwater moves through the soil at the same rate and is a function only of the pore water velocity. The advection component of groundwater flow does not consider velocity distributions within the pores, the tortuosity of flow through the pores or molecular diffusion. These three elements are considered in the dispersion component. The advection term alone would predict that the pesticide would appear down gradient as a step (go from zero to maximum concentration at a discrete time) at a time given by the distance divided by the pore water velocity. The incorporation of dispersion into the prediction would result in a portion of the pesticide appearing sooner (due to that portion of the pores with groundwater velocity greater than the average pore water velocity) and a portion of the pesticide appearing later (due to that portion of the pores with groundwater velocity less than the average pore water velocity). The dispersion component is thus used to describe the spreading observed about the step breakthrough predicted by advection

(plug flow) alone. The combination of advection and dispersion would predict a continuous breakthrough (as opposed to the step breakthrough for advection alone) of a sigmoidal shape. Some of the factors affecting the amount of dispersion observed include soil particle size distribution, pore size distribution, soil packing, pore water velocities and chemical molecular diffusion.

Adsorption and desorption

Advection and dispersion modeling of solute transport assumes that the solute (pesticide) moves with the groundwater and does not interact with the soil. For nonpolar pesticides, the organic nature of pesticides and the organic content of the soil commonly result in the adsorption of the pesticides onto the soil during groundwater flow. Adsorption of the pesticides onto the soil acts as a sink for the pesticides until the adsorptive capacity of the soil is satisfied. The adsorption of the pesticides on the soil will serve to slow down (retard) the appearance of the pesticides down gradient. The level of adsorption (and thus level of retardation) is a function of the pesticide and the organic content (for nonpolar pesticides) of the soil.

The mentality seems to be prevalent that once the pesticide adsorbs to the soil it no longer threatens groundwater resources down gradient. However, the adsorption of nonpolar pesticides to soil organic matter has been observed to be reversible. This suggests that when the concentration of the pesticide in the groundwater decreases (as the pesticide front passes) that desorption of the pesticide from the soil

phase to the pore water phase will occur.

Both adsorption and desorption are mechanisms active in the soil environment which will amend the solute transport predictions made by the advection and dispersion model. This leads to the need for predictive models able to describe advection, dispersion and adsorption / desorption.

Other interactions

Adsorption acts to slow down the movement of pesticides in groundwater. This allows more time for the pesticides to experience other interactions during transport in the soil environment. For pesticides, examples of other interactions that may take place in the subsurface include chemical and biological degradation. In the presence of these interactions, it would be necessary to include additional components to the solute transport model. For purposes of this research, it was assumed that adsorption and desorption are the only interactions occurring in the soil. Thus, the solute transport model of interest to this research contained components for advection (plug flow), dispersion and adsorption / desorption.

Fundamentals of Adsorption and Desorption

Adsorption and desorption are two major processes affecting the transport of pesticides in groundwater. It is vital to have a fundamental understanding of these processes in order to understand and predict the effect of these processes on pesticide transport. Adsorption

is the result of intermolecular forces between the solid phase and the solute.

Intermolecular forces

It is presently believed that there are four distinct forces of nature (Israelachvili, 1985). Two of these forces (strong and weak interactions) act between neutrons, protons, electrons and other elementary particles and are responsible for holding protons and neutrons together in atomic nuclei (strong interactions) and are involved in electron emission (weak interactions). The other two forces, electromagnetic (electrostatic) and gravitational, are more dominant at the atomic size and larger ranges. Electrostatic forces are more evident at the atomic and molecular scales and account for intermolecular interactions which determine the properties of solids, liquids and gases and account for the properties of particles in solution and the nature of chemical reactions. Gravitational forces are more evident at larger scales and account for the movement of the planets and objects within the planets' realm of influence. For purposes of this discussion, intermolecular forces (electrostatic forces) are the forces of interest.

A brief history of the development of the present understanding of intermolecular forces, as outlined by Israelachvili (1985), will be presented. As scientists began to explore laws to account for intermolecular forces, it was believed that one simple law would be determined (much as one gravitational law had been determined). Some of the first attempts included the mass of the molecules in the models (no

doubt patterned after the gravitational law). Eventually it was realized that purely mechanistic views of intermolecular forces could not alone account for their behavior. This resulted in the development of thermodynamic and probabilistic concepts such as free energy and entropy to account for intermolecular behavior. With the advent of quantum theory it was possible to understand the origin of intermolecular forces and derive expressions for interaction potentials. However, the solutions for these expressions are very difficult. Various classifications for intermolecular forces have evolved (e.g., ionic, covalent, van der Waals, hydrogen bonding, hydrophobic) when, fundamentally, all these categories have a common origin (electrostatic interactions). One example of the manifestation of intermolecular forces is adsorption.

Adsorption

Adsorption, absorption and sorption are three terms that refer to similar phenomena. Weber (1972) defines adsorption as occurring at an interface, absorption as occurring within the adsorbent (solid phase) and sorption as including both adsorption and absorption. Often the term adsorption is used interchangeably with sorption, such will be the case for purposes of this document. Fundamentally, adsorption is the concentration of a chemical from one phase (gas or liquid) at the interface or internally to another phase (solid). The adsorbate is the solute (pesticide) being adsorbed out of the solution (groundwater) and the adsorbent (soil) is the solid phase where the concentration of the

adsorbate is occurring.

Historically, adsorption studies were conducted to investigate the concentration of gases at solid surfaces. A few of these studies will be reviewed to provide background for current research efforts investigating the adsorption of pesticides from groundwater.

Langmuir (1918) investigated the adsorption of gases on the plane surfaces of glass, mica and platinum. He stated that the internal bonding of the adsorbent (solid phase) left unsaturated surface atoms and thus resulted in adsorption of a monolayer of gases to satisfy the deficiency. The following assumptions were made by Langmuir in developing his conceptual model of adsorption: (1) adsorption occurs at points of valency on the surface of the adsorbent, (2) a monomolecular layer of adsorption results, (3) all adsorption sites have equal affinity for adsorbate and (4) adsorbed molecules do not affect adsorption at adjacent sites.

In 1926, Freundlich published an empirical equation to describe adsorption. Benefield et al. (1982) state that the development of this equation was based on the assumption that the adsorbent is comprised of a heterogeneous surface composed of different classes of adsorption sites with each class being of the nature described by Langmuir.

In 1938, a model was developed by Brunauer et al. that generalized the Langmuir model by assuming that molecules were adsorbed in multiple layers during adsorption. This model, referred to as the BET model, assumed that the adsorbent surface was composed of uniform sites and that adsorption at one site does not affect adsorption at neighboring sites.

The BET model assumed that the energy of adsorption holds the first monolayer of molecules but that the condensation energy is responsible for the successive layers adsorbed.

The Freundlich model, or a linear simplification of this model, has been most widely used to predict the adsorption of nonpolar pesticides from groundwater. For nutrients or metals, the Langmuir model, or modifications thereof, have been most widely used. For purposes of this research, the linear or Freundlich model will be utilized.

Adsorption motivation and types

In a general sense, adsorption may be classified as adsorbent or solvent motivated (Weber, 1972). Adsorbent motivated adsorption occurs when an attraction occurs between the solute (pesticide) and the adsorbent (soil). An example of adsorbent motivated adsorption would be a polar or ionizable pesticide (such as diquat or paraquat) interacting with the cation exchange sites of clays in a soil. Solvent motivated adsorption occurs when the presence of the solute (pesticide) in the solvent (groundwater) is not thermodynamically favorable. Such a pesticide has a low water solubility and is considered hydrophobic (disliked by water). Hydrophobic pesticides will find it more thermodynamically favorable to be associated with the organic phase (organic matter) of the soil rather than the polar groundwater phase. An example of solvent motivated adsorption would be the interaction of chlordane (hydrophobic insecticide) with the organic content (organic matter) of the soil.

The adsorption attachment may be the result of one or a combination of several different mechanisms (different categories of electrostatic forces). Fundamentally, the adsorption attachment may be classified as exchange, physical or chemical (Weber, 1972). Exchange adsorption refers to accumulation of the pesticide at the adsorption sites due to the electrostatic attraction between the charged sites of the soil and the charged sites or polar moieties of the pesticide. Physical adsorption (physisorption) is the result of van der Waals attractions between the pesticide and the adsorption sites. Chemical adsorption is the result of a chemical reaction between the adsorbent (soil) and the solute (pesticide). While it is fundamentally expedient to separate the adsorption forces into these three categories, in actuality it is typically a combination of several or all of these forces that cause the adsorption of a given pesticide onto a given soil. Hamaker and Thompson (1972) include the following as electrostatic adsorptive forces between pesticides and soils: (1) van der Waals - London forces, (2) hydrogen bonding, (3) charge transfer, (4) ligand exchange, (5) ion exchange, (6) direct and induced ion-dipole and dipole-dipole interactions, and (7) chemisorption. These electrostatic forces may be divided up among the exchange, physical and chemical categories discussed above.

Exchange adsorption is the result of coulombic forces of interionic attraction. These attractions occur between the charged sites of the soil (especially cation exchange sites of clays) and the charged functional groups or polar moieties of the pesticide. Under favorable conditions the pesticide will exchange for the ions previously adsorbed

on the ion exchange sites of the soil (ion exchange). Binding energies of up to 50 kilocalories/mole may be experienced for exchange adsorption (Hamaker and Thompson, 1972).

Physical adsorption is the result of van der Waals or London dispersion forces. These forces are evidenced for molecules with no permanent dipoles or higher order moments and are the result of the continuous motion of electrons in an atom or molecule (Rigby et al., 1986). The continuous motion of the electrons results in temporary dipoles or higher order moments for the atom or molecule while on the average no moment is present. This temporary (instantaneous) dipole (or higher order moment) can in turn induce a dipole (or higher order moment) in a neighboring atom or molecule and a net attraction will occur. The magnitude of this interaction is the sum of the multipole interactions (dipole-dipole, dipole-quadropole, dipole-octopole, quadropole-quadropole, etc.). The contribution of the dipole-dipole interaction is proportional to the minus sixth power of the molecular distance, the dipole-quadropole interaction is proportional to the minus eighth power of the molecular distance and so forth. Thus, the controlling multipole interaction is typically the dipole-dipole interaction (if it is present). In the absence of the dipole-dipole interaction the dipole-quadropole interaction typically becomes dominant (Rigby et al., 1986). Energies of adsorption for the van der Waals interactions are generally of the order of 1 to 2 kilocalories/mole (Hamaker and Thompson, 1972). The energy of adsorption for physical adsorption is significantly lower than typically experienced for exchange or chemical adsorption. For this

reason the adsorbate (pesticide) is considered to be free to move from adsorption site to adsorption site within the soil (Weber, 1972) and is more readily desorbed when the pesticide concentration decreases in the groundwater phase (when the pesticide front passes).

Chemical adsorption occurs as the result of the formation of a chemical bond between the pesticide and the soil. The energy of adsorption for chemisorption is generally higher than the energy of adsorption for exchange or physical adsorption with levels for chemisorption commonly exceeding 50 kilocalories/mole and values as high as 194 kilocalories/mole having been reported (Hamaker and Thompson, 1972). This high energy of adsorption suggests that an activation energy may be necessary for the reaction to take place and also suggests that the pesticide, once adsorbed, is relatively immobile on the soil surface. These high energies of adsorption account for the high level of pesticide adsorption that can occur at low concentrations for some pesticides. The high energy of adsorption also accounts for the continued adsorption that occurs at elevated temperatures (provides necessary activation energy) in spite of the fact that the adsorption process is assumed to be exothermic (Ruthven, 1984).

The adsorption of many pesticides falls into the category of hydrophobic adsorption (adsorption of nonpolar, hydrophobic pesticides). This adsorption typically is solvent motivated and the attachment is due to physical adsorption. The nature of hydrophobic chemicals was originally attributed to "like attracts like", that nonpolar solutes (e.g., alkanes - unsubstituted hydrocarbons) prefer to be in nonpolar

phases. This assumed that the dislike of hydrophobic chemicals for polar solvents was motivated by their preference for hydrocarbon chains. It is now believed that the attraction between nonpolar groups plays only a minor role in the hydrophobic effect and that it is actually the strong attractive forces that occur between water molecules (hydrogen bonds) which result in the hydrophobic effect (Tanford, 1980). The intermolecular distance between hydrogens and oxygens of adjacent water molecules (0.165 nm) is less than predicted by summing the van der Waals radii (0.26 nm) but is still larger than the intramolecular covalent bond distance between hydrogen and oxygen (0.10 nm) (Israelachvili, 1985). Thus, a bond intermediate between the covalent and the van der Waals bond is suggested. This intermolecular bond is referred to as the hydrogen bond. Water molecules find the formation of these hydrogen bonds thermodynamically favorable. Polar or ionic solutes are able to form strong bonds with the water which serve to compensate for the disruption or distortion of the hydrogen bonds (Tanford, 1980) and thus are highly soluble in water. Nonpolar molecules, however, are not capable of forming hydrogen bonds. The water molecules will attempt to adjust their orientation in an effort to fit the chemical into its structure without making it necessary to break a hydrogen bond. However, depending on the size of the nonpolar solute, this may not be possible. This causes many of the nonpolar organic compounds (pesticides) to be thermodynamically unfavorable in the aqueous phase and results in the low aqueous solubilities for these pesticides. It is thus seen why adsorption resulting from the hydrophobic effect is referred to as solvent (water)

motivated adsorption.

Factors affecting pesticide adsorption in soils

Having developed a fundamental framework of the adsorptive forces at work between pesticides and soils, some of the physical and chemical factors within the soil environment which affect the level of adsorption will be discussed. Detailed reviews of this subject are available in the literature (Bailey and White, 1970; Mortland, 1970; Hamaker and Thompson, 1972; Calvet, 1980; Karickhoff, 1984) and are beyond the scope of this document. A brief summary of several of the soil, solvent (water) and adsorbate (pesticide) properties that affect the level of adsorption will be presented here.

Research has shown that, for hydrophobic pesticides, the organic content of the soil and the octanol/water partition coefficient for the pesticide are able to predict the level of adsorption that will occur for a given soil and pesticide (Karickhoff et al., 1979; Rao and Davidson, 1980; Brown and Flagg, 1981; Miller, 1984). The octanol/water partition coefficient (K_{ow}) for a pesticide is determined by placing a pesticide into a reactor (separatory funnel) with a polar (water) and relatively nonpolar (1-octanol) phase. The reactor is mixed until partitioning of the pesticide between the two phases is complete. The concentration of the pesticide in each phase is determined and the ratio of the pesticide concentration in the octanol phase and the water phase is the octanol/water partition coefficient. This parameter indicates the hydrophobicity of the pesticide and is thus a relative indicator of the

adsorptive potential of the pesticide with an organic phase. The fraction organic carbon content (f_{OC}) of the soil provides an organic phase in which the hydrophobic pesticide may concentrate. The octanol/water partition coefficient (K_{OW}) of the pesticide and the fraction organic carbon content (f_{OC}) of the soil have been used in empirical relationships to predict the level of adsorption between a soil and a pesticide. These empirical relationships will be discussed in a later section.

The pH of a groundwater system may affect the form of functional groups both on the pesticide and the soil. Thus, for ionizable pesticides, pH may become a significant factor (especially as the pK_a or pK_b value of the pesticide - the pH where the pesticide functional group changes - is approached). Harris and Warren (1964) found the level of adsorption of atrazine to bentonite to be significantly higher at a pH of 4.1 than at a pH of 8.2 but found adsorption of atrazine to organic matter to be relatively independent of pH. The pK_a value for atrazine has been reported as 1.7 (Weber et al., 1980). Farmer and Aochi (1974) found the level of picloram adsorption to slightly increase for decreasing values of pH for six different soils. The pH during this study did not go below 5, well above the pK_a value for picloram of 3.6. For nonpolar and nonionizable pesticides the pH would be expected to play a lesser role in the level of adsorption.

The temperature of the system may affect the level of adsorption realized. The adsorption process is considered to be exothermic (Benefield et al., 1982). Thus, based on the enthalpy of the reaction,

increasing temperature would tend to decrease the extent of the reaction (adsorption). An indirect effect of temperature on adsorption is the increasing solubility with increasing temperature. Both the solubility and enthalpy of the system would work to predict decreasing adsorption with increasing temperatures. However, the rate of the reaction is taken to be a function of the necessary activation energy for the reaction and increasing temperatures would tend to favor the kinetics of the adsorption reaction. Harris and Warren (1964) found increasing levels of pesticide adsorption on bentonite with decreasing temperature but found the level of pesticide adsorption on organic matter to be relatively independent of temperature. Farmer and Aochi (1974) found a very slight increase in pesticide adsorption with decreases in temperature on six different soils. In general, for the range of temperatures typically encountered, the effect of temperature on adsorption is assumed to be minor (Weber, 1972).

The presence of more than one pesticide may affect the level of pesticide adsorption due to competition for adsorption sites. Chiou et al. (1983) found no evidence of competitive adsorption (partition) when more than one nonionic organic (aromatic) compound was present. The authors interpreted this to indicate that the concentration at the solid interface was the result of solvent motivated partitioning (hydrophobic) rather than adsorbent motivated adsorption. Schwarzenbach and Westall (1981) found the adsorption of nonpolar organics to be independent of the number of solutes present. Abdul and Gibson (1986) found slight decreases (10 to 20%) in the level of adsorption for polynuclear aromatic

hydrocarbons (PAH) when present as a mixture. It appears that for the adsorption of hydrophobic compounds little competitive adsorption would be expected. In the case of polar or ionizable pesticides (when exchange or chemical adsorption would be more evident), the presence of competitive adsorption would be more likely.

The presence of background ions (and corresponding changes in ionic strength) may affect the level of pesticide adsorption in soils. Increasing valencies of ions and increasing ionic strength of the groundwater would serve to reduce electrostatic repulsions that exist due to charges on the soil particles (especially clays and organics). Farmer and Aochi (1974) observed increasing levels of picloram adsorption for increasing ionic strength (concentration and valency) of the solution. The authors attribute this effect to the ionizable nature of the picloram. Khan and Khan (1986) found the presence of divalent cations to increase the level of adsorption for organophosphorous (ionizable) pesticides. For neutral (nonionic) pesticides, changes in the electrostatic forces of repulsion of the soil surfaces would not be expected to affect the level of adsorption. Fusi and Corsi (1968) noticed only slight variations in the level of adsorption of atrazine (less than 20%) when the salt concentration was increased from 0.01 N to 0.5 N at neutral values of pH.

Other environmental factors affecting the level of pesticide adsorption with soils could be discussed, but lie beyond the scope of this document.

Batch and column adsorption techniques

Adsorption of pesticides on soils is commonly investigated in the laboratory by use of batch or column studies. The batch study consists of placing a known quantity of the soil and a known mass of the pesticide into a reactor and shaking until equilibrium adsorption is reached. The purpose of batch studies is to determine the equilibrium level of pesticide adsorption and the shaking serves to eliminate mass transfer limitations. The column study more closely mimics the soil environment and includes the corresponding mass transfer limitations. A column is filled with the soil media, the pesticide solution is introduced at the top of the column and the appearance of the pesticide in the effluent of the column is monitored. The specific methodologies utilized for conducting batch and column studies in this research will be discussed in the materials and methods section.

Modeling of Solute Transport with Adsorption

Having discussed the fundamental concepts of advection, dispersion and adsorption, techniques for mathematically modeling these processes will be reviewed.

Types of modeling approaches

Various approaches may be utilized in an attempt to model solute transport with adsorption. Only mathematical models will be considered here (as opposed to physical and analog models). Various mathematical models can be classified as follows: (1) conceptual (mechanistic) versus

empirical (functional) - based on theoretical derivation from fundamentals versus derived from observations without consideration for fundamental mechanisms, (2) stochastic versus deterministic - model incorporates random nature of process and output varies for a given set of inputs, versus discrete output for a given set of inputs (3) static versus dynamic - steady state with respect to time for input parameters versus time dependent variations of input parameters and (4) spatial dimensionality - one-, two- or three-dimensional. The fundamental solute transport model to be considered here will be mechanistic, deterministic, dynamic and one-dimensional. For a discussion of stochastic modeling the reader is referred to Jury (1983) and for a treatment of functional modeling the reader is referred to Sposito et al. (1986). Macropore flow models will not be discussed here; the reader is referred to Beven and Germann (1982), van Genuchten et al. (1984) and Germann and Beven (1985) for treatment of this topic.

One-dimensional solute transport

The fundamental governing equation for pesticide transport in saturated groundwater is the advection, dispersion and adsorption / desorption equation. This equation is derived from flux balance considerations about an elemental volume and, for the one-dimensional flow case, results in the partial differential equation shown in Equation 1 (Lapidus and Amundson, 1952; Freeze and Cherry, 1979). The development of the basic advection dispersion equation assumes that dispersion can be described as a Fickian process. This assumption has been criticized

$$\frac{\partial C}{\partial t} = - v_x \frac{\partial C}{\partial x} + D_x \frac{\partial^2 C}{\partial x^2} - \frac{\rho_s(1-\eta)}{\eta} \frac{\partial q}{\partial t} \quad (1)$$

where: C = liquid phase solute concentration (M/L³)
t = time (t)
D_x = hydrodynamic dispersion coefficient (L²/t)
x = dimension of solute transport (L)
v_x = pore water velocity (L/t)
ρ_s = solid phase particle density (M/L³)
η = pore water fraction (L³/L³)
q = ratio of solute on solid phase versus in liquid phase (M/M)

(Anderson, 1984) but is widely used. Equation 1 is a parabolic partial differential equation and is second order with respect to space (x) and first order with respect to time (t). The solution of this governing equation will thus require two spatial (boundary) conditions and one temporal (initial) condition. For cases of simple boundary conditions and adsorption expressions, analytical solutions to this one-dimensional equation are available (van Genuchten and Alves, 1982). For more complicated boundary conditions or adsorption expressions it may become necessary to utilize numerical approximation solutions (finite difference, finite element, etc.).

The term on the left of Equation 1 is the change of the pesticide concentration in the liquid phase within the elementary volume with respect to time. The first term on the right of Equation 1 is the advection (plug flow) term as noted by the presence of the pore water velocity parameter. The second term on the right of Equation 1 is the

hydrodynamic dispersion term which accounts for pore water velocity gradients, tortuosity of the flow path through the porous media and the molecular diffusion of the solute. The third term on the right of Equation 1 is the adsorption term which accounts for the loss (or gain) of the solute from the liquid phase into the soil phase. Equation 1 thus predicts the change in solute concentration as affected by advection, dispersion and adsorption. As in the development of all governing equations, various assumptions were made in the derivation of Equation 1. Some of the assumptions made in the derivation include the following: saturated soil conditions, nonconsolidating soil (porosity constant) with respect to space and time, one-dimensional flow (pore water velocity only in the x dimension), dispersion only in the x dimension, pore water velocity and dispersion constant with respect to x and adsorption is the only interaction between the solute and the soil. These assumptions are often satisfied for laboratory column studies; however, they are less likely to apply in field situations.

The hydrodynamic dispersion coefficient accounts for velocity gradients within the pores, the tortuosity of the flow path for flow through porous media and the molecular diffusion of the solute. The first two elements are functions of the soil configuration and the pore water velocity and these two elements are referred to collectively as mechanical mixing. Molecular diffusion is a function of the solute and is independent of the pore water velocity (although the relative significance of the molecular diffusion is a function of pore water velocity). Equation 2 demonstrates the relationship commonly used to

$$D_x = \alpha_x v_x + D_m \quad (2)$$

where: α_x = soil dispersivity (L)
 D_m = molecular diffusion coefficient (L^2/t)

define the hydrodynamic dispersion coefficient. While some researchers have included an exponent on the pore water velocity term, it has generally been found that the value of this exponent is 1.0 (Gillham and Cherry, 1982). The dispersivity (α_x) is the soil specific parameter that, when combined with the pore water velocity, accounts for the mechanical mixing portion of the hydrodynamic dispersion. An increase in either the dispersivity of the soil or the pore water velocity will act to increase the mechanical mixing portion of the hydrodynamic dispersion coefficient. For a given soil, the molecular diffusion portion of the hydrodynamic dispersion coefficient becomes significant at low pore water velocities (low gradients and/or soils with low hydraulic conductivities). The molecular diffusion coefficient is typically on the order of 10^{-2} to 10^{-1} cm^2/hr (Gillham and Cherry, 1982). For most laboratory column studies, pore water velocities are in the range of 1 to 50 cm/hr and soil dispersivities are in the range of .01 to 1.0 cm (Freeze and Cherry, 1979). It is only for the very low values of pore water velocities and dispersivities that the molecular diffusion coefficient becomes significant. In the case where the contribution of the molecular diffusion coefficient is relative insignificant, Equation 2 can be simplified to Equation 3. In most cases Equation 3 is the

$$D_x = \alpha_x v_x \quad (3)$$

form used for defining the hydrodynamic diffusion coefficient (Gillham and Cherry, 1982).

A useful parameter for evaluating the relative significance of the advection and dispersion terms is the Peclet (Pe) number. This is a dimensionless number (such as the Reynolds number) which indicates the relative significance of advection and dispersion in solute transport for a given set of conditions. Equation 4 gives the general form of the

$$Pe = \frac{v_x L}{D_x} \quad (4)$$

where: Pe = Peclet number
L = column length (L)

relationship used to define Pe. The numerator of the Pe parameter indicates the advective tendency of the system and the denominator represents the dispersive tendency of the system. Thus, high values for Pe would suggest advection as dominant and the solute breakthrough curve would tend towards a plug flow (step) shape. Low values for Pe would suggest that dispersion is dominant and the solute breakthrough curve would tend towards a sigmoidal shape - earlier appearance of the solute and increased time for complete breakthrough to occur. Figure 1 demonstrates a comparison of breakthrough curves for Pe values of 5 and 100 and also demonstrates the retardation (lag) effect of a sorbing solute. Substituting for D_x from Equation 3 into Equation 4 yields

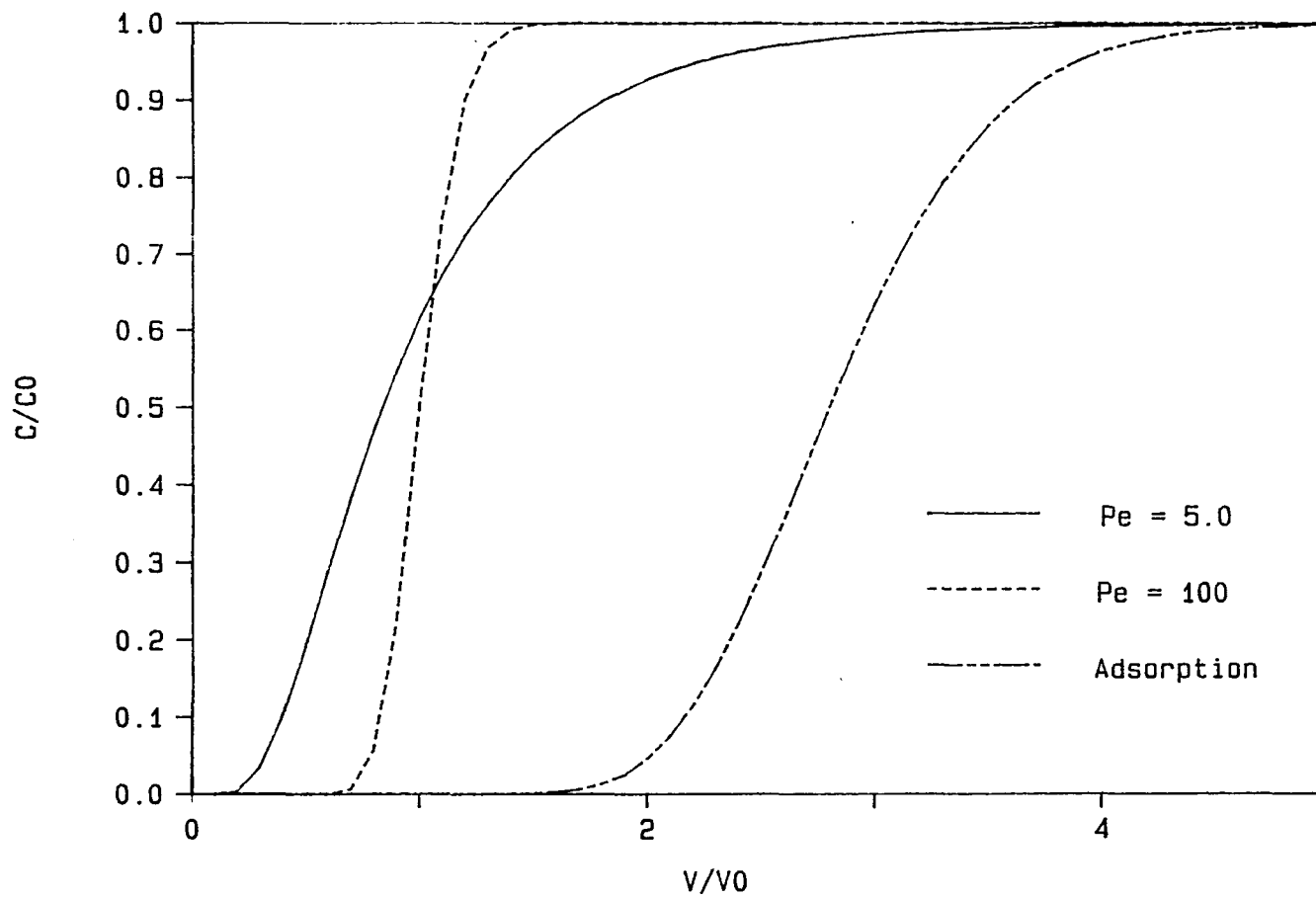


Figure 1: Breakthrough curve - effect of Pe and adsorption

Equation 5. This demonstrates that, when Equation 3 is valid, the

$$Pe = \frac{L}{\alpha_x} \quad (5)$$

value of Pe is independent of the pore water velocity and is a function of the column length and the dispersivity of the soil. It can be observed from Equation 5 that increasing column lengths favor advection and increasing dispersivities favor dispersion.

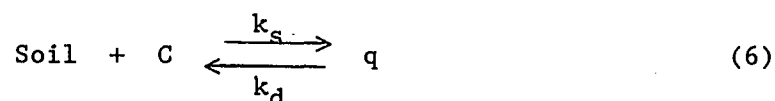
Equilibrium versus nonequilibrium adsorption

The retarding effect of adsorption on the appearance of a solute in a breakthrough curve was demonstrated in Figure 1. The last term on the right hand side of Equation 1 accounts for the removal of solute from the liquid phase due to adsorption. Many researchers have assumed the adsorption process to be instantaneous relative to the groundwater flow rates and have assumed equilibrium adsorption to be valid. Others have observed experimental deviations from equilibrium adsorption predictions and have utilized nonequilibrium adsorption expressions to account for these deviations.

Equilibrium Adsorption and Desorption Expressions

Equilibrium adsorption assumes that the rate of adsorption (kinetics) is relatively fast and that the use of an instantaneous adsorption expression is justified. Equation 6 shows the adsorption process written in terms of a reaction between the soil and the chemical

(C) resulting in adsorbed chemical (q). An example of a kinetic adsorption expression to describe this reaction is shown in Equation 7. The term on the left of Equation 7 defines the time rate of change of the amount of the pesticide adsorbed in the solid phase normalized to the amount of pesticide in the water phase (q). The forward rate of this reaction (adsorption) is taken to be proportional to the solute concentration (C) and the reverse rate of this reaction (desorption) is assumed to be proportional to q with k_s and k_d being the rate coefficients for sorption and desorption, respectively. For equilibrium conditions, the left hand side of Equation 7 is zero and the expression simplifies to Equation 8. At equilibrium, the rates of adsorption and desorption are constant (and thus k_s and k_d are constant). This allows the terms inside of the brackets in Equation 8 to be simplified into an overall constant (K_p). Valocchi (1985) and Parker and Valocchi (1986) have discussed criteria for determining the validity of the local



$$\frac{\partial q}{\partial t} = k_s \frac{\eta}{\rho_s(1-\eta)} C - k_d q \quad (7)$$

$$q = \left[\frac{k_s}{k_d} \frac{\eta}{\rho_s(1-\eta)} \right] C_e = K_p C_e \quad (8)$$

where: k_s = first order adsorption rate constant (1/t)
 k_d = first order desorption rate constant (1/t)
 C_e = liquid phase equilibrium concentration (M/L³)
 K_p = linear equilibrium partition coefficient (L³/M)

equilibrium assumption for a given set of conditions. It can thus be seen that equilibrium adsorption is actually a simplifying condition for the kinetic adsorption process. When the kinetics of adsorption are not limiting, the equilibrium simplification of the adsorption process can be successfully applied.

Linear equilibrium adsorption expression

Various equilibrium adsorption expressions have been utilized by researchers. The simplest form of the equilibrium adsorption expressions is the linear equilibrium adsorption expression. This is the expression shown in Equation 8 which resulted when equilibrium was assumed for Equation 7. Equation 8 is presented again in Equation 9 for the purpose of clarity. This expression is referred to as linear equilibrium adsorption, linear partitioning, and Henry's adsorption by various

$$q = K_p C_e \quad (9)$$

researchers. The distinguishing factor of this adsorption expression is that a linear relationship is assumed between q and C at equilibrium with K_p (K_d used by some researchers) as the proportionality constant. This equation suggests that plotting of a range of q versus C_e values on arithmetic scales would result in a linear plot with a slope of K_p . A plot of q versus C_e at constant temperature is known as an adsorption

isotherm. An example of a linear adsorption isotherm is given in Figure 2. If the isotherm plot is not linear on arithmetic paper, a nonlinear adsorption expression is suggested (such as the Freundlich isotherm).

Some researchers have found the assumption of linear equilibrium adsorption to be valid for pesticides and soils (Brown and Flagg, 1981) while others have observed nonlinear adsorption isotherms (Hamaker and Thompson, 1972; Rao and Davidson, 1980). Even when nonlinearity is observed at higher concentrations, the isotherm is often observed to be linear at lower concentrations.

Linear isotherms at lower concentrations, with nonlinearity becoming evident at higher concentrations, is consistent with Langmuir's conceptual model of adsorption. This model assumes a finite number of adsorption sites each with equal affinity for the adsorbate (pesticide). As more of the adsorption sites become occupied, the probability of the pesticide mass still in solution finding one of the remaining adsorption sites becomes less favorable. This results in nonlinearity of the isotherm at higher concentrations (at higher concentrations a smaller fraction of the pesticide originally in solution ends up adsorbed to the soil). Another conceptual model, based on a distribution of adsorption sites with varying affinities for the adsorbate, would also predict nonlinearity of the isotherm at higher concentrations. The most favorable adsorptive sites would be filled first with less favorable sites being utilized at higher concentrations. At lower concentrations it may be that only the most favorable sites are utilized, predicting linear adsorption isotherms at lower concentrations. The reduction in

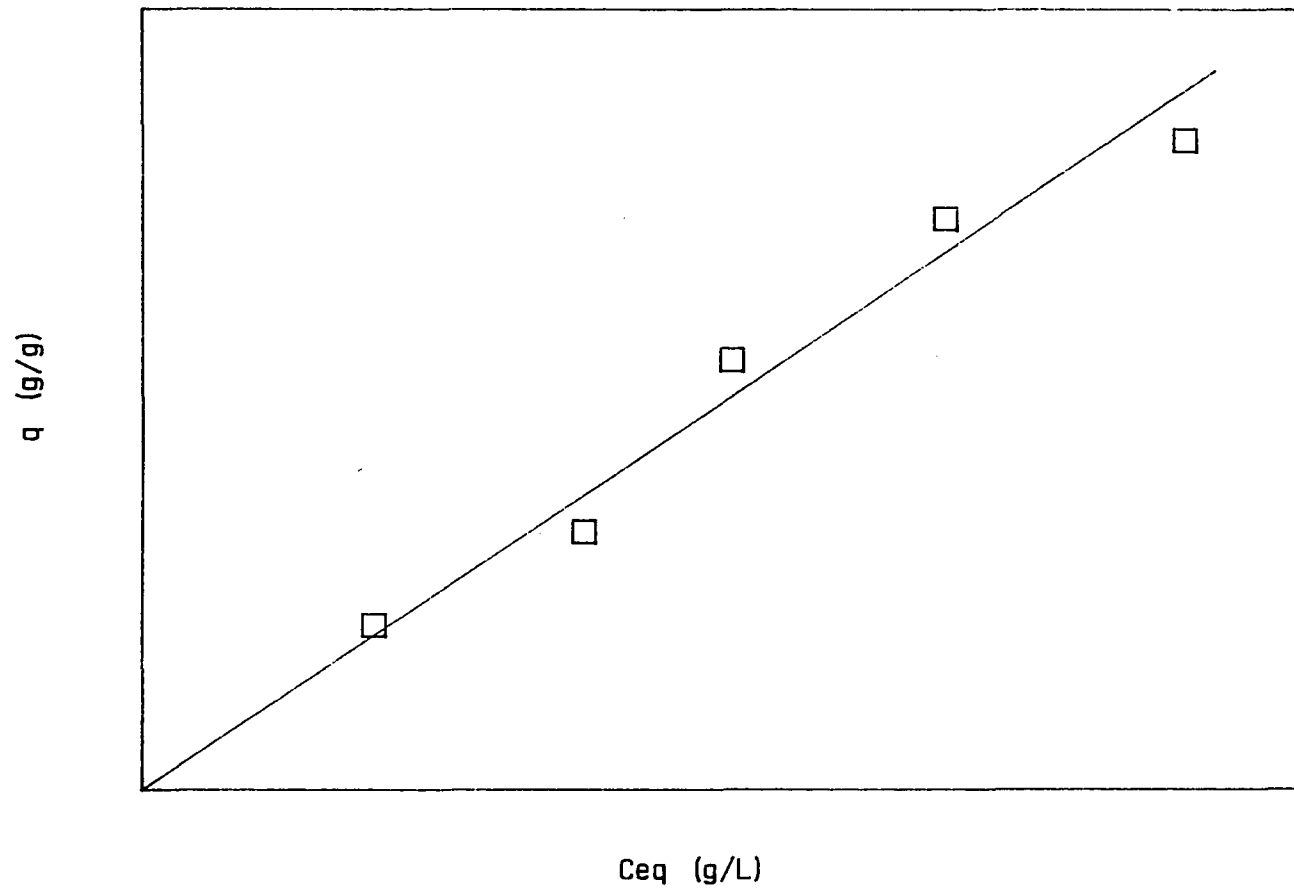


Figure 2: Linear adsorption isotherm

incremental adsorption with increasing adsorbate concentrations would result in the adsorption isotherm being nonlinear (less overall efficiency of adsorption) at higher equilibrium concentrations.

Some researchers have found adsorption isotherms for a solute to be linear over the entire solubility range of the solute (Chiou et al., 1983; Mingelgrin and Gerstl, 1983). Chiou et al. (1983) suggest that the lack of isotherm curvature at equilibrium concentrations of 60 to 90% of solubility for the solute indicates hydrophobic motivated adsorption (partitioning) rather than adsorbent motivated adsorption. This construct has some basis for solvent motivated adsorption which is basically a partitioning of the adsorbate between two phases and, in some situations, is independent of the adsorption sites. Mingelgrin and Gerstl (1983), however, state that for chemicals with low solubility, the conclusions of Chiou et al. (1983) may be inaccurate. For compounds with low solubility, the solubility range may not be great enough to cause nonlinearity of the isotherm due to the low level of adsorption realized. This low level of adsorption may be inadequate to cause nonlinearity, in agreement with the discussions of the Langmuir model and the distribution of adsorption sites model reviewed above. Thus, the conclusions of Chiou et al. (1983) are not adequate to support that the adsorption isotherm for nonionic organics will always be linear and that a linear isotherm over the solubility range of the chemical indicates solvent motivated (hydrophobic) adsorption (partitioning).

Incorporation of the linear equilibrium adsorption expression into the governing partial differential equation (Equation 1) requires an

expression for the $\partial q/\partial t$ term (the last term on the right of Equation 1). The $\partial q/\partial t$ term can be expanded as shown in Equation 10. Substituting for the $\partial q/\partial C$ term (as follows from Equation 9) results in Equation 11.

$$\frac{\partial q}{\partial t} = \frac{\partial q}{\partial C} \frac{\partial C}{\partial t} \quad (10)$$

$$\frac{\partial q}{\partial t} = K_p \frac{\partial C}{\partial t} \quad (11)$$

Substituting Equation 11 into the last term of Equation 1 and collecting the $\partial C/\partial t$ terms on the left hand side results in Equation 12. The values inside the brackets on the left hand side of Equation 12 are constants and can be simplified into a single constant (r_f), as shown in Equation 13. This term (r_f) is referred to as the retardation factor, as it is the factor that differentiates solute transport with linear adsorption from solute transport of a nonadsorbing (conservative) solute.

Simplifying Equation 12 by substituting for r_f results in Equation 14.

For a value of $r_f = 1.0$ ($K_p = 0$), Equation 14 simplifies

$$\left[1 + \frac{\rho_s(1-\eta)}{\eta} K_p\right] \frac{\partial C}{\partial t} = D_x \frac{\partial^2 C}{\partial x^2} - v_x \frac{\partial C}{\partial x} \quad (12)$$

$$r_f = \left[1 + \frac{\rho_s(1-\eta)}{\eta} K_p\right] \quad (13)$$

where: r_f = retardation factor

$$r_f \frac{\partial C}{\partial t} = D_x \frac{\partial^2 C}{\partial x^2} - v_x \frac{\partial C}{\partial x} \quad (14)$$

to the advection dispersion equation with no reactions. For simple boundary conditions, analytical solutions are available for Equation 14. Equation 15 is an example of one such analytical solution (Freeze and Cherry, 1979) with the initial and boundary conditions as specified in Equations 16 through 18. Usage of this analytical solution

$$\frac{C}{C_0} = 0.5 \left[\operatorname{erfc} \left(\frac{x r_f - v_x t}{2(D_x r_f t)^{1/2}} \right) + \exp \left(\frac{v_x x}{D_x} \right) \operatorname{erfc} \left(\frac{x r_f + v_x t}{2(D_x r_f t)^{1/2}} \right) \right] \quad (15)$$

$$C(x, 0) = 0.0 \quad x \geq 0 \quad (16)$$

$$C(0, t) = C_0 \quad t \geq 0 \quad (17)$$

$$C(\infty, t) = 0.0 \quad t \geq 0 \quad (18)$$

where: erfc = complementary error function

for $r_f = 1.0$ will provide the analytical solution for nonadsorbing (conservative) solutes. For utilization of numerical approximation solutions to Equation 14, the lower boundary condition (Equation 18 above) can be modified to Equation 19 (where L is the length of the column). Neither Equation 18 nor Equation 19 is exact for laboratory

$$\frac{\partial C}{\partial x} = 0.0 \quad x = L \quad (19)$$

or field conditions. However, the errors introduced by these assumed boundary conditions are similar and minimal under typical conditions (Miller, 1984).

Freundlich equilibrium adsorption expression

In the case where the adsorption isotherm is nonlinear, it is necessary to utilize a nonlinear equilibrium adsorption expression. Figure 3 demonstrates isotherms plotted for one set of data and two subsets of the same data. This figure points out the danger of extrapolating data beyond the experimental range from which the data were collected. Individual plots for the two subsets of the data can appear to be linear while when the two subsets are combined it becomes apparent that the data is nonlinear. Extrapolating the linear results from the lower range to the higher concentrations would have resulted in higher values of q predicted than would actually occur. This would result in the prediction that the soil would have a greater adsorptive capacity for the pesticide than it actually does. Thus, the pesticide would appear down gradient sooner than predicted. Rao and Davidson (1979) observed this when attempting to extrapolate information from pesticide adsorption at the $\mu\text{g/L}$ range to the mg/L range. Equilibrium studies at the higher concentrations resulted in nonlinear isotherms with Freundlich exponents in the range of 0.75 to 0.92 while previous work at the lower concentrations had indicated linear adsorption. Modeling efforts using linear equilibrium parameters predicted a greater lag in the appearance of the pesticide than observed. Utilizing the Freundlich nonlinear

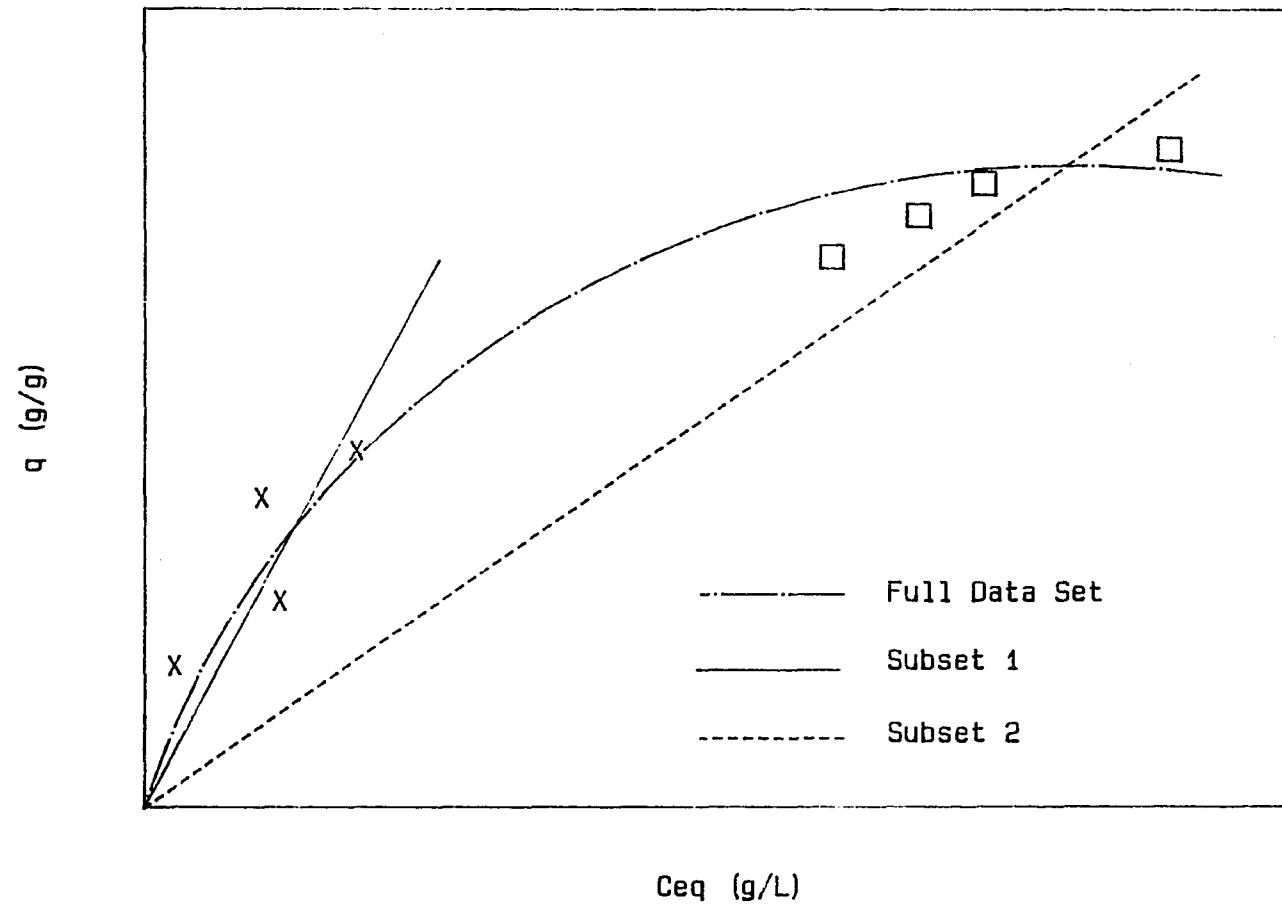


Figure 3: Linear versus nonlinear isotherm

adsorption expression in the modeling resulted in improved predictive capabilities.

The Freundlich equilibrium adsorption expression is the most commonly utilized nonlinear equilibrium adsorption expression for organics and soils (Karickhoff et al., 1979; Rao and Davidson, 1980; Karickhoff, 1984). The Langmuir adsorption expression has found greater utilization for electrolytes and soils (e.g., nutrients, metals) (Harter and Baker, 1977; Veith and Sposito, 1977; Sposito, 1984; Brown and Combs, 1985). The Freundlich expression is shown in Equation 20. It is observed that when the Freundlich exponent (N) is equal to 1.0 that Equation 20 is the same as Equation 9 above with K_{fr} the same as K_p . The Freundlich expression requires the determination of two parameters (K_{fr} and N). These parameters are typically determined by plotting q versus C_e on log-log paper. Equation 21 shows the log form of the Freundlich

$$q = K_{fr} C_e^N \quad (20)$$

$$\log q = \log K_{fr} + N \log C_e \quad (21)$$

where: K_{fr} = Freundlich partition coefficient $((L^3/M)^N)$
 N = Freundlich exponent

expression. The slope of the log-log plot of q versus C_e is N and the value of q at $C_e = 1.0$ ($\log C_e = 0.0$) is K_{fr} .

Incorporation of this adsorption expression into the governing partial differential equation (Equation 1) requires an expression for the $\partial q/\partial t$ term. For the Freundlich isotherm this expression is as shown in

Equation 22. Making use of Equation 10 for $\partial q/\partial t$, substituting Equation 22 into Equation 1 and consolidating the $\partial C/\partial t$ terms on the left hand side results in Equation 23. The terms inside the bracket on the left

$$\frac{\partial q}{\partial t} = N K_{fr} C_e^{N-1} \frac{\partial C}{\partial t} \quad (22)$$

$$\left[1 + \frac{\rho_s(1-\eta)}{\eta} N K_{fr} C_e^{N-1} \right] \frac{\partial C}{\partial t} = D_x \frac{\partial^2 C}{\partial x^2} - v_x \frac{\partial C}{\partial x} \quad (23)$$

hand side of Equation 23 are not constant, C_e is specific to the given situation. It may become necessary to utilize numerical approximation solution techniques for this governing equation.

Other equilibrium adsorption expressions

Other nonlinear equilibrium adsorption expressions besides the Freundlich expression have seen use by researchers. The Langmuir, BET and Gibbs adsorption models are examples of other nonlinear adsorption models utilized by researchers (Bailey and White, 1970). The Langmuir model, and variations thereof, have found widespread utilization in considering the transport of electrolytes (e.g., nutrients, metals) in soils (Harter and Baker, 1977; Veith and Sposito, 1977; Brown and Combs, 1985). These equilibrium adsorption models were not utilized during this study.

Estimating adsorption of pesticides on soils

Adsorption isotherms are determined in the laboratory by using a series of reactors with varying ratios of soil mass to solvent chemical concentration and shaking until equilibrium adsorption is known to exist (often 24 hours is used). The equilibrium pesticide concentration in the liquid is determined for each reactor and the pesticide adsorbed to the soil is calculated by mass balance. Each reactor produces a point on the isotherm (plot of q versus C_e). Figure 2 shows an example of a linear adsorption isotherm.

Due to the time and expense required to determine equilibrium adsorption parameters for all possible combinations of soils and pesticides, much research has been conducted investigating relationships capable of predicting the linear adsorption coefficients based on readily available or easily obtainable parameters. For nonionic pesticides and soils, the main predictive parameters isolated are the fraction organic carbon content (f_{oc}) of the soil and the octanol-water partition coefficient (K_{ow}) for the pesticide (Bailey and White, 1970; Karickhoff et al., 1979; Rao and Davidson, 1980; Brown and Flagg, 1981).

Bailey and White (1970) attribute the importance of the soil organic carbon content in the level of pesticide adsorption to the fact that the organic matter of the soil has the highest combined cation exchange capacity and surface area of the soil size separates. Hamaker and Thompson (1972) list typical values of f_{oc} for surface soils as high as 0.08 while alluvial sand aquifers have been reported to have f_{oc} values as low as 0.0002 (Schwarzenbach and Westall, 1981; Abdul, Gibson and Rai,

1986; Bouchard et al., 1988).

The octanol-water partition coefficient is a parameter which describes the partitioning of a pesticide between a polar phase (water) and a relatively nonpolar phase (1-octanol). The octanol-water partitioning is likened to the partitioning (solvent motivated adsorption) of a pesticide between the groundwater and the organic carbon content of the soil. One of the advantages of the use of the octanol-water partition coefficient is that this parameter is widely available for many compounds (Leo et al., 1971; Hansch and Leo, 1979; Rao and Davidson, 1980; Lyman, 1982). Table 1 shows a partial listing of K_{ow} values compiled by Rao and Davidson (1980). In the event that measured K_{ow} values are not available for a given pesticide, Lyman (1982) has summarized estimation methods for predicting K_{ow} values for a chemical based on either fragment constants or other solvent/water partition coefficients for the chemical. Some researchers have attempted to correlate the adsorption of a pesticide to its aqueous solubility. Karickhoff et al. (1979) state that the octanol-water partitioning more closely parallels the pesticide adsorption in the soil system and thus proves to be a better estimator than the aqueous solubility.

Normalizing of linear partition coefficients (K_p) by the fraction organic carbon content of the soil has been shown to reduce the variations in the resulting partition coefficient (K_{oc}). This normalization is demonstrated in Equation 24. The merit of this

$$K_{oc} = K_p / f_{oc} \quad (24)$$

Table 1. Log K_{ow} values for various pesticides^a

Pesticide	Log K_{ow}
<u>Herbicide:</u>	
Alachlor	2.64
Atrazine	2.33
Diuron	2.81
Simazine	1.94
2,4-D	2.64
2,4,5-T	0.85
<u>Insecticide:</u>	
Aldicarb	0.70
Chlordane	3.32
DDT	5.57
Dieldrin	3.69
Lindane	2.81

^aTaken from Rao and Davidson (1980).

normalization has been supported by research in which the organic content of the soil was removed and significant decreases in the level of adsorption was realized (Weber et al., 1983; Miller, 1984). Karickhoff et al. (1979) investigated the adsorption of chemicals from two chemical classes (PAH and chlorinated hydrocarbons) and three natural river and lake sediments. Linear adsorption was observed and the expression shown in Equation 25 was proposed. Brown and Flagg (1981) investigated the adsorption of chemicals from the triazine and dinitroaniline families with natural lake sediments and observed linear adsorption isotherms. Combining their data with that of Karickhoff et al. (1979), Brown and Flagg (1981) developed the expression shown in Equation 26. Other

$$\log K_{OC} = 1.00 \log K_{OW} - 0.21 \quad (25)$$

$$\log K_{OC} = 0.937 \log K_{OW} - 0.006 \quad (26)$$

researchers have successfully applied these relationships to predict measured linear adsorption coefficients using alluvial aquifer materials with low organic content (Schwarzenbach and Westall, 1981) and pesticides (Miller, 1984).

From the above relationships, given the K_{OW} value for a pesticide and the f_{OC} value of the soil, an estimate of the K_p value and thus the adsorption of the pesticide on the soil can be made. While the ease of obtaining K_{OW} and f_{OC} values makes the use of these expressions attractive, caution must be taken in applying them. Banerjee et al. (1985) found that at f_{OC} values less than 0.002 or clay content to f_{OC}

ratios greater than 60 the mineral surfaces (clays) may become the dominant soil fraction. The cation exchange capacity may become dominant when considering ionic or polar pesticides, such as diquat or paraquat (Bailey and White, 1970). It is thus important to understand the theory behind the preceding relationships and apply them only when the situation justifies their use.

Desorption and hysteresis of desorption

Often the mentality seems to exist that once the pesticide is adsorbed that it no longer poses a threat to the groundwater. However, pesticide adsorption to soil organic matter has been observed to be reversible. The reversibility of pesticide adsorption indicates physical adsorption (physisorption) as opposed to chemical adsorption (chemisorption) of the pesticide to the soil with physical adsorption having lower energies of attachment. When the pesticide concentration in the soil pore water decreases (as the pesticide front passes), desorption of the pesticide from the solid phase to the pore water phase occurs (the free energy gradient is from the soil to the groundwater). Modeling efforts often assume that desorption is completely reversible (the desorption curve is symmetrical to the adsorption curve). Several researchers have observed asymmetry (hysteresis) in the desorption curve (Swanson and Dutt, 1973). Swanson and Dutt (1973) found that the desorption data could be described by the Freundlich relationship with the value of N_{ads}/N_{des} being 2.3.

Hysteresis of desorption can be evaluated in laboratory batch

studies in conjunction with conducting adsorption isotherm studies. Upon attainment of equilibrium adsorption in a reactor, the supernatant of each reactor is removed and replaced with pesticide free water and shaken until equilibrium desorption occurs. This process is repeated for each reactor resulting in a series of desorption data points for each original adsorption data point. Thus, each reactor from the adsorption study results in a desorption isotherm. Figure 4 shows an example of an adsorption isotherm and three desorption isotherms (indicating hysteresis of desorption). The triangles in Figure 4 correspond to the data points (reactors) that are used to establish the adsorption isotherm. Each triangle is the starting point of a desorption isotherm. The squares along each desorption isotherm correspond to desorption data points which are determined as outlined above. If desorption was completely reversible (no hysteresis of desorption), the desorption data points would fall on the adsorption isotherm.

The effect of hysteresis of desorption on a breakthrough curve is shown in Figure 5. Figure 5 shows one graph in which hysteresis of desorption is modeled and one graph in which desorption is considered as symmetrical. The graphs demonstrate the loss of symmetry when including hysteresis of desorption. Much remains to be learned about the nature, kinetics and modeling of desorption and its influence on the transport of pesticides in groundwater. It is apparent that this phenomena will greatly affect the time and volume of groundwater necessary for "pump and treat" technologies and for determining the time necessary for a slug of pesticides to pass a given point (e.g., a well).

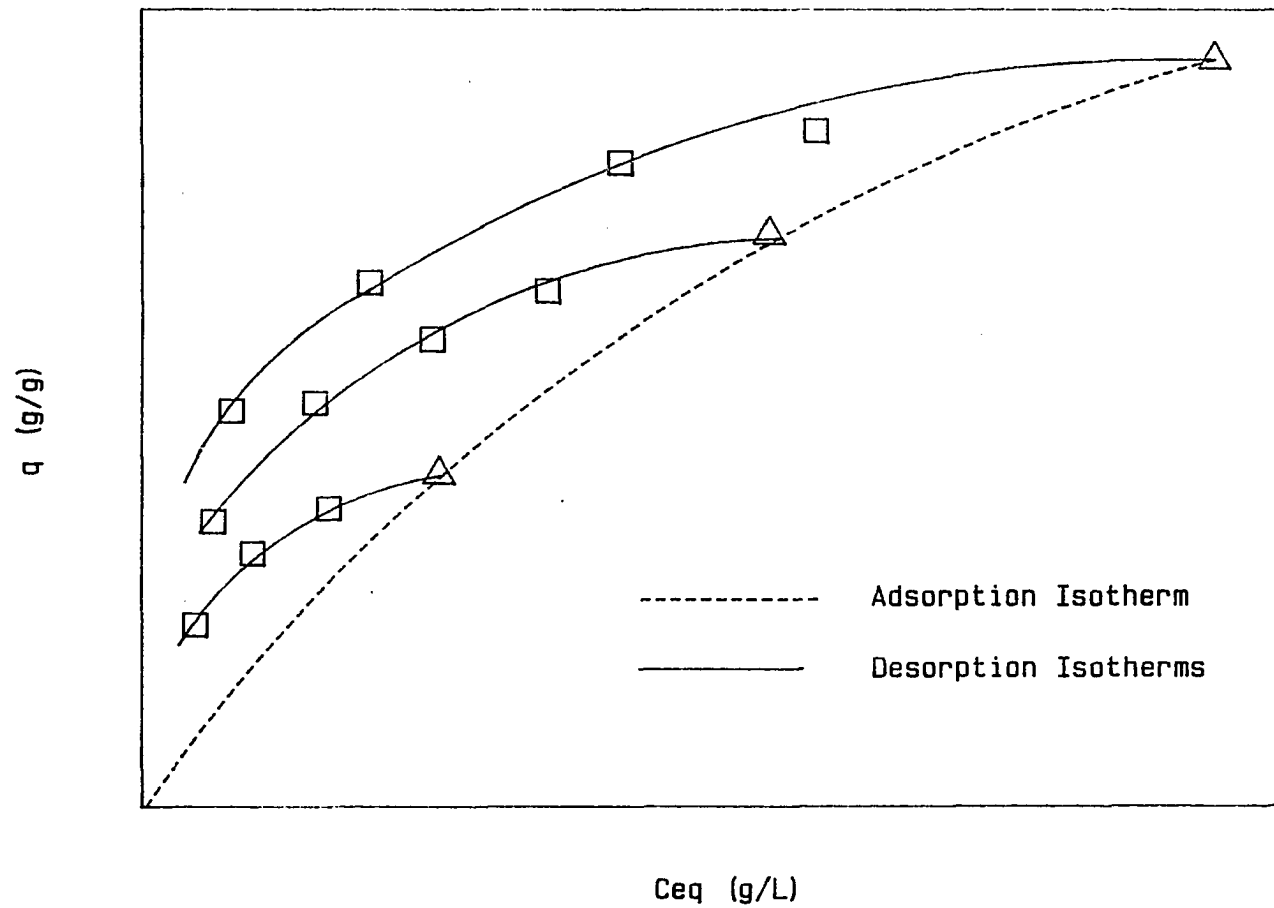


Figure 4: Hysteresis of desorption - isotherms

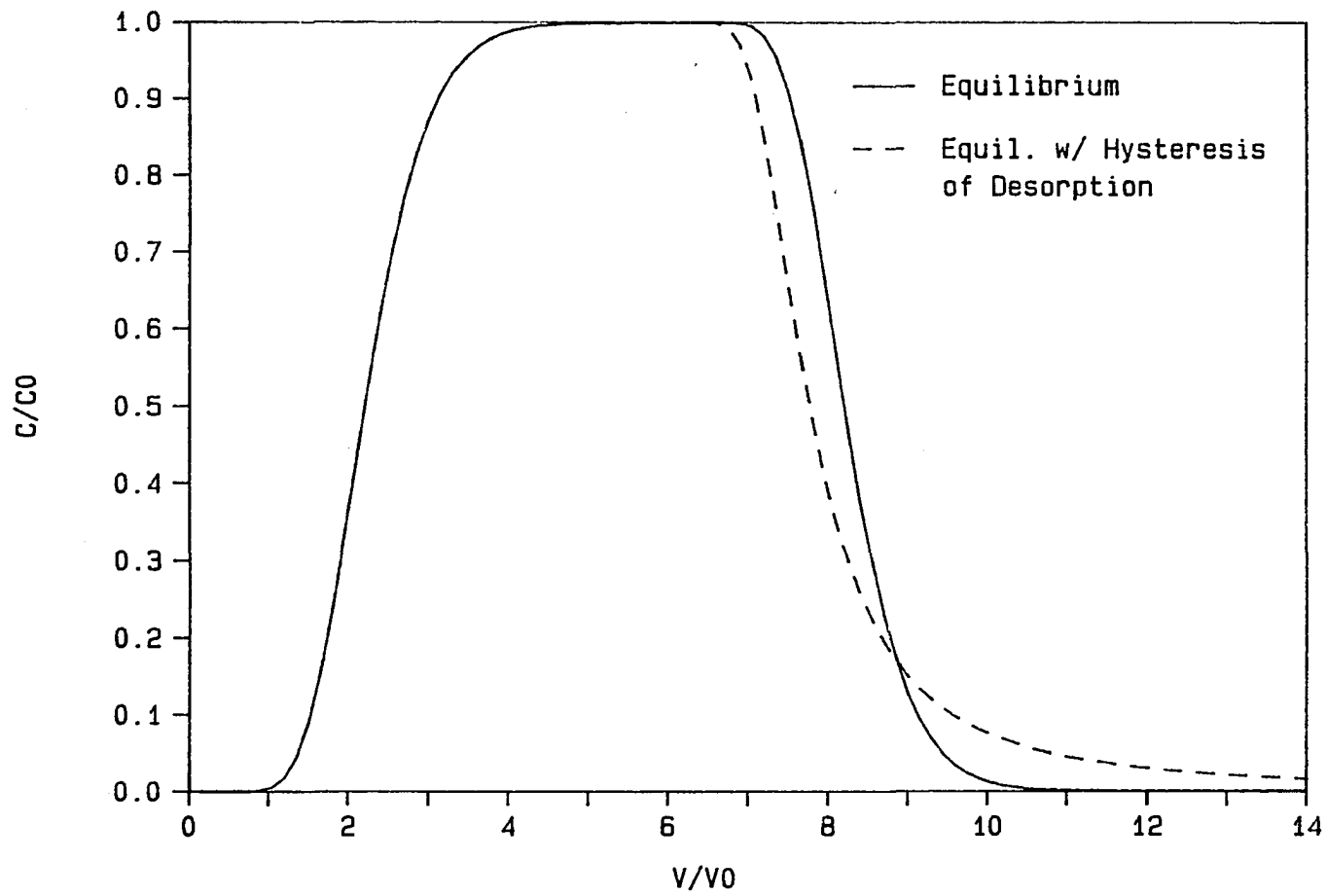


Figure 5: Hysteresis of desorption - breakthrough curves

Nonequilibrium Adsorption and Desorption Expressions

Early research showed that equilibrium adsorption expressions were not always able to predict accurately the results observed in column studies with the greatest deviations occurring at higher pore water velocities (Kay and Elrick, 1967; van Genuchten et al., 1974; Valocchi, 1985). In attempting to predict the nonequilibrium adsorption experimentally observed, it is necessary to have a conceptual framework of the adsorption process and to isolate the rate limiting step(s). The adsorption process is considered to consist of three basic steps (Weber, 1972; Benefield et al., 1982). First, the adsorbate must diffuse from the aqueous phase (bulk liquid) to the soil or aggregate surface (film transport). Second, the adsorbate must diffuse through the intra-aggregate or intraparticle pores to the adsorption site (intraparticle diffusion). Third, the adsorbate undergoes the actual adsorption step (adsorption). This conceptualization is demonstrated in Figure 6. Rate limitations by the film transport and/or the intraparticle diffusion steps would be classified as physical nonequilibrium while rate limitations of the adsorption step would be classified as chemical nonequilibrium. Figure 7 illustrates the difference in the shapes of breakthrough curves for equilibrium and nonequilibrium conditions.

Chemical versus physical nonequilibrium

The first attempts by researchers to describe nonequilibrium adsorption during solute transport assumed the adsorption step was rate

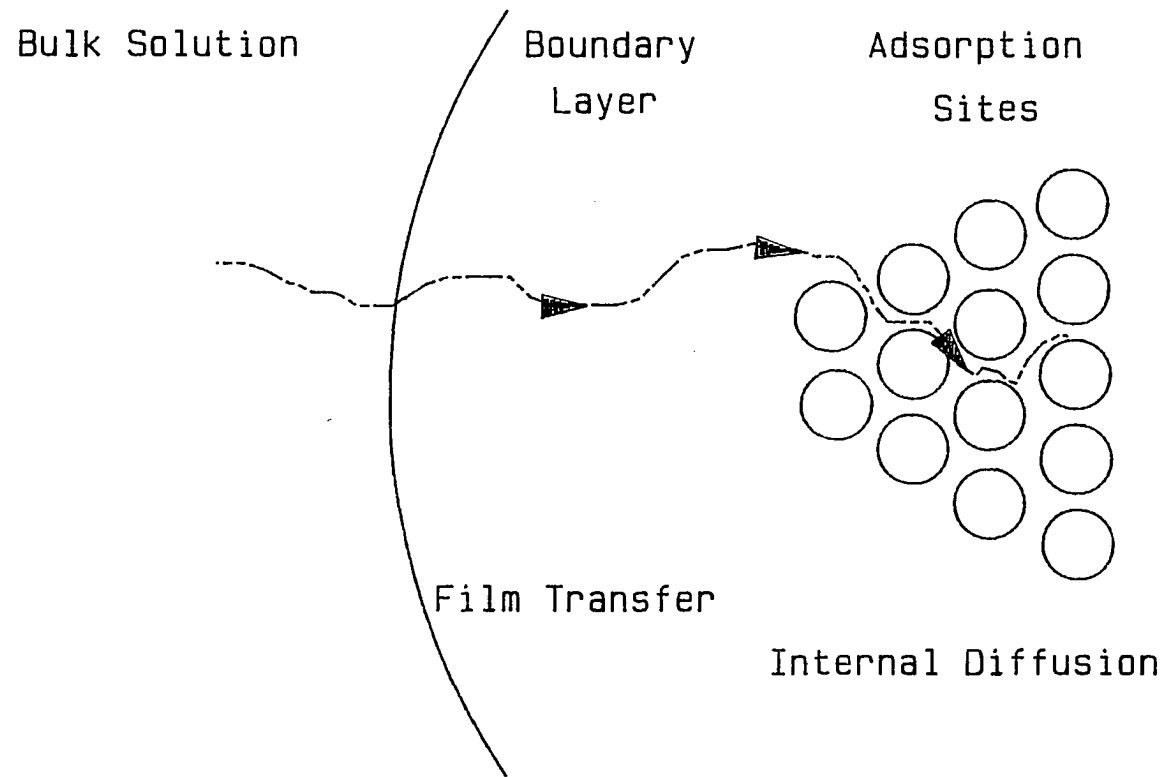


Figure 6: Adsorption conceptualization

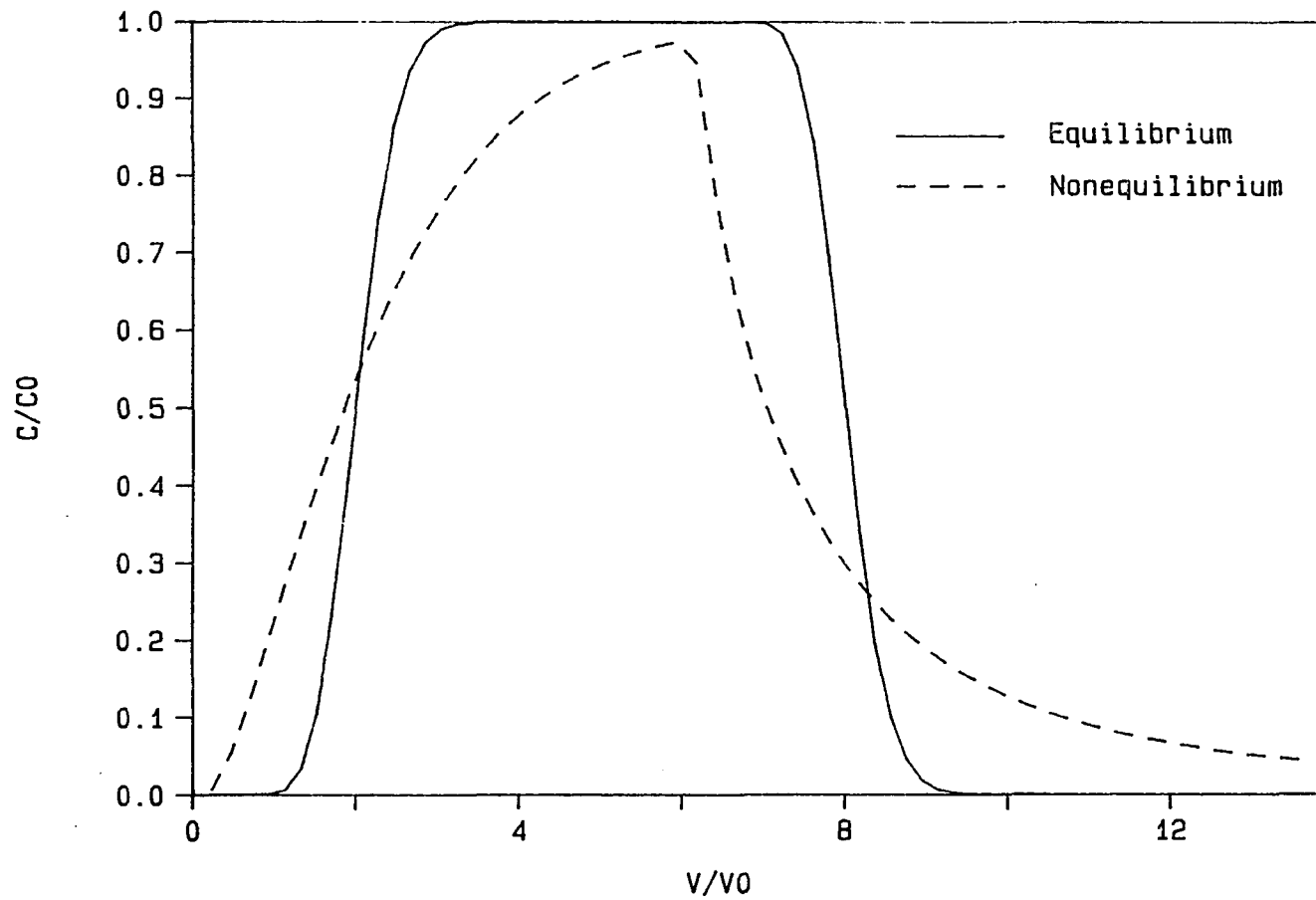


Figure 7: Equilibrium versus nonequilibrium breakthrough curves

limiting. It was felt that the higher pore water velocities did not allow sufficient contact time (residence time) for the adsorption to reach equilibrium. A later hypothesis was that the actual chemical adsorption step was not limiting but that diffusion of the pesticide from the aqueous phase (bulk liquid) to the final adsorption site becomes limiting at higher pore water velocities (physical nonequilibrium). While fundamentally physical and chemical nonequilibrium approaches are different, some researchers have argued that it is difficult to distinguish between the two processes by evaluating experimental data or by modeling attempts (van Genuchten, 1981; Nkedi-Kizza et al., 1984; Skopp, 1986).

A complete review of the chemical and physical nonequilibrium expressions that have been proposed is beyond the scope of this effort. The interested reader is directed to other references for nonequilibrium adsorption expressions not covered (Travis and Etnier, 1981; Rao and Jessup, 1983). The goal here will be to briefly review some of the nonequilibrium adsorption expressions which have been proposed in an effort to establish the types of modeling approaches which have been utilized. Specific details of experimental conditions for column studies and solution techniques for the models will not be covered. The reader is directed to the original references for these details.

Chemical nonequilibrium expressions

Davidson and McDougal (1973) proposed the use of a first order kinetic adsorption expression as shown in Equation 7. This expression is

first order with respect to both C and q with rate coefficients for adsorption and desorption (k_s and k_d , respectively). These rate coefficients were determined by the authors by calibrating (fitting) the model with the observed data. This first order expression reduces to the linear adsorption expression at equilibrium ($\partial q/\partial t = 0.0$) and thus assumes that the adsorption is linear and completely reversible ($N_{ads} = N_{des} = 1.0$). Pesticides evaluated in the study were fluometuron, picloram and prometryne and a Norge loam soil was utilized. Earlier appearance of the pesticide breakthrough curves was observed with increasing pore water velocities (0.57 to 5.6 cm/hr). The use of the kinetic adsorption expression was able to predict the leftward shift of the breakthrough curve but did not predict the shape of the breakthrough curve.

Hornsby and Davidson (1973) utilized a kinetic adsorption expression which was first order with respect to q but N^{th} order with respect to C . This expression, as shown in Equation 27, simplifies to the Freundlich expression at equilibrium. The expression was used in the model in

$$\frac{\partial q}{\partial t} = k_s \frac{\eta}{\rho_s(1-\eta)} C^N - k_d q \quad (27)$$

such a way that hysteresis of desorption ($N_{des} \neq N_{ads}$) could be modeled. The pesticide fluometuron, a Norge loam soil and pore water velocities of 0.6 and 5.5 cm/hr were utilized in this study. The authors found the use of asymmetric desorption aided in the modeling of the tailing elution curve. The authors concluded that, while the kinetic relationship did

assist in describing the nonequilibrium situation, the fit was not significantly better than the equilibrium model.

van Genuchten et al. (1974) evaluated the ability of three different adsorption models (two kinetic and one equilibrium) to predict the movement of picloram through a Norge loam soil. The equilibrium model utilized was the Freundlich expression. The kinetic adsorption expressions utilized by the authors included Equation 27 above and Equation 28 after Lindstrom et al. (1971). The model by Lindstrom et al. (1971) includes the parameter b which is the surface stress coefficient ($\text{g}/\mu\text{g}$) as described by Fava and Eyring (1956). Five

$$\frac{\partial q}{\partial t} = [k_d \exp (b q)] \left[\frac{k_s}{k_d} \exp (-2 b q) \frac{\eta C}{(1-\eta)\rho_s} - q \right] \quad (28)$$

different pore water velocities were investigated in the range of 0.6 to 6.0 cm/hr. The inclusion of hysteresis of desorption improved the predictive capabilities of the models. Nonequilibrium breakthrough was evidenced with increasing pore water velocities. Rate parameters determined by fitting breakthrough curves at a lower pore water velocity were not able to predict the breakthrough curves experienced at higher pore water velocities. Since the adsorption rate constants should be independent of the pore water velocity, this lack of predictive ability led the authors to suspect the validity of the adsorption expressions utilized. Sensitivity analyses were conducted for the kinetic models using a wide range of adsorption rate constants and the resulting breakthrough curves were compared to the experimentally observed curves.

It was apparent that the kinetic models alone were not sufficient to predict the shapes of breakthrough curves experimentally observed. This led the authors to suspect diffusion limited adsorption sites as the cause for the nonequilibrium breakthrough curves observed.

Cameron and Klute (1977) discussed the use of a combined equilibrium and kinetic adsorption (two site or bicontinuum) model. This approach was justified by the authors based on heterogeneities present in the soil. The authors state that quite different processes, such as rapid adsorption on the soil organic matter (equilibrium) and slow adsorption on mineral surfaces (kinetic), may be involved in the overall adsorption process. The authors state that diffusion limited sites could fall into the kinetic (physical) site category. Atrazine breakthrough data collected by others were utilized and it was found that the two site model provided good predictive capabilities. Use of a single site model (equilibrium or kinetic) for the same data did not provide good predictive capabilities. The authors state that one disadvantage of this approach is the need to fit the parameters to the data. It would be preferable to be able to determine the parameters separate from the experimental data they are to describe.

Rao et al. (1979) investigated the use of two site (bicontinuum) models to describe nonequilibrium breakthrough curves. Two conceptual models using the bicontinuum concept were investigated in this study. In both models one of the soil sites was assumed to experience instantaneous nonlinear equilibrium while the second site was assumed to be described by nonlinear reversible kinetics (chemical) in one conceptual model and

by diffusion controlled kinetics (physical) in the other model. The physical nonequilibrium bicontinuum model will be discussed in the next section. The nonlinear reversible kinetic expression utilized is as shown in Equation 27 above and the equilibrium expression utilized was the Freundlich expression. Some fraction of the adsorption sites (F) was assumed to participate in equilibrium adsorption while the remainder of the sites ($1-F$) was assumed to participate in kinetic (physical or chemical) adsorption. Data from Rao and Davidson (1979) for atrazine and 2,4-D and three soils were utilized for evaluating the models. Two concentration levels for each pesticide were evaluated (50 and 5000 mg/L for 2,4-D and 5 and 50 mg/L for the atrazine). Parameters determined by fitting the model to the breakthrough data at the lower concentration were used to predict the results at the higher concentrations with good success. However, the rate parameters determined by curve fitting did not agree well with values determined experimentally by others. This discrepancy resulted in uncertainty as to the mechanistic accuracy of this model.

Physical nonequilibrium expressions

As researchers began to realize that chemical nonequilibrium expressions were not able to describe and/or predict the experimentally observed data, the utility of physical nonequilibrium expressions received increased attention. Davidson and McDougal (1973), Hornsby and Davidson (1973) and van Genuchten et al. (1974) are examples of early research efforts that found chemical nonequilibrium expressions to be

inadequate and suggested the investigation of physical nonequilibrium expressions. The fact that researchers often observed pesticide adsorption to be virtually complete in batch kinetic studies in less than one hour (Leenher and Alrichs, 1971) also supported the conclusion that the adsorption step was not rate limiting.

Skopp and Warrick (1974) discussed a two-phase model for describing solute transport of sorptive solutes in soils. The two phases considered by the authors were the mobile phase (bulk liquid) and the stationary phase (boundary layer of pores). Transport in the mobile phase was assumed to occur by advection and dispersion while transport through the stationary phase was assumed to be due to diffusion (advection was assumed to be negligible in this phase). It was assumed that the diffusion across the stationary phase to the adsorption sites is the rate limiting step in the adsorption process.

van Genuchten and Wierenga (1976) developed a model to describe the mass transfer of solute in sorbing porous media. The model development involved dividing the soil matrix into five regions: (1) air spaces, (2) mobile (dynamic) water located in the larger (inter-aggregate) pores, (3) immobile (stagnant) water located inside aggregates and at the contact points of aggregates and/or particles, (4) dynamic soil, located sufficiently close to the mobile water phase for assumed equilibrium to exist between solute in mobile phase and the soil phase and (5) stagnant soil region, where adsorption by soil is diffusion limited through immobile liquid. Equation 29 was developed from these considerations. In Equation 29, the subscript m refers to mobile phase and im refers to

immobile phase. The mass transfer between the mobile and immobile phases was considered to be first order, as shown in Equation 30. Sensitivity analyses were conducted for this model with a range in shapes of predicted breakthrough curves observed. These predicted breakthrough

$$\begin{aligned} \theta_m \frac{\partial C_m}{\partial t} + \theta_{im} \frac{\partial C_{im}}{\partial t} + f \rho_b \frac{\partial q_m}{\partial t} + (1 - f) \rho_b \frac{\partial q_{im}}{\partial t} \\ = \theta_m D_x \frac{\partial^2 C_m}{\partial x^2} - \theta_m v_{x,m} \frac{\partial C_m}{\partial x} \end{aligned} \quad (29)$$

$$\theta_{im} \frac{\partial C_{im}}{\partial t} + (1 - f) \rho_b \frac{\partial q_{im}}{\partial t} = \alpha' (C_m - C_{im}) \quad (30)$$

where: θ_m = mobile phase water content (L^3/L^3)
 θ_{im} = immobile phase water content (L^3/L^3)
 f = fraction adsorption sites in dynamic region
 ρ_b = bulk soil density (M/L^3)
 α' = first order mass transfer coefficient (1/T)

curves include shapes similar to those experimentally observed but which previous modeling attempts had been unsuccessful in predicting. Parker and van Genuchten (1984) produced a bulletin discussing the use of this model (including later additions).

van Genuchten et al. (1977) utilized the model of van Genuchten and Wierenga (1976) to model the transport of 2,4,5-T through a clay loam soil. Pore water velocities evaluated ranged from 0.17 to 0.71 cm/hr. Parameters were fitted to the data with good agreement between observed and modeled results. It was found that the inclusion of intra-aggregate

diffusion was more significant in fitting the data than inclusion of desorption hysteresis. However, no attempts were made to utilize parameters developed under one set of conditions to predict results for a separate set of conditions (the validity of the fitted parameters was not established).

Rao et al. (1976) discussed the use of a capillary bundle model for describing solute transport in an aggregated soil. The model enabled the use of several classes of pore sizes (a bundle of pores was treated as different sized capillary tubes) and thus allowed the use of pore water velocity distributions rather than necessitating the use of an average pore water velocity. The pore size distribution was determined from soil water characteristic data. The breakthrough curves predicted with the capillary bundle model were extremely skewed and did not agree well with observed breakthrough data. The variations in the observed and predicted results were attributed to the failure of the capillary bundle model to include mixing of the solute between adjacent flow paths. The authors stated that the prediction of the dependence of solute transport on soil pore geometry necessitates a method for describing the pore accessibility and interconnectedness of pore sequences.

Rao et al. (1979) investigated the use of two-site (bicontinuum) models to describe nonequilibrium breakthrough curves. One of the sites was considered to experience equilibrium adsorption and the other site was considered to experience nonequilibrium (physical or chemical) adsorption. The chemical nonequilibrium case was discussed above. The physical nonequilibrium condition suggests that diffusion limited sites

exist. Diffusion from the mobile phase to the immobile phase was assumed to be first order (see Equation 30 above). In this case, the bicontinuum model is conceptually the same as the two phase model of van Genuchten and Wierenga (1976). Data from Rao and Davidson (1979) for atrazine and 2,4-D and three soils were utilized for evaluating the model. Two concentration levels for each pesticide were evaluated (50 and 5000 mg/L for 2,4-D and 5 and 50 mg/L for the atrazine). Parameters determined by fitting the model to the breakthrough data at the lower concentration were used to predict the results at the higher concentrations. Although the location of the breakthrough curve was predicted with fairly good success, the model overestimated the tailing (slow approach to C/C_0 of 0.0) of the breakthrough curve at the higher concentration. Fitting the model to the higher concentration data resulted in parameters of questionable value. This led the authors to question the applicability of the equilibrium - first order diffusion nonequilibrium bicontinuum model to the systems investigated.

De Smedt and Wierenga (1984) discussed the solute transport of nonadsorbed $^{35}\text{Cl}^-$ through a column of nonaggregated glass beads. The beads ranged in size from 74 to 125 μm . Unsaturated conditions in the column resulted in early breakthrough and tailing, much as experienced under saturated aggregated conditions. The breakthrough curves could be modeled by fitting the dispersion coefficient to the data, but this required the use of a dispersion coefficient twenty times greater than observed under saturated conditions at a similar pore water velocity. It was possible to use dispersion coefficients from saturated conditions and

use a mobile - immobile model with first order diffusion between the two phases to model the observed breakthrough data successfully under unsaturated nonaggregated conditions.

Miller (1984) proposed a physical nonequilibrium model which incorporated film transport and intraparticle diffusion (see Figure 6 for conceptualization) as the source of the nonequilibrium breakthrough. This effort differed from ones previously discussed in that diffusion was considered to be Fickian rather than first order. This approach has been labeled the Fickian physical nonequilibrium model. This model was developed using mass transfer and mass balance concepts and resulted in the relationships shown in Equations 31 and 32. Aquifer sand materials

$$\frac{\partial q}{\partial t} = D_s \frac{1}{r^2} \frac{\partial}{\partial r} \left[r^2 \frac{\partial q}{\partial r} \right] \quad (31)$$

$$k_f (C - C_s) = D_s \rho_s \frac{\partial q}{\partial r} \quad @r = R \quad (32)$$

where: D_s = intraparticle diffusion coefficient (L^2/T)
 r = radial dimension for particle (L)
 k_f = external film transfer coefficient (L/T)
 C_s = equilibrium pesticide concentration at exterior of particle (M/L^3)
 R = radius of particle (L)

and lindane were utilized to investigate this modeling approach with the necessary model parameters determined in completely mixed batch reactors. Good predictive capabilities for the laboratory column studies were observed using parameters determined in a completely mixed batch reactor.

Crittenden et al. (1986) developed a Fickian physical nonequilibrium model similar to that of Miller (1984). The model of Crittenden et al. (1986) was based on the presence of aggregates (or diffusion limited regions in the absence of physical aggregates) in the soil which caused the nonequilibrium breakthrough curves (see Figure 6 for conceptualization). This model included intraaggregate diffusion both in the pore space and along the pore surfaces. The authors referred to the model as the dispersed flow, pore and surface diffusion (DFSPDM) model. The authors conducted sensitivity analyses on the model to determine the relative significance of dispersion, film transport and intraparticle (intraaggregate) diffusion on the shape of the breakthrough curve. The authors concluded that under most conditions the intraparticle diffusion would be the limiting case. The authors also discussed techniques for determining the model parameters separate from the column data by estimation techniques.

Hutzler et al. (1986) utilized the model of Crittenden et al. (1986) to predict the movement of TCE and bromoform in a sandy loam. The model was calibrated to the data by fitting the aggregate radii. However, the model was not able to predict the leftward shift of the breakthrough curve or the increased asymmetry when the pore water velocity was increased from 12 to 36 cm/hr. Hutzler et al. (1986) concluded that, while the DFSPDM appeared to be an improved mechanistic model, their work suggested that an additional kinetic mechanism should be included in the model.

Roberts et al. (1987) utilized the model of Crittenden et al. (1986)

in an attempt to predict the data of Nkedi-Kizza et al. (1982). Estimation techniques were utilized for predicting the necessary parameters separate from the column data with good predictive results realized. The authors concluded that hydrodynamic dispersion governed the nonequilibrium breakthrough curves at low velocities and that internal pore diffusion dominated at higher pore water velocities (3 to 143 cm/hr). The external mass transfer was concluded to play a minor role under all the experimental conditions investigated.

It is not necessary for a soil to be aggregated for diffusion limited physical nonequilibrium to be experienced. Bouchard et al. (1988) designed their column experiments to minimize aggregation effects on solute transport. Investigating the movement of atrazine, diuron and hexazinone in low organic carbon aquifer materials, the authors found the level of nonequilibrium to increase with increasing organic carbon content of the soil. The adsorption was determined to be linear for the solutes studied in the concentration ranges investigated eliminating nonlinear isotherms as the cause for the nonequilibrium breakthrough curves observed. It was thus concluded that the nonequilibrium was caused by diffusion limitations into the organic carbon matrix of the soils investigated. Lee et al. (1988) came to similar conclusions concerning nonequilibrium breakthrough curves observed while investigating the movement of TCE and p-xylene in two sand aquifer materials. Bouchard et al. (1988) noted a leftward shift in the breakthrough curves for atrazine and diuron with increasing pore water velocities (2.4, 8.1 and 22.6 cm/hr).

Equivalence of nonequilibrium expressions

While physical and chemical nonequilibrium expressions are mechanistically different, researchers have questioned the ability to distinguish between these processes based on experimental data or modeling efforts.

Nkedi-Kizza et al. (1984) discussed the equivalence of two conceptual models. The models investigated were both two site (bicontinuum) models with both models having instantaneous sorption on one of the sites and adsorption on the other site being either physical or chemical nonequilibrium. The equilibrium expression utilized was the linear reversible model. The physical nonequilibrium model used incorporated first order diffusion limitations and the chemical nonequilibrium model used incorporated first order reversible kinetics. Introduction of dimensionless variables into each model resulted in exactly the same dimensionless form of the equations. Thus, both models proved equally capable of describing the experimental results. The authors concluded that it is not possible from the breakthrough curves alone to determine which conceptual model is accurate. Skopp (1986) further supported this conclusion in his discussion of time dependent chemical processes in soils.

Valocchi (1985) evaluated the time moments for various equilibrium and nonequilibrium solute transport models. The nonequilibrium models investigated included the diffusion (Fickian) physical nonequilibrium, the first order physical nonequilibrium and the first order linear

chemical nonequilibrium. The temporal moments serve as indicators of the shape of the breakthrough curves. The first, second and third moments describe the mean breakthrough time (retardation), the degree of spreading (dispersion) and the degree of nonequilibrium (asymmetry), respectively (Lee et al., 1988). Valocchi (1985) showed that the first moment for all models had the same dimensionless expression. Thus, all models predict the same average time of appearance of the breakthrough curve. It is the spreading of the breakthrough curve about the average time of appearance that varies from model to model. By comparing the second moments for equilibrium and nonequilibrium it was possible to establish relative criteria for when equilibrium conditions would be satisfied and also when chemical and physical nonequilibrium models would be equivalent.

Parker and Valocchi (1986) further discussed the utilization of time moment analyses for solute transport studies. The authors stated that the nonequilibrium shapes of breakthrough curves observed could be attributed to hydrodynamic spreading of the breakthrough front and spreading of the front due to diffusion limitations. The use of an effective dispersion coefficient was proposed. This effective dispersion coefficient would account for all the spreading (hydrodynamic and physical) about the mean time of appearance of the solute. The mean time of appearance would be established using an equilibrium adsorption expression and the spreading would be accounted for by using an effective dispersion coefficient. This would greatly simplify the solution techniques for the resulting equilibrium model versus the models for

nonequilibrium solute transport. Lee et al. (1988) found the technique of the effective dispersion coefficient to provide good results for the prediction of breakthrough curves using TCE and p-xylene in two sand aquifer materials.

Adsorption Studies with Atrazine and Alachlor

The purpose of this section is to review some of the results investigating the adsorption of the herbicides atrazine and alachlor (to be investigated in this study) on soils.

Batch results - atrazine

Hamaker and Thompson (1972) provided a review of adsorption studies with pesticides and soils. Data for atrazine included linear and Freundlich parameters. For a range of equilibrium atrazine concentrations of 0.7 to 12 mg/L and a range of f_{oc} values of 0.001 to 0.44, the K_p values ranged from 1 to 74 and the K_{oc} values ranged from 50 to 400 with an average K_{oc} value of 105 ± 3.3 . Table 2 summarizes the K_{oc} values from this and other studies. The Freundlich exponents (N) ranged in value from 0.52 to 0.98 with the lower values of N (increased nonlinearity) corresponding to the higher organic content soils (mucks).

Swanson and Dutt (1973) investigated the adsorption and desorption of atrazine on a sandy loam (Mohave) and a silty loam (Walla Walla) soil. The sandy loam soil had an f_{oc} value of 0.0026 and the silty loam had an f_{oc} value of 0.015. Atrazine was added to the batch reactors at concentrations of 5, 10, 15, 20 and 25 mg/L with equilibrium

Table 2. K_{oc} values for pesticides (atrazine and alachlor) and fluorescent dyes (rhodamine WT and fluorescein)

K_{oc}	Reference
<u>Atrazine:</u>	
105 ± 3.3	Hamaker and Thompson (1972)
80	Swanson and Dutt (1973)
122 ± 25	Rao and Davidson (1980)
216	Brown and Flagg (1981)
48 to 121	Bouchard and Wood (1988)
64 to 237	Bouchard et al. (1988)
<u>Alachlor:</u>	
191 ± 49	Peter and Weber (1985)
<u>Rhodamine WT</u>	
1000 to 1600	Trudgill (1987)
<u>Fluorescein</u>	
108	Omoti and Wild (1979)

concentrations ranging from 5 to 18 mg/L for the low f_{oc} soil (sandy loam) and 3 to 13 mg/L for the high f_{oc} soil (silty loam). The lower removals of the aqueous phase atrazine for the sandy loam as well as the greater q values indicate that less atrazine was adsorbed on the sandy loam than the silty loam. This would agree with the lower f_{oc} value for the sandy loam. The isotherm for the sandy loam was observed to be linear while the isotherm for the silty loam was observed to be nonlinear. The lesser adsorption realized for the lower f_{oc} soil and the smaller organic carbon content (and concomitant increase in adsorption site availability) would predict a higher probability for a linear adsorption isotherm. The K_p value for the sandy loam soil was 0.21 and the K_{fr} and N values for the silty loam soil were 2.61 and 0.85, respectively. The K_{oc} value for the sandy loam is calculated to be 80. Desorption isotherms were observed to be nonreversible. The Freundlich expression was shown to be capable of describing the nonreversible desorption with the $N_{ads}:N_{des}$ ratio being 2.3.

Rao and Davidson (1979) evaluated the adsorption of atrazine on three soils (silty clay loam, sandy loam and fine sand) ranging in f_{oc} values from 0.0056 to 0.039. Adsorption studies were conducted by varying the initial atrazine concentration in the adsorption reactor from zero to the solubility limit (33 mg/L). Linear and Freundlich expressions were utilized to describe the adsorption data. The average K_{oc} value for the soils was 121.8 ± 25 . The Freundlich exponent (N) ranged from 0.73 for the high f_{oc} soil to 1.04 for the low f_{oc} soil.

Brown and Flagg (1981) evaluated the adsorption of atrazine on the

bottom sediments of a pond ($f_{oc} = 0.0327$). The equilibrium concentration of atrazine in the batch reactors ranged from zero to 16 mg/L (one-half the aqueous solubility). The resulting K_{oc} value for the atrazine and the bottom sediment was 216.

Bouchard and Wood (1988) utilized column studies to investigate the adsorption of atrazine on three soils with f_{oc} values of 0.00033, 0.0026 and 0.0069. The K_{oc} values for the three soils and atrazine (determined from the retardation factors) were 48, 83 and 121, respectively. Bouchard et al. (1988) utilized batch studies for the same soils and atrazine concentrations not exceeding 12% of aqueous solubility (4 mg/L) and determined K_{oc} values of 237, 106 and 64, respectively.

Batch results - alachlor

Peter and Weber (1985) investigated the adsorption of alachlor on nine soils with organic contents ranging in f_{oc} values from 0.003 to 0.051. Equilibrium alachlor concentrations investigated in the batch studies were as high as 16 mg/L with the average K_{oc} value for the soils of 191 ± 49 .

Column results - atrazine

Elrick et al. (1966) investigated the transport of atrazine using column studies and a silt loam soil. The influent atrazine concentration utilized was 21.9 mg/L and the pore water velocity utilized was 0.64 cm/hr. Nonequilibrium breakthrough was observed and the authors attributed this to intra-aggregate adsorption sites or dead end pores.

Rao and Davidson (1979) have shown atrazine adsorption to be nonlinear in this concentration range and this could also account for the nonequilibrium shape of the breakthrough observed.

Swanson and Dutt (1973) investigated the transport of atrazine using column studies with a sandy loam (Mohave) and a silty loam (Walla Walla) soil. The sandy loam soil had an f_{oc} value of 0.0026 and the silty loam had an f_{oc} value of 0.015. The atrazine was added dry to the top layer of the soil and the appearance of the atrazine in the effluent was monitored. Unit gradients were maintained for both soils and flow rates of 0.3 cm/hr for the silty loam and 1.5 cm/hr for the sandy loam were observed. The authors utilized the Freundlich adsorption expression and found good agreement between predicted and observed results.

Rao and Davidson (1979) evaluated the column breakthrough curves of atrazine at two concentrations (5 and 50 mg/L) in a fine sand soil ($f_{oc} = 0.0056$). The atrazine utilized was Aatrex 80W (80% wettable powder). The pore water velocity, 0.22 cm/hr, was selected to allow near equilibrium conditions to occur. The breakthrough appeared earlier for the higher atrazine concentration (50 mg/L) than the lower concentration. This agreed with the nonlinear isotherm observed during batch studies. The nonequilibrium shape of the breakthrough curves was attributed to the nonlinear nature of the adsorption and thus the changing capacity of the soil for the atrazine as the breakthrough progressed.

Bouchard et al. (1988) evaluated the breakthrough curves for atrazine in a fine sand aquifer material ($f_{oc} = 0.007$) at three pore water velocities (2.4, 8.1 and 22.6 cm/hr). The breakthrough was

observed to appear sooner (shifted to the left) with increasing pore water velocity.

Column results - alachlor

While batch and leaching studies have been reported for alachlor, no column breakthrough studies were found in the literature for alachlor with surface or subsurface soils.

Fluorescent Dyes as Groundwater Tracers

Due to the expense and health implications of conducting field scale studies with pesticides, researchers have investigated the use of tracers to mimic the pesticide movement. One class of compounds which has been utilized for groundwater tracing purposes is fluorescent dyes. The majority of the research investigating fluorescent dyes as groundwater tracers has centered on their use as conservative (nonadsorbing) tracers to indicate the rate of groundwater flow. Less work has centered on determining the ability of fluorescent dyes to serve as sorbing tracers to mimic the flow of pesticides.

Fluorescent dyes

Fluorescent dyes are those dyes which, when exposed to ultraviolet light, fluoresce - adsorb the lower wavelength ultraviolet light and emit a higher wavelength light which is in the visible range. This property of the fluorescent dyes allows them to be detected at the $\mu\text{g/L}$ and ng/L ranges using a fluorometer.

Fluorescent dyes as water tracers

Feuerstein and Selleck (1963) investigated the behavior of three fluorescent dyes, including fluorescein, for use in water tracing studies. The following parameters were found to affect analysis of the dyes: (1) temperature, (2) salinity, (3) pH, (4) background level of dye and (5) turbidity or suspended solids. Fluorescein exhibited high photochemical decay and high levels of background fluorescence were encountered when analyzing for fluorescein. The fluorescence of fluorescein was seen to decrease at pH values below 5. The fluorescein was the least adsorbed of the three dyes investigated on suspended solids and algae.

Smart and Laidlaw (1977) discussed the use of eight fluorescent dyes, including rhodamine WT and fluorescein, in water tracing studies. The fluorescence of both rhodamine WT and fluorescein was shown to be a function of temperature. The fluorescence of the dyes was seen to decrease at low pH and was observed to be a function of the ions causing the pH change and the buffering system. For fluorescein, pH values below 6 resulted in decreases in fluorescence and for rhodamine WT pH values below 5 resulted in decreases in fluorescence. The pH effect was attributed to the ionization of the dyes or to structural changes to the dye with changing pH. Fluorescein exhibited no decrease in fluorescence with increasing salinity while rhodamine WT fluorescence was observed to decrease with increasing salinity. The background fluorescence of water samples was shown to be more significant for fluorescein (especially in

the presence of organic matter) than rhodamine WT. Photochemical decay was observed to be significant for fluorescein (greater for sunlight than artificial light) but relatively insignificant for rhodamine WT.

Rhodamine WT was observed to be more strongly adsorbed to organic and inorganic solid phases than fluorescein. The organic phases (sawdust, humus, heather) were observed to result in more adsorption than inorganic phases (clays, limestone, orthoquartzite) for both rhodamine WT and fluorescein.

Omoti and Wild (1979) investigated the use of fluorescein as a groundwater tracer. In a column study utilizing a loamy sand soil (85% sand, 10% clay and 2% organic matter - $f_{oc} = 0.012$) and a pore water velocity of 2.44 cm/hr, the K_p value was determined to be 1.3. The corresponding value of K_{oc} is 108.

Bencala et al. (1983) studied the use of rhodamine WT as a water tracer in a mountain stream environment. Batch studies between the rhodamine WT and streambed sediments resulted in a K_p value of 5.6. The f_{oc} for the sediment was not given.

Trudgill (1987) investigated the use of fluorescent dyes for soil water tracing. Batch experiments with rhodamine WT and a silty loam soil (f_{oc} of 0.034 to 0.053) resulted in a K_p value of 54. This corresponds to a K_{oc} value of 1000 to 1600 for the rhodamine WT.

MATERIALS AND METHODS

The experimental efforts in this study utilized two aquifer materials, two herbicides (atrazine and alachlor) and two fluorescent dyes (rhodamine WT and fluorescein) in batch and column studies to investigate the research objectives (as stated in the introduction). The materials and methods used are discussed in this section.

Aquifer Materials

Two alluvial aquifer sand samples were obtained for use in this study. The first soil sample was obtained south of Ames, Iowa, in a sand layer thirty feet below the ground surface with a clay layer directly above the sand layer. This sample was obtained during the drilling of a water supply well using the rotary bucket technique. The second soil sample was obtained from a site located on the Halletts Pit property north of Ames, Iowa. The site where the sample was obtained had not been utilized by the pit as a production site. A backhoe was utilized to cut through the topsoil and a clay layer to the desired sand layer, located six feet below the ground surface. The sample was obtained prior to sloughing of the topsoil into the hole and prior to appearance of groundwater into the hole in an effort to prevent organic carbon content entering the sample from these sources. Table 3 lists values for relevant parameters of the soils with respect to this study. The sieve analysis was conducted according to ASTM procedures (1988). The fraction organic content was conducted according to the modified Mebius method

Table 3. Soil parameters for alluvial aquifer materials

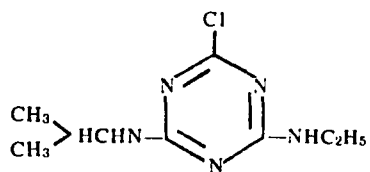
Parameter	South Ames	Halletts Pit
Median grain size diameter - d_{50} (mm)	0.58	1.2
Uniformity Coefficient - d_{60}/d_{10}	3.5	4.7
Percent sand (%)	97.3	98.4
Percent silt (%)	2.2	1.3
Percent clay (%)	0.5	0.3
Fraction organic carbon content (f_{oc})	0.0027 ± 0.00029	0.0013 ± 0.00012
Soil pH	7.9	8.0
Cation Exchange Capacity (meq/100g)	13.3	15.1
Hydraulic Conductivity (cm/s)	8.6×10^{-3}	4.7×10^{-2}

(Nelson and Sommers, 1982). Hydraulic conductivity was determined in the columns by determining the flowrate through the soil, measuring the head loss across the soil sample and utilizing Darcy's Law. The cation exchange capacity was determined according to Rhoades (1982).

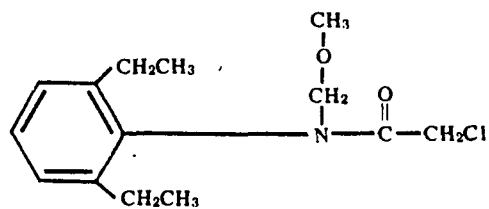
Chemicals

The herbicides investigated in this study were atrazine (Aatrex) and alachlor (Lasso). The chemical structures of atrazine and alachlor are shown in Figure 8. Atrazine is a triazine pesticide and alachlor is an amine pesticide. Other physical and chemical parameters for atrazine and alachlor which are pertinent to this study are given in Table 4. The atrazine and alachlor utilized for standards and stock solutions were analytical grade (99% pure) and were obtained from Chem Service, Inc. (Westchester, PA).

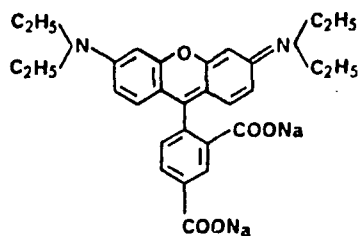
Atrazine and alachlor were analyzed according to USEPA method 619 (USEPA, 1982) and 645 (USEPA, 1985), respectively. These two procedures are virtually the same and it was thus possible to analyze for both atrazine and alachlor simultaneously. The analytical procedure involved extracting the samples three times in a separatory funnel (1.0 L) with methylene chloride. The samples (40 to 100 mL) were brought to 500 mL using Nanopure II water (Barnstead, Inc.) prior to extraction. Thirty mL of methylene chloride was used for each of the three extractions. After each extraction, the methylene chloride was filtered through a drying column of anhydrous sodium sulfate. For the combined extract, the methylene chloride was exchanged to hexane and concentrated to 2 mL using



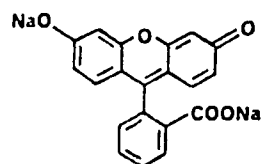
atrazine



alachlor



rhodamine WT



fluorescein

Figure 8: Chemical structures of pesticides (atrazine and alachlor) and dyes (rhodamine WT and fluorescein)

Table 4. Physical and chemical properties of atrazine and alachlor

Parameter	Atrazine	Alachlor
Trade name	Aatrex	Lasso
Molecular Formula ^a	C ₈ H ₁₄ ClN ₅	C ₁₄ H ₂₀ ClNO ₂
Molecular Weight ^a	215.7	269.8
Water Solubility ^a @ 25 °C (mg/L)	33	242
Log K _{ow} ^b	2.34	2.64
pK _a ^c	1.7	n/a
Vapor pressure ^a @ 25 °C (mm Hg.)	8 x 10 ⁻⁷	2.2 x 10 ⁻⁵
Henry's constant ^d @ 25 °C (dimensionless)	2.8 x 10 ⁻⁷	1.3 x 10 ⁻⁶

^aWeed Science Society of America (1983).

^bRao and Davidson (1980).

^cWeber et al. (1980).

^dEstimated according to Thomas (1982).

Kuderna-Danish glassware and a water bath. The 2 mL concentrates were placed in sealed vials and stored at $-20\text{ }^{\circ}\text{C}$ prior to gas chromatographic analysis (one to two weeks). Recovery efficiencies for atrazine were $87.4\% \pm 4.5\%$ and for alachlor were $84.3\% \pm 7.3\%$, respectively. Pesticide data were corrected for these recovery efficiencies prior to presentation and manipulation. Optima grade (Fisher Scientific) hexane and methylene chloride were utilized during this study.

A Perkin Elmer Sigma 1 gas chromatograph (GC) was used with a nitrogen / phosphorous (N/P) thermionic detector in the nitrogen mode. The glass column utilized was 1.8 m long x 2 mm (inside diameter) and was packed with 5% Carbowax 20M-TPA on Supelcoport (80/100 mesh). During GC operation, the injection temperature was $250\text{ }^{\circ}\text{C}$, the oven temperature was $200\text{ }^{\circ}\text{C}$, the carrier gas was helium, the carrier flowrate was 30 mL/min and the sample injection volume was 5.0 μL . For these operating conditions, the peak detention time for alachlor was 8.4 min and for atrazine was 13.2 min. For a 40 mL original sample size, the detection limit (taken as twice the chromatogram noise level) for atrazine was 0.5 $\mu\text{g/L}$ and for alachlor was 1.0 $\mu\text{g/L}$.

The fluorescent dyes investigated were rhodamine WT and fluorescein. The chemical structures of rhodamine WT and fluorescein are shown in Figure 8. Smart and Laidlaw (1977) classified rhodamine WT as an orange fluorescent dye and fluorescein as a green fluorescent dye. Other available physical and chemical parameters for rhodamine WT and fluorescein which are pertinent to this study are given in Table 5. While pKa values were not found in the literature for rhodamine WT or

Table 5. Physical and chemical properties of rhodamine WT and fluorescein

Parameter	Rhodamine WT	Fluorescein
Molecular Formula	$C_{29}H_{29}N_2O_5Na_2Cl$	$C_{20}H_{10}Na_2O_5$
Molecular Weight	531	376
Log K_{ow} ^a	-1.33	-0.39

^aSmart (1984).

fluorescein, both of these dyes have been shown to be ionizable at pH values less than 5 to 6 (Smart and Laidlaw, 1977). The rhodamine WT used in this study was obtained as a 20% solution from Pylam Products, Inc. (Garden City, NY) and the fluorescein was a powder obtained from Fisher Scientific (listed as Uranine by Fisher Scientific).

Rhodamine WT and fluorescein were analyzed using a Turner 110 fluorometer according to United States Geological Survey procedures (Wilson et al., 1986). The primary filters utilized for rhodamine WT were 1-60 + 58 and for fluorescein were 47B + 2A. The secondary filter utilized for rhodamine WT was 25 and for fluorescein was 58. While these were not the optimal filters for detecting rhodamine WT and fluorescein (Smart and Laidlaw, 1977), the results were sufficient for the concentration ranges of concern in this study. Using these filters, the detection limit (taken as one dial reading on the most sensitive scale) for rhodamine WT was 1.0 $\mu\text{g/L}$ and for fluorescein was 0.2 $\mu\text{g/L}$.

Batch Methods.

Batch studies for the herbicides and dyes were conducted by placing a constant mass of aquifer material and a constant volume of chemical solution at varying concentrations in a series of reactors and shaking for a predetermined amount of time sufficient for equilibrium conditions to exist. The initial and equilibrium concentration of the chemical(s) were determined for each reactor and the mass of chemical(s) adsorbed was calculated from mass balance considerations. Duplicates were evaluated for each initial chemical concentration. Chemical and soil blanks were

conducted during each isotherm study. The reactors utilized were 250 mL Erlenmeyer flasks and the shaker utilized was a horizontal motion Eberbach water-bath shaker. Batch tests were conducted at room temperature (25 °C).

Preliminary efforts established the use of 50 grams of the aquifer material and 100 mL of the chemical solution for each batch reactor. This gave a soil to solution ratio of 1:2. Increasing the soil to solution ratio above 1:2 resulted in inadequate mixing of the soil with the solution. Preliminary work established that equilibrium conditions existed for the fluorescent dyes within one to two minutes and for the pesticides within 2 hours. Shaking times of 2 hours for the fluorescent dyes and 24 hours for the pesticides were utilized to assure that equilibrium conditions had been established.

Upon completion of shaking, the reactors were removed from the shaker and the soil and solution phases were separated. For the fluorescent dyes, gravity filtering with Whatman #2 or #5 filter paper (8 and 2.5 μm , respectively) and plastic funnels was used for the solid liquid separation. No change in the dye concentrations was observed using this solid liquid separation technique. Problems were encountered in eliminating the background fluorescence from the soil when analyzing for fluorescein. Use of 0.45 μm filter paper, 0.2 μm filter paper and high speed centrifuging (17,000 rpm) was not observed to decrease the background fluorescence observed, leading to the hypothesis that the background fluorescence was the result of colloidal or dissolved organics. The problem of background fluorescence for fluorescein has

been reported by others (Feuerstein and Selleck, 1963; Smart and Laidlaw, 1977). Soil blanks (with no fluorescein present) resulted in readings of 1 to 10 $\mu\text{g/L}$. Solid liquid separation for the pesticides was achieved by using high speed centrifuging (17,000 rpm). This technique was chosen for the pesticides to eliminate any potential interferences from the filter paper or the plastic funnels in the extraction or GC analysis steps. For the batch tests, the pH of the solution phase was observed to be neutral (7.5 to 8.0).

Column Methods

The laboratory column studies were conducted using glass columns 5.0 cm in diameter (cross sectional area of 19.6 cm^2) and 35.0 cm in length. The glass column had an internal ledge (slight decrease in the internal column diameter) 2.5 cm from the bottom of the column where a fine mesh stainless steel screen was supported. The fine mesh stainless steel screen served to maintain the soil within the column. The column was fitted with rubber stoppers with glass tubes on the top and bottom of the column. When pesticides were present, the bottom rubber stopper was covered with aluminum foil and a small air gap (3 cm) was left below the top rubber stopper to prevent potential interactions between the pesticides and the rubber stoppers. A schematic illustration of the glass column is shown in Figure 9. A known mass of soil was added in small increments to the column with water present. This method provided saturated conditions in the soil while minimizing stratification of the soil. The depth of the soil within the column averaged approximately

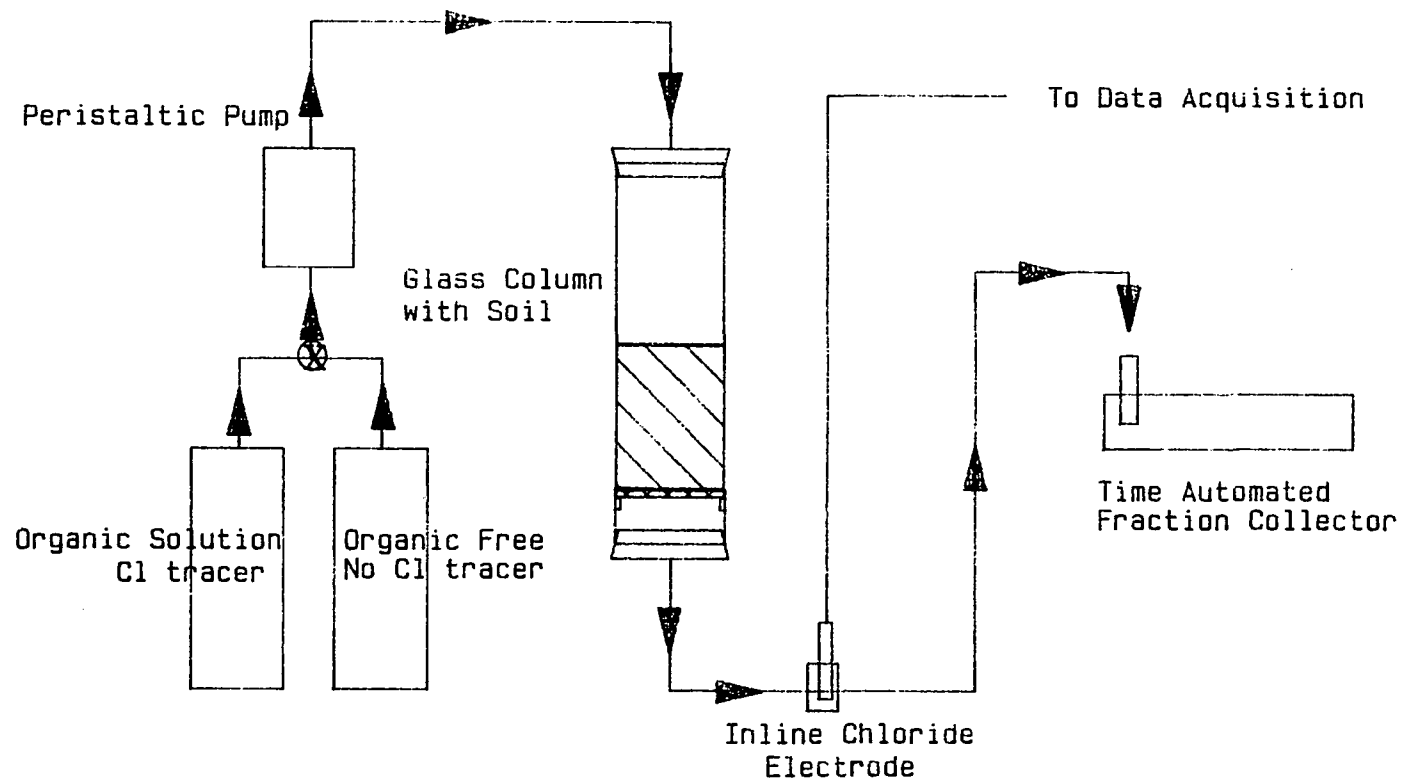


Figure 9: Schematic of column apparatus

12.0 cm. Masterflex peristaltic pumps were utilized to establish a constant flowrate through the column. Silicone tubing was utilized in the pump heads and Teflon tubing elsewhere to eliminate any adsorptive losses of the chemicals to the tubing. A time controlled fraction collector was utilized to gather samples for dye or pesticide analysis. The breakthrough of a conservative tracer (chloride) was monitored utilizing an inline chloride specific electrode and a continuous data acquisition system interfaced with a microcomputer. Figure 9 illustrates schematically the column apparatus utilized during this study. The pH of the column effluent remained relatively neutral (7.5 to 8.0) for all column runs. Column studies were conducted at room temperature (25 °C).

For purposes of determining the hydrodynamics of flow through the column, the breakthrough of a conservative tracer (chloride) was monitored. The chloride breakthrough curves verified saturated soil conditions and allowed the determination of the hydrodynamic dispersion coefficient (D_x) for each combination of soil and column conditions. The chloride was introduced as 0.01 N CaCl_2 . In the absence of chloride, 0.01 N CaSO_4 was utilized to maintain the chemical environment of the soil column. The CaCl_2 was added to the pesticide or dye solutions and the breakthroughs of the conservative and nonconservative chemicals were obtained simultaneously. Upon completion of the breakthrough portion of the study, a CaSO_4 solution was utilized for the pesticide and dye free solution during the desorption portion of the column study. The CaSO_4 solution was also eluted through the column prior to introduction of the dyes or pesticides to establish equilibrium conditions in the soil.

Distilled water was utilized for the dye studies and Nanopure II water (Barnstead, Inc.) was utilized during pesticide studies.

BATCH STUDIES

Batch studies were conducted to evaluate the equilibrium adsorption of the pesticides and the dyes with the aquifer materials. While the environment of an equilibrium batch reactor differs from that of porous media flow, the relative ease of obtaining adsorption information in batch reactors encourages their use. The raw data for the batch studies appear in Appendix A.

Pesticides

Preliminary batch tests for atrazine and alachlor showed that equilibrium conditions existed within 2 hours. Shaking times of 24 hours were used to assure equilibrium conditions in the reactors. Preliminary batch studies showed no effect of background ions on the level of pesticide adsorption to the soils (as expected for relatively nonpolar organics). Due to the time and expense of pesticide analysis, it was decided to evaluate adsorption isotherms only for the South Ames aquifer material. The potential for competitive adsorption between atrazine and alachlor was evaluated.

Adsorption of atrazine and alachlor

Batch studies were conducted for atrazine and alachlor using the South Ames aquifer material. The resulting isotherms (based on averages of duplicate samples) for atrazine and alachlor are shown in Figures 10 and 11, respectively. The isotherms are seen to be linear for atrazine

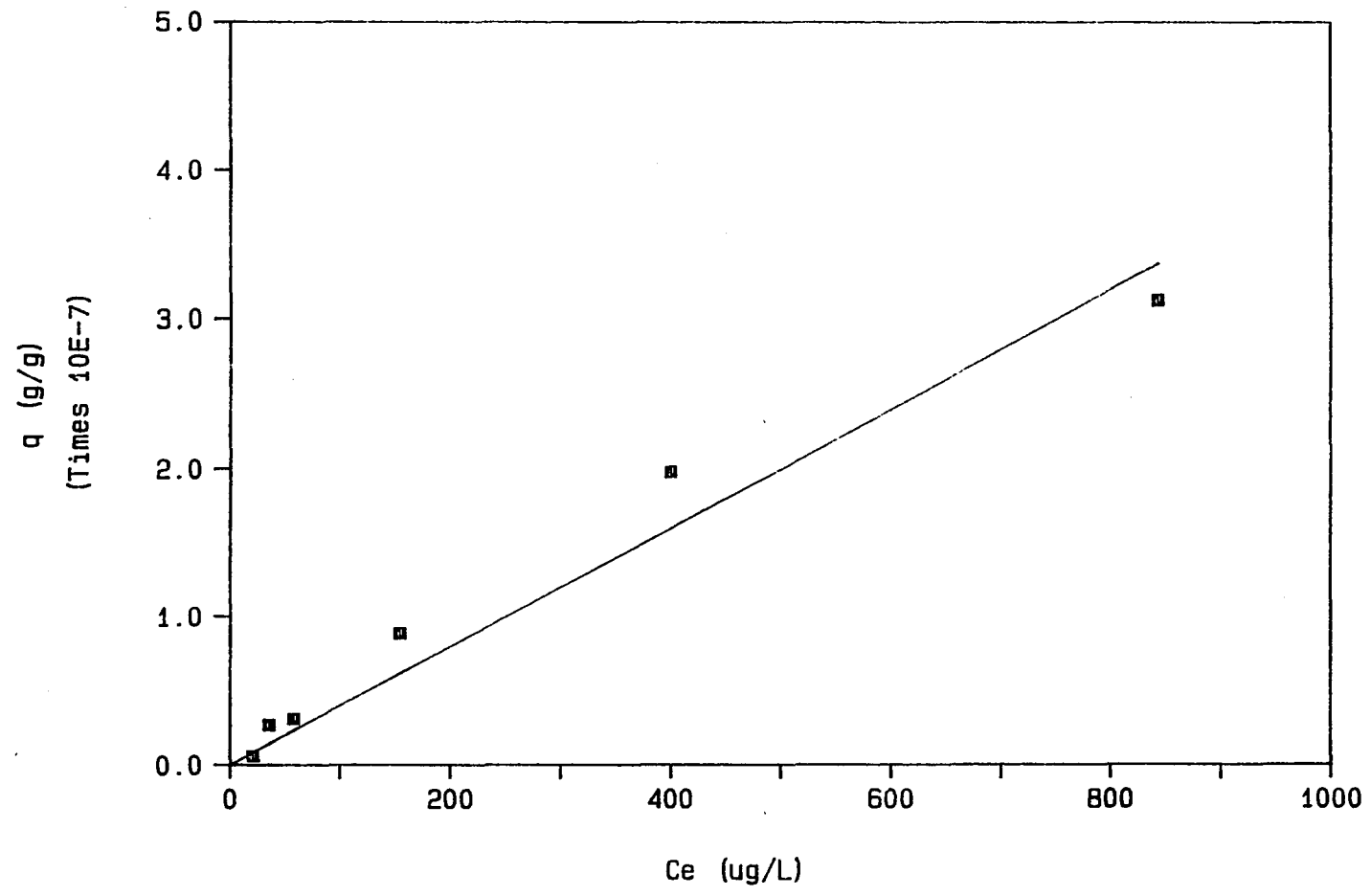


Figure 10: Atrazine adsorption isotherm

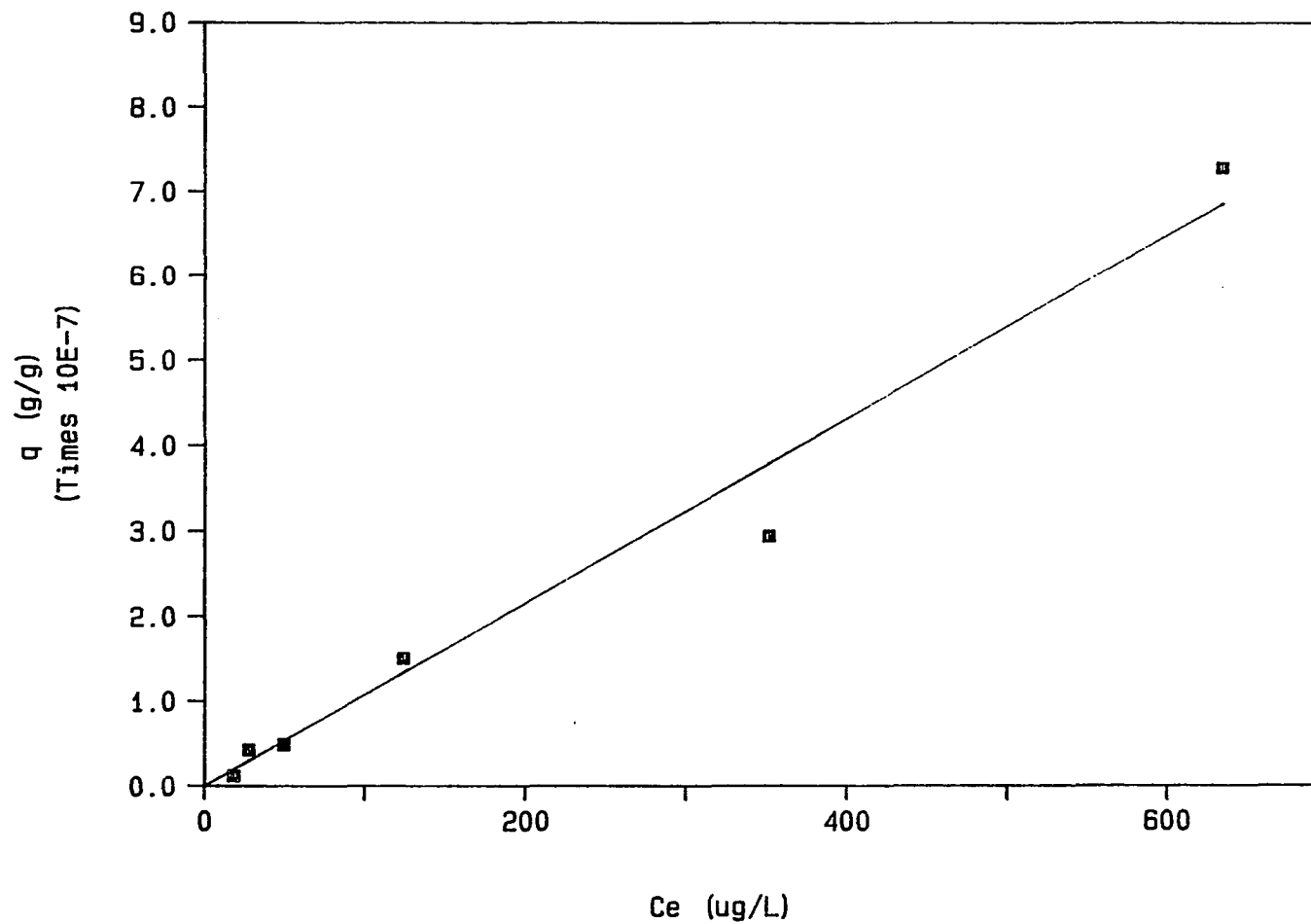


Figure 11: Alachlor adsorption isotherm

and alachlor over the equilibrium concentration ranges investigated. The K_p values for these isotherms and the corresponding K_{oc} values are shown in Table 6. The experimental K_{oc} values of 148 for atrazine and 400 for alachlor are similar to values reported in the literature. For atrazine, K_{oc} values have been reported in the range of 48 to 237 and for alachlor a K_{oc} value of 191 ± 49 was measured (see Table 2 for a summary of K_{oc} values in the literature).

Atrazine isotherms have been observed by others to be nonlinear at higher equilibrium concentrations. Rao and Davidson (1979) found adsorption of atrazine to be nonlinear using equilibrium concentrations up to the solubility limit of atrazine (33 mg/L). Peter and Weber (1985) investigated the adsorption of alachlor at equilibrium concentrations up to 16 mg/L (it is not clear what the lower limit of the equilibrium concentrations investigated was) and determined a K_{oc} value of 191 ± 49 . The K_{oc} value of Peter and Weber (1985) for alachlor is less than the K_{oc} value determined in this study (400). If alachlor equilibrium concentrations investigated by Peter and Weber (1985) were in the mg/L range, one explanation for the variation in K_{oc} values could be that alachlor is nonlinear over the $\mu\text{g/L}$ to mg/L range. For the concentrations ($\mu\text{g/L}$) and soils investigated in this study, the atrazine and alachlor isotherms did not evidence nonlinearity.

Estimated linear partition coefficient

The ability of empirical expressions (based on K_{ow} values) to estimate the observed K_{oc} values for atrazine and alachlor was

Table 6. Batch adsorption parameters for atrazine and alachlor

Parameter	BATA	BALA
Pesticide	atrazine	alachlor
Soil	South Ames	South Ames
f_{oc}	0.0027	0.0027
K_p (cm ³ /g)	0.40	1.08
r^2	0.96	0.97
K_{oc} (cm ³ /g)	148	400

Table 7. Measured and estimated K_{oc} values for atrazine and alachlor

Parameter	atrazine	alachlor
$(K_{oc})_{observed}$ (cm ³ /g)	148	400
$\log K_{ow}^a$	2.34	2.64
$(K_{oc})_{estimated}^b$ (cm ³ /g)	135	270
$(K_{oc})_{estimated}^c$ (cm ³ /g)	153	293

^aRao and Davidson (1980).

^bEstimated after Karickhoff et al. (1979).

^cEstimated after Brown and Flagg (1981).

investigated. The empirical relationships of Karickhoff et al. (1979), as shown in Equation 25, and Brown and Flagg (1981), as shown in Equation 26, were utilized to estimate K_{OC} values for atrazine and alachlor. Table 7 shows the K_{OC} parameters predicted by these expressions and measured in this study. The error for the estimation expressions ranged from 4 to 10% for atrazine and from 35 to 50% for alachlor. The ability to predict the K_{OC} values with this accuracy based on readily available K_{OW} values is encouraging. It is also an indication that atrazine and alachlor are similar in nature (nonpolar, hydrophobic) to the solutes used to develop the empirical relationships.

Competitive adsorption

The potential for competitive adsorption of atrazine and alachlor with the South Ames aquifer material was evaluated. A batch study was conducted with both atrazine and alachlor present (binary solutes) during the shaking period. The isotherm data obtained with binary solutes were plotted for each pesticide with the previous isotherm data obtained with only a single solute present. These plots are shown in Figure 12 for atrazine and Figure 13 for alachlor. No significant effects of binary solutes on the adsorption isotherms were observed for either atrazine or alachlor under the conditions investigated. This indicates that no competitive adsorption was experienced.

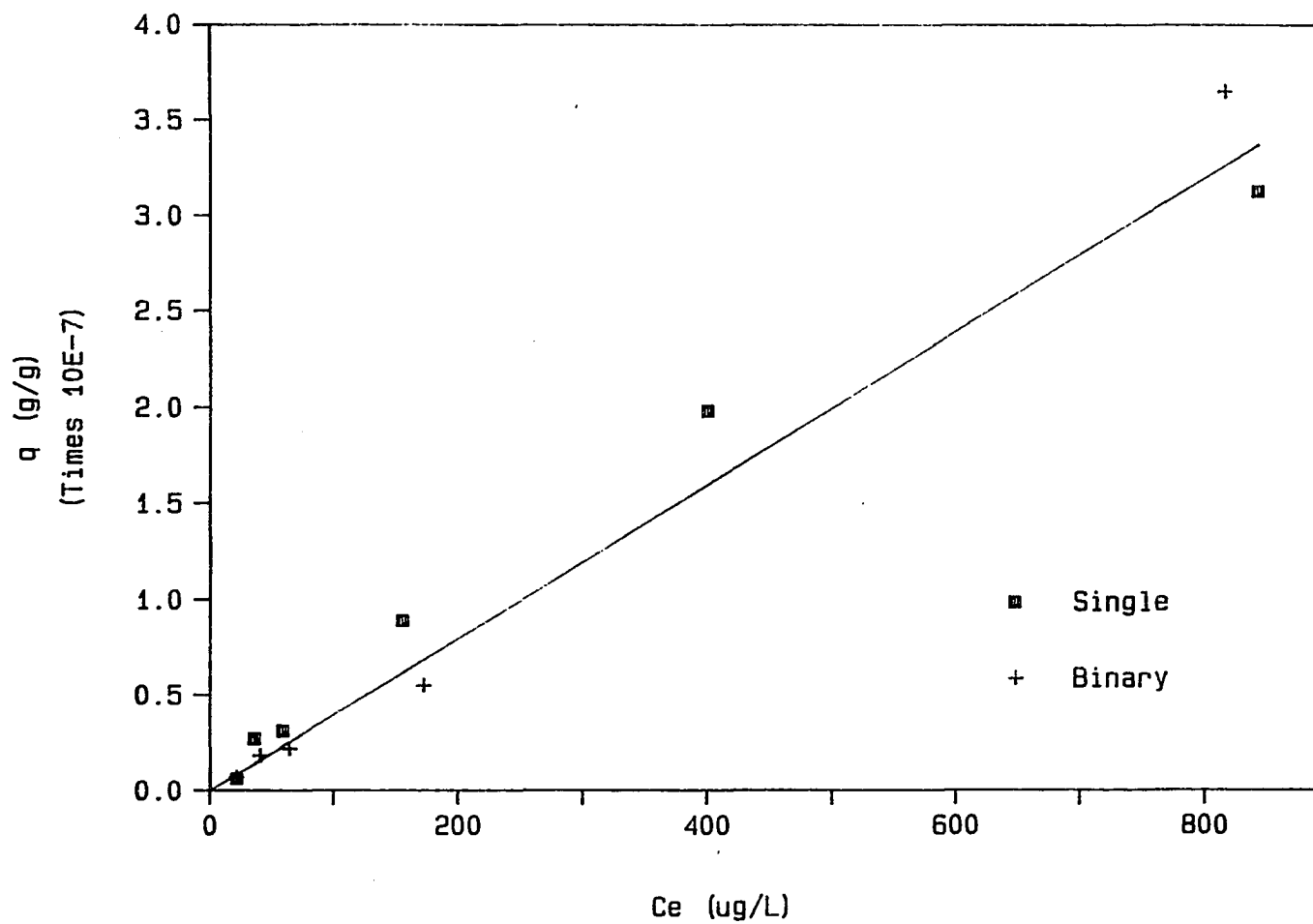


Figure 12: Atrazine adsorption isotherm - single versus binary solutes

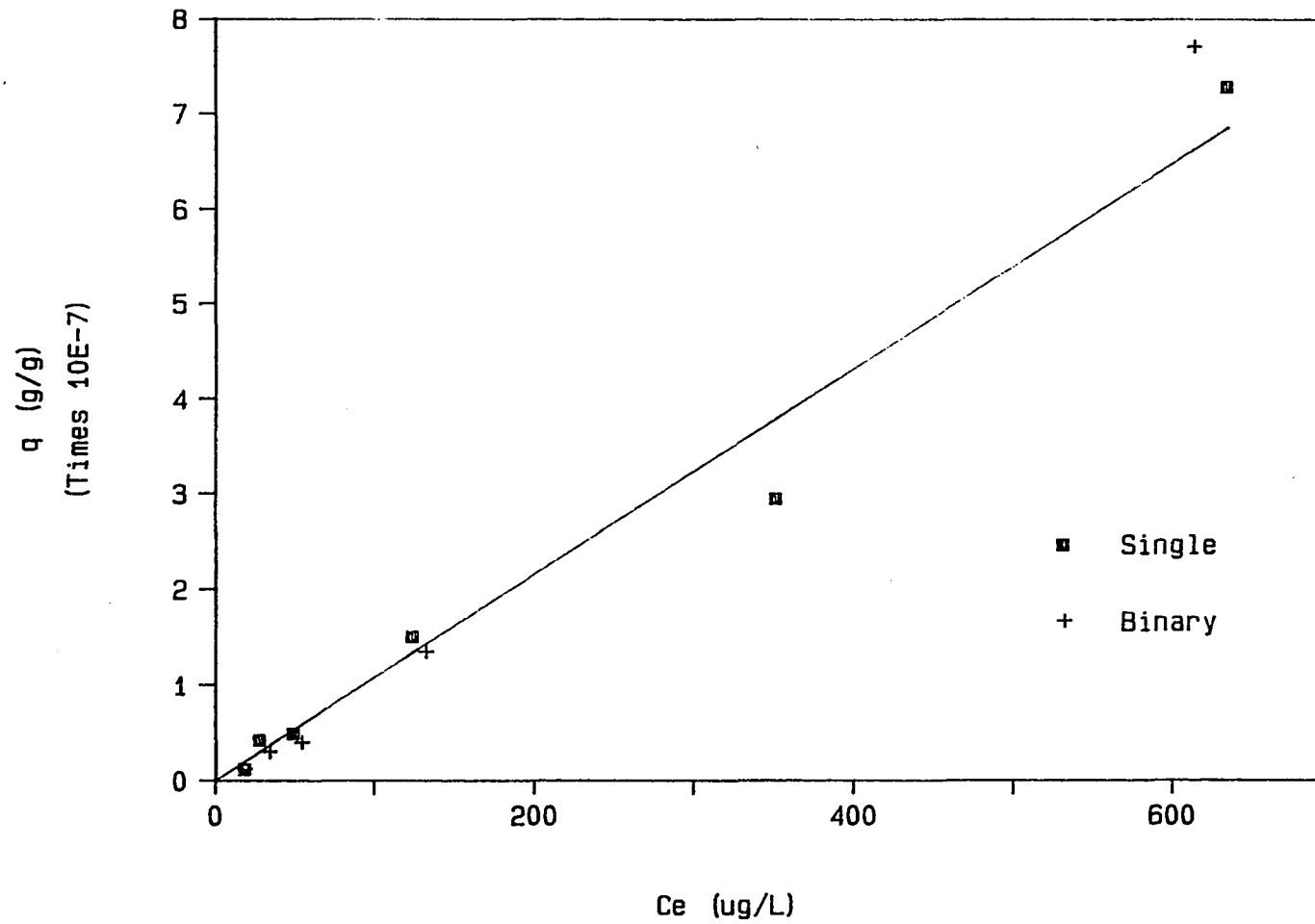


Figure 13: Alachlor adsorption isotherm - single versus binary solutes

Fluorescent Dyes

Preliminary batch studies showed that equilibrium conditions existed for the fluorescent dyes within 1 to 2 minutes. Shaking times of 2 hours were utilized to assure equilibrium conditions in the reactors.

Adsorption of rhodamine WT and fluorescein

Batch studies were conducted for rhodamine WT (RWT) and fluorescein using the South Ames aquifer material. The resulting isotherms for RWT and fluorescein are shown in Figure 14 and Figure 15 respectively. Figure 16 provides increased resolution at the lower concentrations for the RWT isotherm. Table 8 summarizes the experimental conditions and adsorption results for the RWT (BRA) and fluorescein (BFA) batch tests.

As observed by the relative magnitudes of the q values for RWT and fluorescein adsorption isotherms (Figures 14 and 15), the level of adsorption for the fluorescein was much less than that for the RWT. During the fluorescein batch studies, the reductions of the aqueous phase fluorescein concentration were low (5 to 15%). As discussed previously, the soil blanks exhibited background fluorescence when analyzing for fluorescein which varied from blank to blank. These factors complicated the interpretation of the fluorescein batch results. Attempts to increase the level of fluorescein adsorption by increasing the soil to water ratio resulted in increases in the background fluorescence and unsatisfactory mixing of the soil with the solution.

Inspection of the adsorption isotherms for RWT and fluorescein indicates that both dyes demonstrated linearity at low concentrations

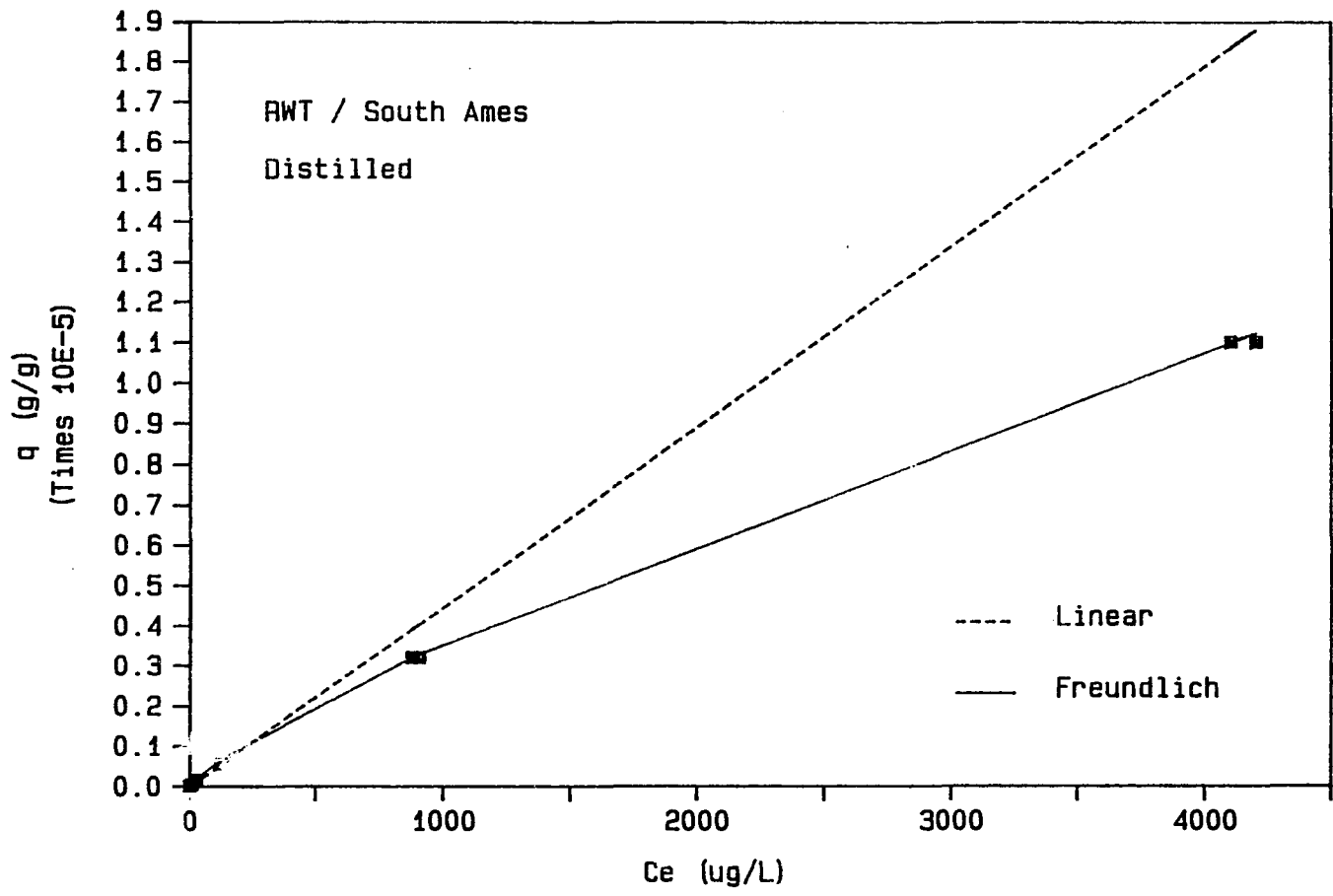


Figure 14: Rhodamine WT adsorption isotherm (South Ames, 0 - 4500 µg/L)

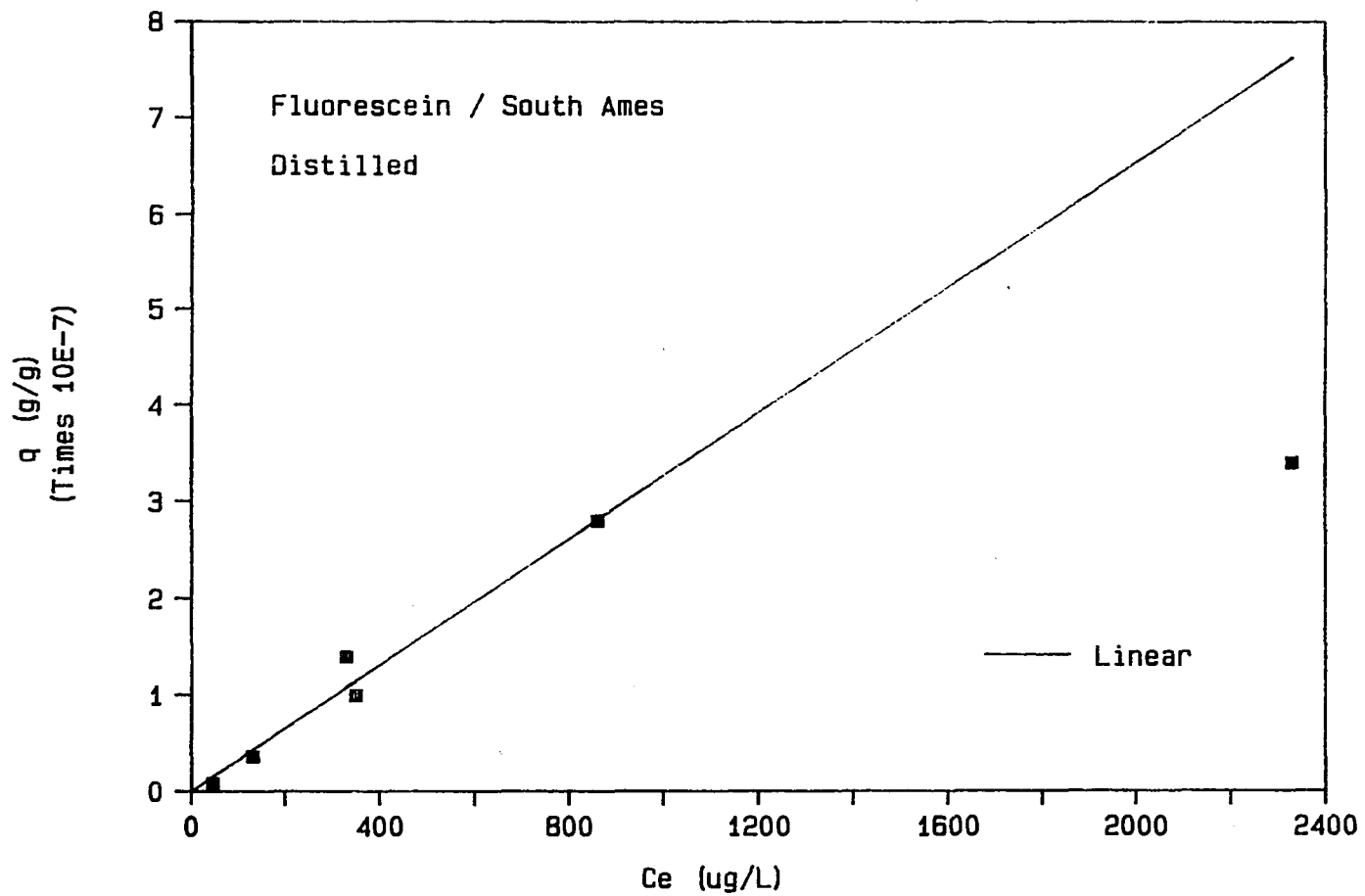


Figure 15: Fluorescein adsorption isotherm (South Ames)

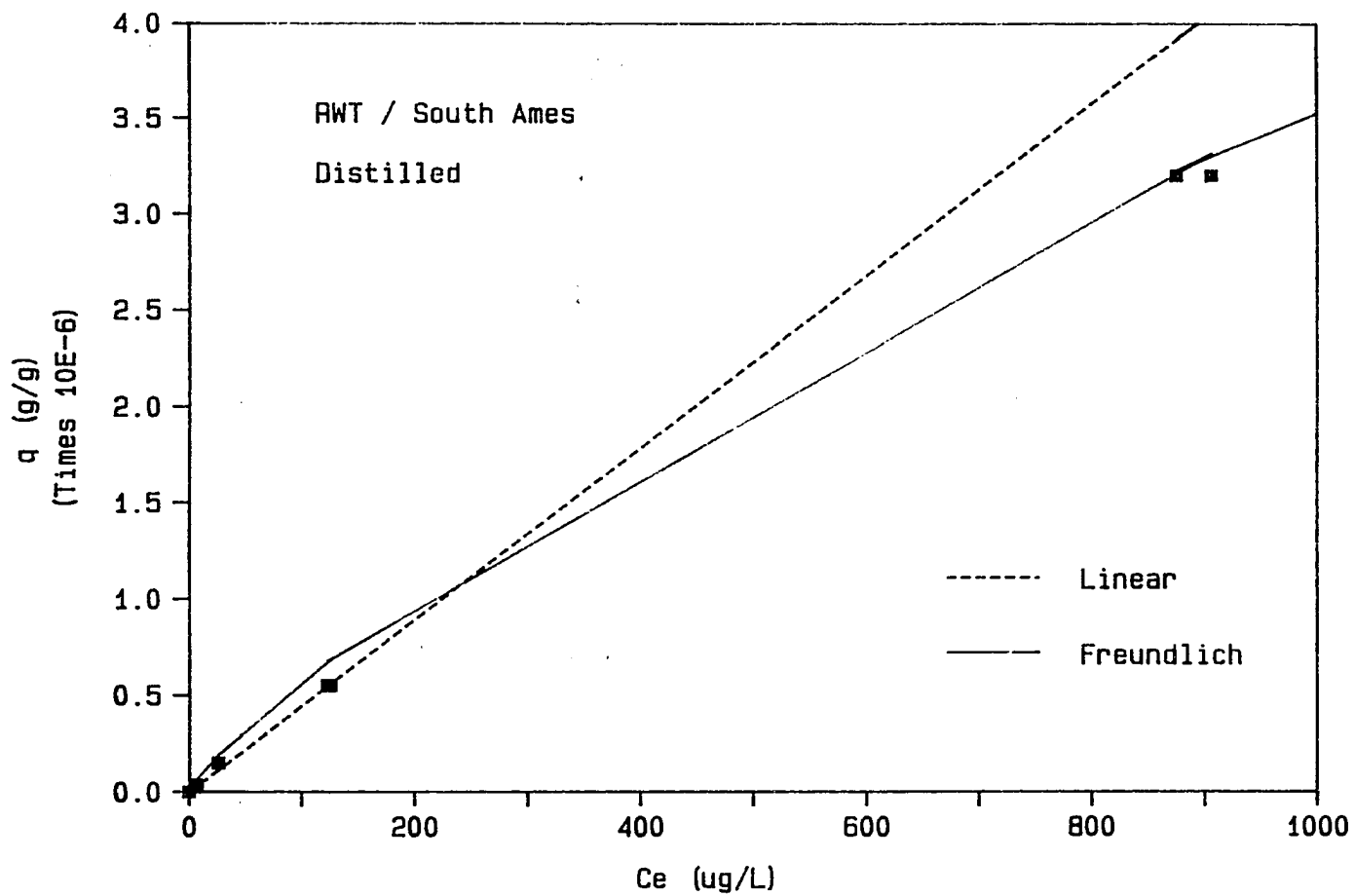


Figure 16: Rhodamine WT adsorption isotherm (South Ames, 0 - 1000 $\mu\text{g/L}$)

Table 8. Batch adsorption parameters for rhodamine WT and fluorescein

Parameter	BRA	BFA	BRH	BRACA
Dye	RWT	Fluorescein	RWT	RWT
Soil	South Ames	South Ames	Halletts	South Ames
f_{oc}	0.0027	0.0027	0.0013	0.0027
Background solution	distilled	distilled	distilled	10^{-2} N $CaCl_2$
K_p (cm^3/g)	4.5	0.33	2.7	9.7
r^2	0.99	0.98	0.99	0.99
$(K_{oc})_{batch}$ (cm^3/g)	1.7×10^3	1.2×10^2	1.4×10^3	3.7×10^3
N	0.80	---	0.85	0.73
K_{fr} (g/g)/(g/L) ^N	8.8×10^{-4}	---	7.6×10^{-4}	7.1×10^{-4}

with nonlinearity experienced at higher concentrations. The linear adsorption expression was used to describe the linear data at the lower concentrations. The K_{oc} values (Table 8) of 1700 for RWT and 120 for fluorescein are similar to values reported by others (see Table 2). Using the data of Trudgill (1987), K_{oc} values for RWT in the range of 1000 to 1600 were determined. Using the data of Omoti and Wild (1979), a K_{oc} value for fluorescein of 108 was determined.

The Freundlich isotherm was able to predict the nonlinear nature of the RWT isotherm observed at higher equilibrium concentrations. However, the discontinuous nature of the fluorescein isotherm (caused by the highest equilibrium concentration data points) prevented the Freundlich expression from providing a good fit to the data. For this reason, only the linear expression is shown for the fluorescein isotherm. The adsorption parameters for the Freundlich (K_{fr} and N) expression are shown in Table 8 for the RWT (BRA) isotherm. The Freundlich parameters were determined utilizing a nonlinear least error method in the Eureka (Borland) microcomputer software package. This method was observed to provide a better fit to the isotherm data than the conventional log transformation method. The failure of the log transformation method to provide as good of results as the nonlinear least error method could be due to the spacing of the data points utilized in the batch tests.

Estimated linear adsorption parameter

The estimation expressions of Karickhoff et al. (1979) (Equation 25) and Brown and Flagg (1981) (Equation 26) were utilized to predict K_{oc}

values for RWT and fluorescein. Table 9 shows the K_{OC} parameters predicted by these expressions and measured in this study. It is observed that the levels of adsorption observed for both dyes in this study were several orders of magnitude greater than that predicted by either estimation technique. The estimation techniques of Karickhoff et al. (1979) and Brown and Flagg (1981) are empirical and were derived utilizing relatively nonpolar chemicals. RWT and fluorescein are polar and ionizable and thus violate the conditions necessary for these empirical relationships to be valid.

Effect of aquifer material

The effect of the aquifer material on the RWT adsorption isotherm was investigated by utilizing the Halletts alluvial material. The Halletts material was coarser and lower in organic carbon content. The RWT adsorption isotherm is shown in Figure 17 and the resulting linear and Freundlich parameters are shown in Table 8 (BRH). The f_{OC} value for the Halletts material was 48% of that for the South Ames material and the K_p value for the Halletts material was 60% of that for the South Ames material. This indicates that the level of adsorption decreased with the decreasing value of f_{OC} . It is noted that the Freundlich parameters were similar for the Halletts and Ames materials (Table 8).

Effect of background ions

The batch studies discussed above were conducted with the dyes in distilled water (no background ions added). Based on the polar nature of

Table 9. Measured and predicted K_{oc} values for rhodamine WT and fluorescein

Parameter	RWT	Fluorescein
$\log K_{ow}$	-1.33	-0.39
$(K_{oc})_{estimated}^a$ (cm^3/g)	0.03	0.25
$(K_{oc})_{estimated}^b$ (cm^3/g)	0.06	0.43
$(K_{oc})_{observed}$ (cm^3/g)	1400 - 3700	120

^aEstimated after Karickhoff et al. (1979).

^bEstimated after Brown and Flagg (1981).

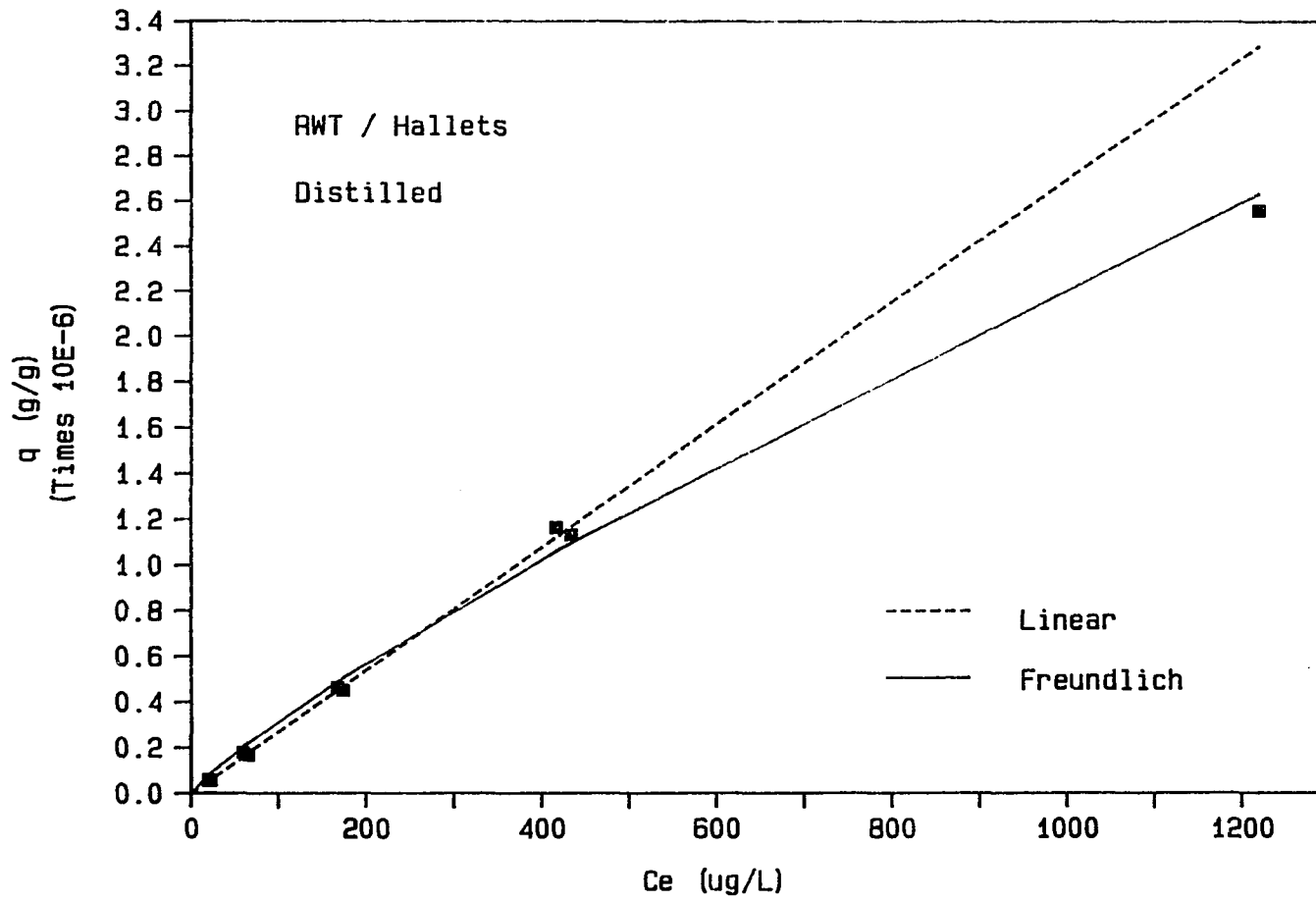


Figure 17: Rhodamine WT adsorption isotherm (Halletts)

RWT, the effects of background ions present along with the RWT were evaluated. The main variations of the background ions investigated were monovalent versus divalent cation, specific cation, specific anion and ion concentration. Preliminary batch tests were conducted (without replication) to evaluate which of the above variations were the most significant. A constant soil to mass ratio and RWT concentration was placed in each reactor. The ionic compound and the concentration of each compound was varied between the reactors. The resulting equilibrium phase RWT concentrations were compared to evaluate the effects of the experimental variations. The compounds and their concentrations utilized in this batch test are summarized in Table 10. Reactors with RWT and with the background ions but with no soil showed no decrease in RWT concentration. Figure 18 shows the measured equilibrium values for each reactor. This preliminary study indicated the following: (1) for constant concentration, the specific cations present (e.g., CaCl_2 versus NaCl) had a greater impact than the specific anions (e.g., CaCl_2 versus CaSO_4), (2) an order of magnitude difference in concentration of the divalent cation calcium (e.g., CaCl_2) was observed to decrease the equilibrium RWT concentration (increase the level of adsorption) while little effect on the equilibrium RWT concentration was noted for an order of magnitude difference in concentration for the monovalent cation sodium (as NaCl).

Based on these preliminary results, several of the above conditions were repeated with replicates. Figure 19 shows the mean and standard deviation for each of the experimental conditions evaluated (as defined

Table 10. Effect of background ions on rhodamine WT adsorption

Item	Chemical	Concentration (M)	Cation	Concentration (mg/L)
KB	KBr	10^{-3}	K	39
KC	KCl	10^{-3}	K	39
NCL	NaCl	10^{-3}	Na	23
NCH	NaCl	10^{-2}	Na	230
NBC	NaHCO ₃	10^{-3}	Na	23
MGL	MgSO ₄ ·7H ₂ O	10^{-3}	Mg	24
MGH	MgSO ₄ ·7H ₂ O	10^{-2}	Mg	240
GCL	CaCl ₂	10^{-3}	Ca	40
GCH	CaCl ₂	10^{-2}	Ca	400
CS	CaSO ₄	10^{-3}	Ca	100
BLK	Blank	-----	--	---

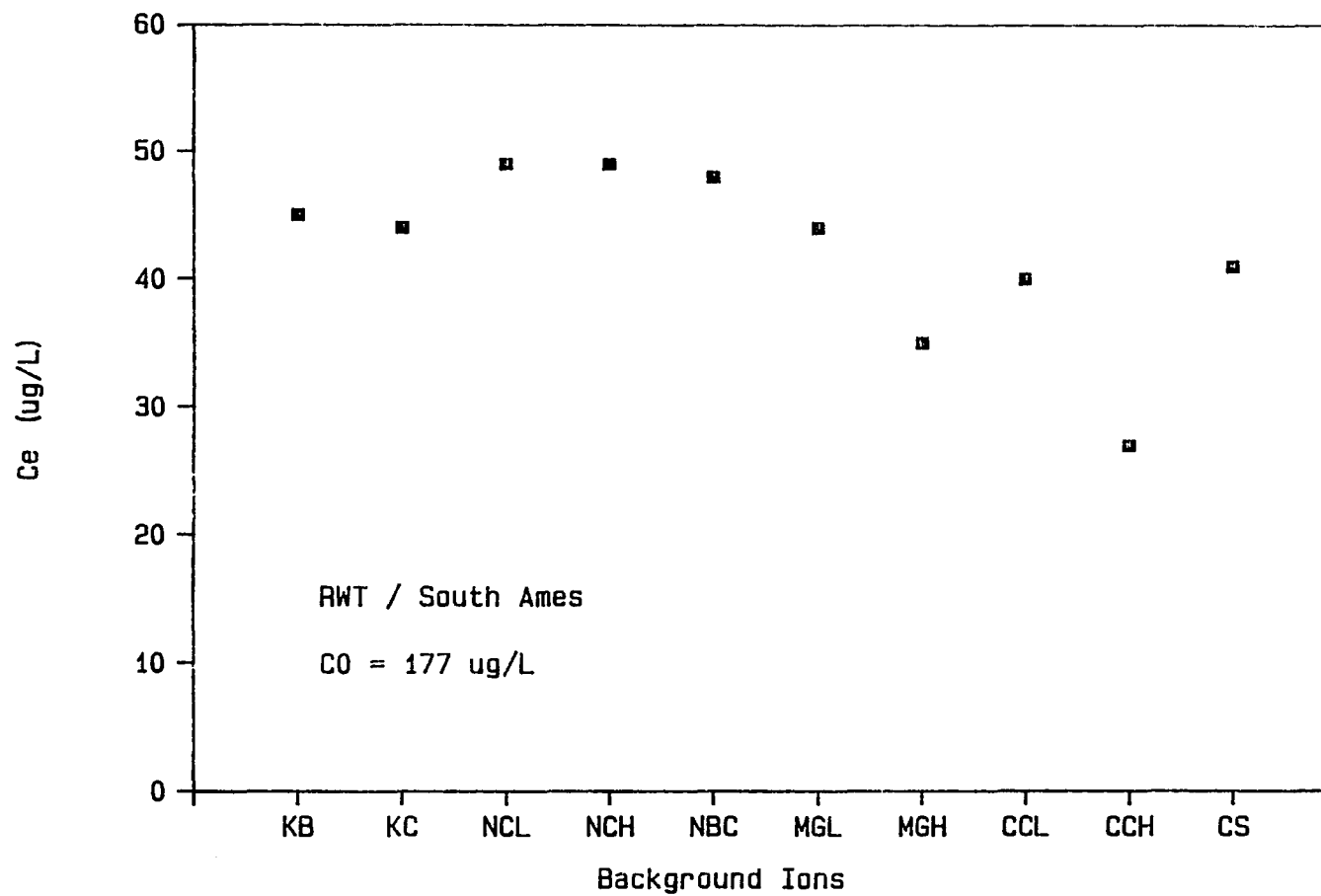


Figure 18: Effects of background ions on rhodamine WT adsorption - preliminary batch tests

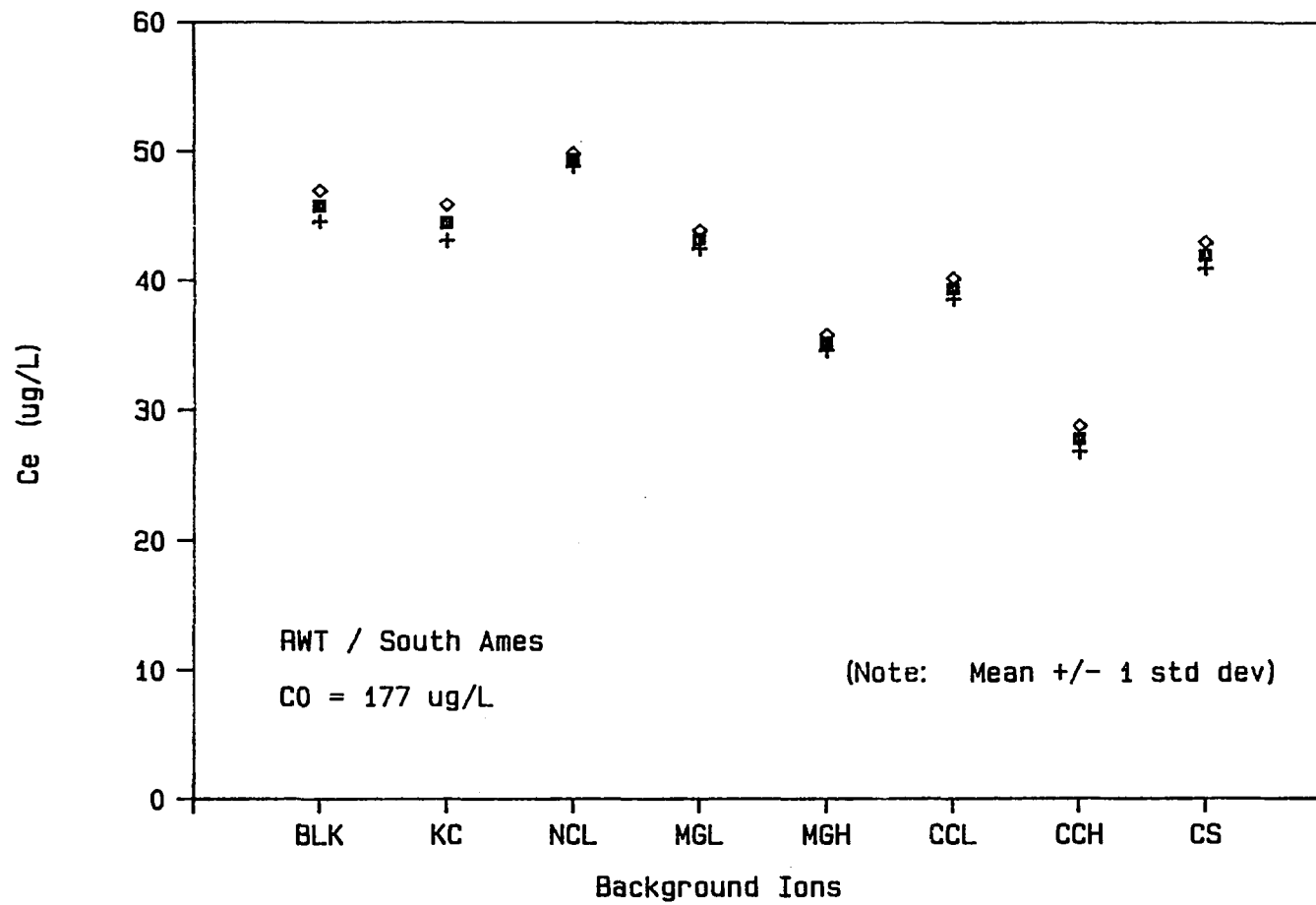


Figure 19: Effects of background ions on rhodamine WT adsorption - batch tests with replicates

in Table 10). These results indicate the following: (1) with concentration constant, increased adsorption was realized for divalent versus monovalent cations (e.g., calcium versus sodium), (2) with concentration and valency constant, certain cations were observed to increase the adsorption realized (e.g., calcium versus magnesium) and (3) with cation constant, increasing concentration resulted in increases in the level of adsorption. It is hypothesized that these effects are the result of the suppression of diffuse double layers present in the alluvial material. For the polar RWT, suppression of the diffuse double layer would allow easier access of the RWT to the adsorption sites. This would explain the increase in RWT adsorption to the soil (as evidenced by the decrease in RWT equilibrium aqueous phase concentration) with increased suppression of the diffuse double layer (with increasing valency and concentration). The polar nature of RWT adsorption (evidenced by these results) helps to explain the deviation of the level of RWT adsorption from that estimated based on empirical relationships which were developed using nonpolar solutes.

An isotherm was determined for RWT with background ions added (10^{-2} N CaCl_2) and using the South Ames alluvial material (BRACA in Table 8). Figure 20 shows the resulting isotherm with the linear and Freundlich parameters summarized in Table 8. This isotherm (BRACA) differs from a previous isotherm (BRA) by the addition of the CaCl_2 . The K_p value for BRACA (9.7) was greater by a factor of more than two than that with no background ions added. Figure 21 shows the two isotherms (BRA and BRACA) plotted jointly. For a given equilibrium concentration it is observed

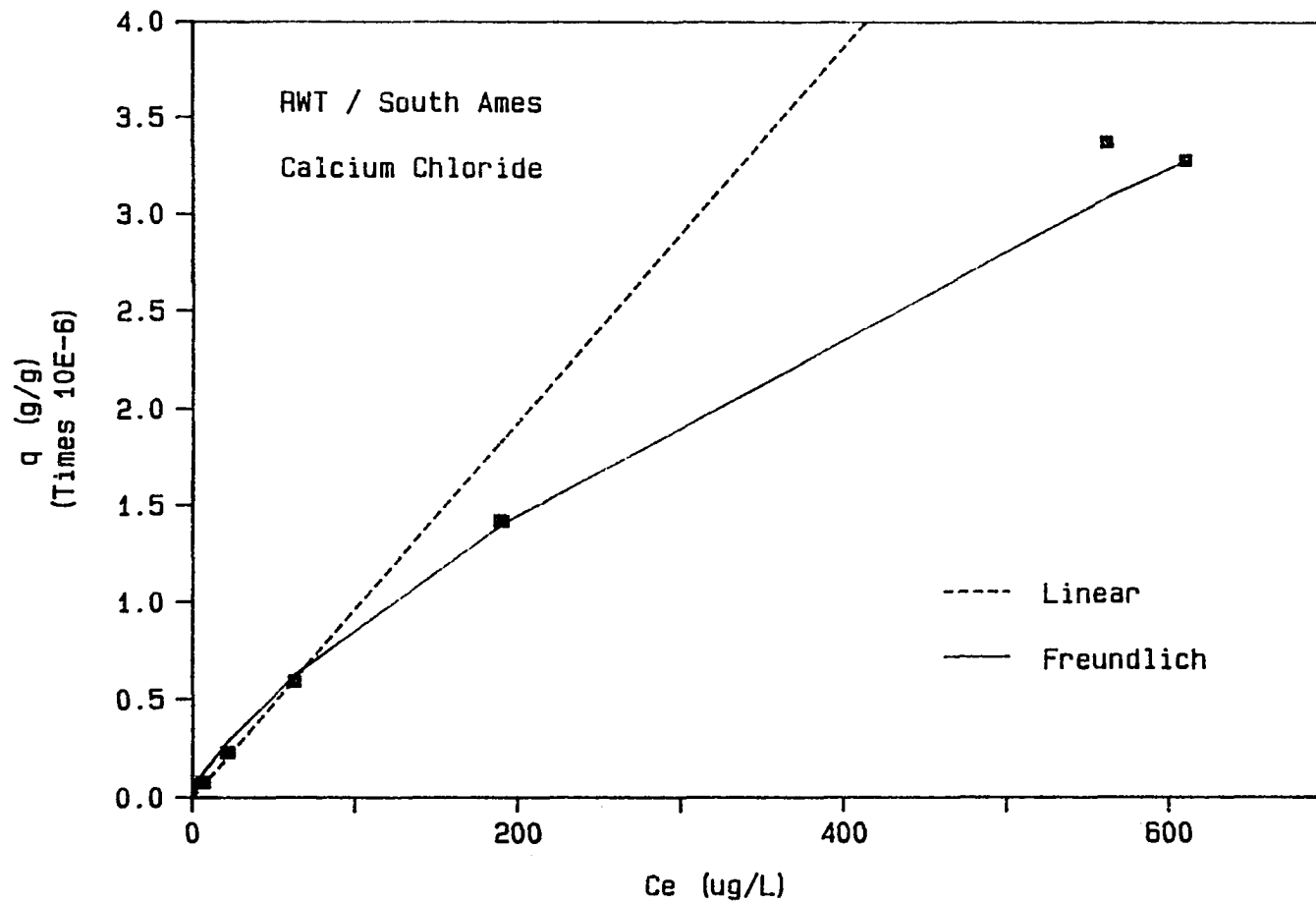


Figure 20: Rhodamine WT adsorption isotherm (South Ames, CaCl₂)

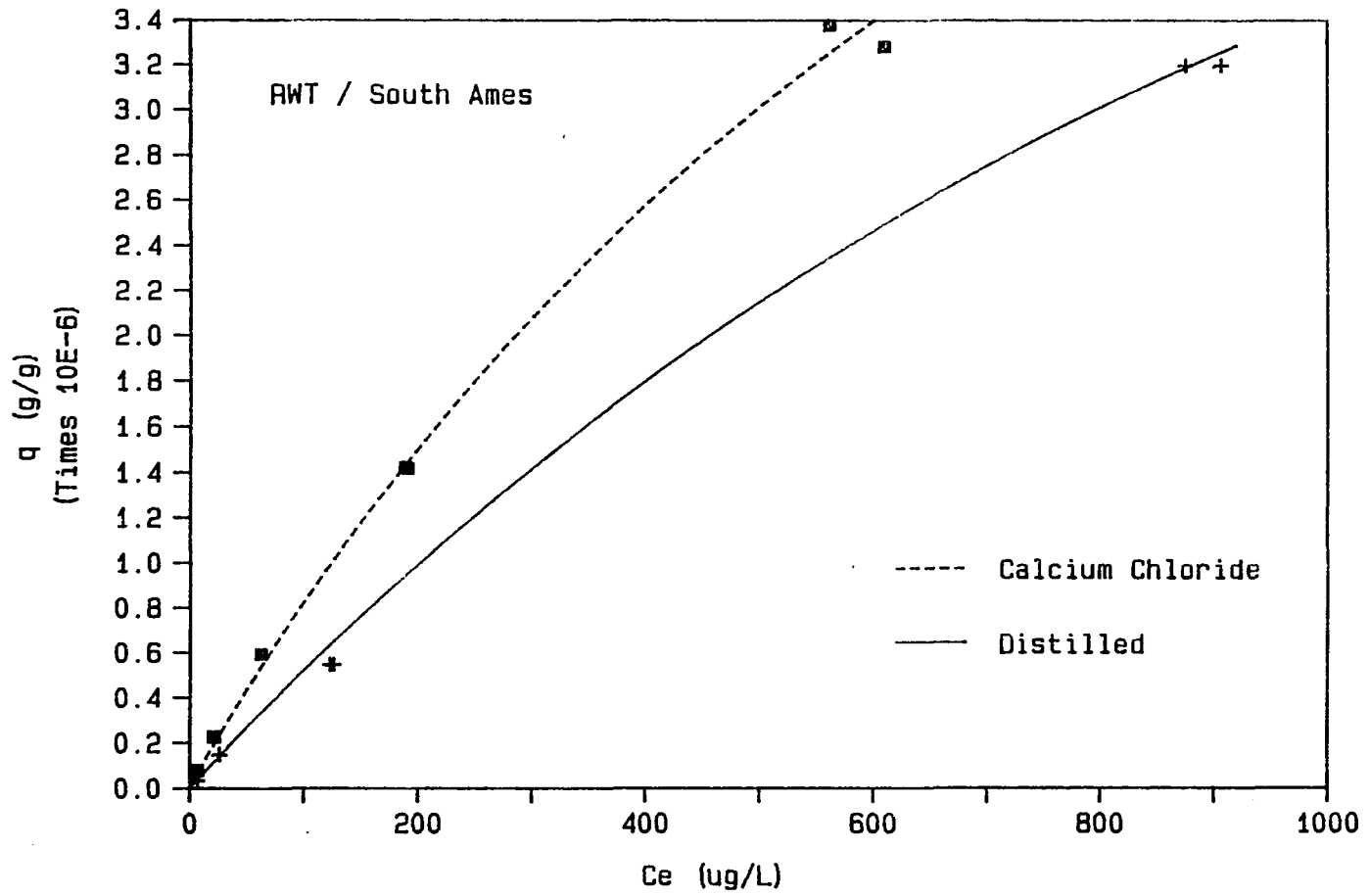


Figure 21: Rhodamine WT adsorption isotherm with and without CaCl_2 (South Ames)

that the level of adsorption (q) is greater with the addition of CaCl_2 . The isotherm is observed to vary from linearity at a lower equilibrium concentration with CaCl_2 than with no background ions added. Using the point of deviation of the linear and the Freundlich plots as the point where nonlinear adsorption becomes evident, the deviation from linearity occurs at $230 \mu\text{g/L}$ without CaCl_2 (Figure 16) versus $80 \mu\text{g/L}$ with CaCl_2 (Figure 20). However, the mass of RWT adsorbed at $80 \mu\text{g/L}$ with CaCl_2 and $230 \mu\text{g/L}$ without CaCl_2 is similar (0.75×10^{-6} versus 1.0×10^{-6} , respectively). This suggests that, while the background ions reduce the driving force (concentration gradient) necessary to achieve a certain level of adsorption, the adsorption limitations which cause nonlinear adsorption are not affected as significantly by the background ions. This would agree with the hypothesis that the background ions serve to suppress the diffuse double layer.

COLUMN STUDIES

While adsorption information is relatively easy to obtain with batch studies, the environment of continuous flow column studies more closely resembles that of porous media flow. For this reason, column breakthrough (adsorption) and elution (desorption) curves for the pesticides and the fluorescent dyes were measured. The raw data for the column studies appear in Appendix B.

The breakthrough of a conservative tracer (chloride) was evaluated in each column run. The chloride breakthrough curve was complete within two pore volumes for all runs and this information was utilized to obtain the hydrodynamic dispersion coefficient (D_x) for each column run. The chloride breakthrough curves indicated that saturated conditions existed during the column runs, that the flow through the porous media occurred without significant preferential flow and that the P_e number (relative magnitude of advective and dispersive transport) was relatively independent of pore water velocity (Table 11).

Pesticides

Breakthrough and elution curves were collected for atrazine and alachlor. Due to the time and expense involved in analyzing pesticides, only the South Ames alluvial aquifer material was investigated during column runs. Preliminary batch tests for atrazine and alachlor indicated no significant effect of background ions on the level of adsorption realized. The adsorption of atrazine and alachlor was observed to be

Table 11. Column parameters for atrazine and alachlor column runs

Run	CO ($\mu\text{g/L}$)		PWV (cm/h)	Length (cm)	Weight (g)	Porosity	D_x (cm^2/h)	P_e	Switch to Desorption (V/V0)
	Atrazine	Alachlor							
CPA10	200	200	10.6	11.8	380.0	0.38	9.7	12.9	11.8
CPA5	200	200	5.5	11.8	384.3	0.37	5.0	13.0	18.3
CPA30	200	200	30.3	12.4	387.4	0.40	33.3	11.3	19.5

linear during the batch tests for the concentration ranges investigated and competitive adsorption was not evidenced. Thus, the pesticide column runs were conducted with atrazine and alachlor present jointly and the major variables investigated were the effect of pesticide and pore water velocity (detention time) on the breakthrough curves.

Breakthrough curves for atrazine and alachlor

Breakthrough and elution curves for atrazine and alachlor were analyzed in a single column run using the South Ames material and a pore water velocity of 10.6 cm/h. The conditions for the column run are summarized in Table 11 (CPA10) for atrazine and alachlor and the breakthrough curves are shown in Figure 22. The alachlor was observed to be more highly adsorbed (retarded) than the atrazine, as observed during the batch tests. The alachlor did not reach a value of C/C_0 of 1.0 during the column breakthrough but instead appeared to level off at a value of C/C_0 of 0.85. The adsorption of atrazine and alachlor was observed to be reversible (desorption occurred) during the elution studies, indicating physical adsorption. Mass balances showed 105% recovery for the atrazine and 68% recovery for the alachlor. The lower recovery of the alachlor suggests that some other mechanism (e.g., degradation, volatilization) may have been responsible for alachlor loss during the column breakthrough. The chromatograms showed no evidence of new peaks during the column run (the presence of new peaks would have suggested the appearance of metabolites) and no evidence of volatilization was observed for the stock solution during the column run.

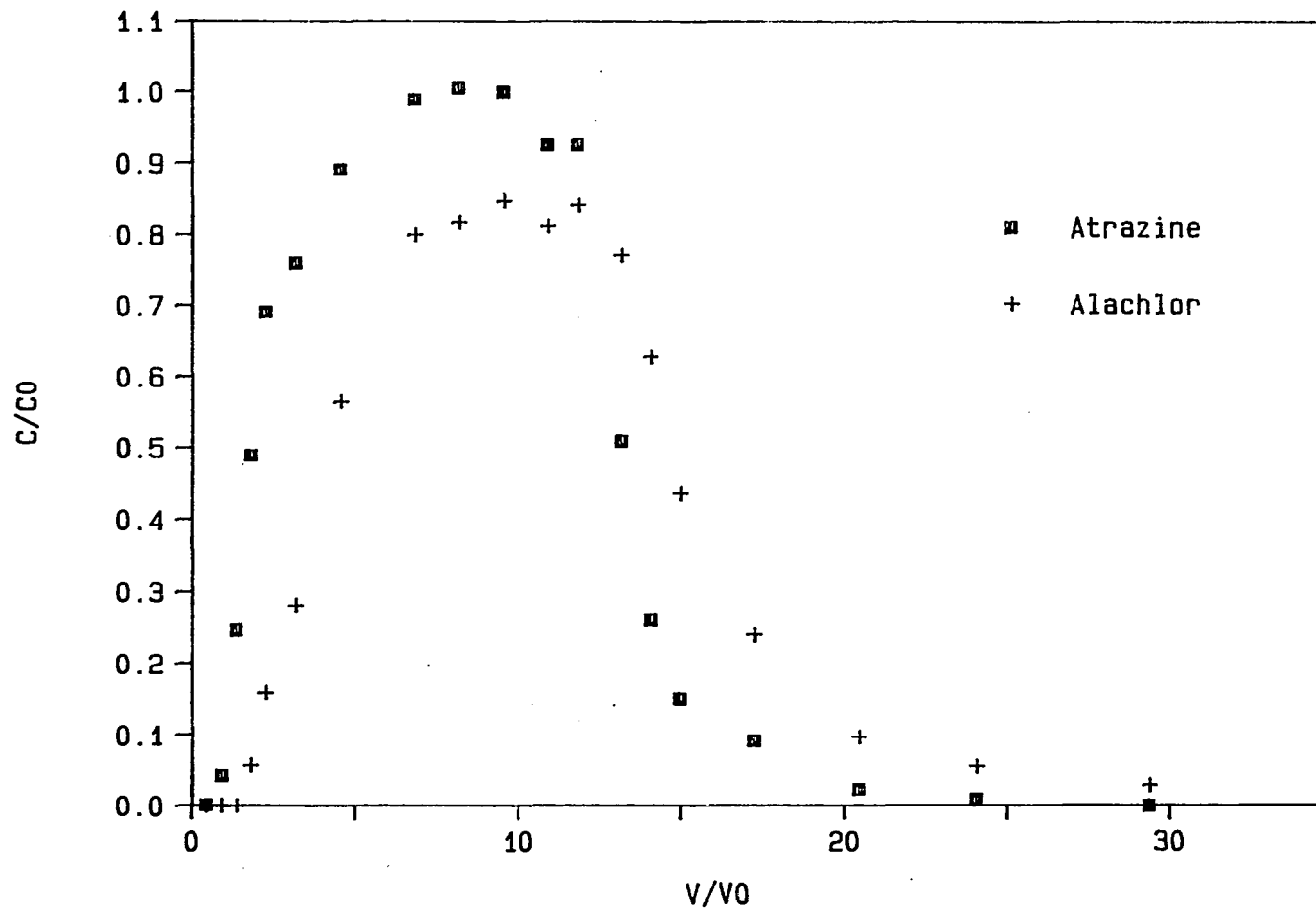


Figure 22: Atrazine and alachlor breakthrough curves (10.6 cm/h)

Subsequent column runs were conducted for additional pore volumes to determine if the alachlor would reach complete breakthrough.

Several techniques may be used to compare the results observed in column studies with those obtained in batch studies. For a sigmoidal breakthrough curve, the retardation factor (r_f) may be established by determining the relative pore volume corresponding to C/C_0 equal to 0.5. The value of K_p may then be determined from r_f according to Equation 13. For nonsigmoidal breakthrough curves (as evidenced for RWT in this study and nonequilibrium breakthrough curves in general), this method of determining the K_p value is not adequate (Bouchard et al., 1988). As an alternative for determining K_p values, the following method was utilized. As the breakthrough curve reaches completion (C/C_0 of 1.0), it is possible from mass balance considerations to calculate the mass of chemical adsorbed to the soil. Combining the mass of the chemical adsorbed with the mass of the soil in the column results in a value for q (g chemical adsorbed / g soil). At complete breakthrough, the liquid phase concentration throughout the column is the same (C_0). This is the equilibrium chemical concentration (C_e) throughout the column which determines the level of adsorption (q) determined above. The q and C_e values correspond to a single point isotherm and a K_p value can be determined. Values for K_p determined from the column run by this method and those determined from the batch studies are compared in Table 12.

From Table 12, the K_p values determined from the column run are seen to be less than those determined in the batch tests for both the atrazine and the alachlor. Bouchard et al. (1988) reported data that gave ratios

Table 12. Column adsorption parameters from column run CPA10 for atrazine and alachlor

Parameter	atrazine	alachlor
Mass Soil (g)	380.0	380.0
Mass pesticide adsorbed (g)	2.2×10^{-5}	7.1×10^{-5}
C_e ($\mu\text{g/L}$)	200	200
$(K_p)_{\text{column}}$ (cm^3/g)	0.30	0.93
$(K_{oc})_{\text{column}}$ (cm^3/g)	111	344
$(K_p)_{\text{batch}}$ (cm^3/g)	0.40	1.08
$(r_f)_{\text{batch}}$	2.7	5.7
$(r_f)_{\text{column}}^a$	1.9	4.3
$(r_f)_{\text{column}}^b$	2.3	5.0
$(r_f)_{\text{column}}^b / (r_f)_{\text{column}}^a$	1.2	1.2

^aDetermined from $C/C_0 = 0.5$.

^bDetermined from $(K_p)_{\text{column}}$.

of column to batch K_p values in the range of 0.43 to 0.74. The ratios of column to batch K_p values for atrazine and alachlor from Table 12 are 0.75 and 0.87, respectively. If the leveling of the breakthrough curve at a value of C/C_0 of 0.85 for the alachlor breakthrough was due to some mechanism other than adsorption, then the K_p value determined from the column run was artificially high (the mass actually adsorbed was less than calculated based on mass balance considerations). This would account for the higher ratio of column to batch K_p values for alachlor, and may explain why this ratio was outside the range of Bouchard et al. (1988).

Researchers have suggested that the relative degree of nonequilibrium for a breakthrough curve may be determined by taking the ratio of values for r_f determined at $C/C_0 = 0.5$ and r_f determined using the K_p value determined from the column run (Bouchard et al., 1988). For a sigmoidal breakthrough curve (and linear adsorption conditions), the ratio of r_f values determined by each method will be unity. As the ratio deviates from unity, increased nonequilibrium conditions are indicated (fronting and/or tailing of the breakthrough curve). The ratios for atrazine and alachlor (as seen in Table 12) are both 1.2 and indicate nonequilibrium conditions (as observed by visual inspection of the breakthrough curves). Bouchard et al. (1988) reported ratios in the range of 0.96 to 1.64 with the higher ratios being for higher organic carbon content soils.

The relative pore volume when desorption was initiated is shown in Table 11. The elution curves for atrazine and alachlor did not return to

$C/C_0 = 0.0$ in the same number of pore volumes that it took to reach equilibrium breakthrough ($C/C_0 = 1.0$ for atrazine and 0.85 for alachlor). Thus, hysteresis of desorption was observed for atrazine and alachlor.

Effect of pore water velocity

To evaluate the kinetics of adsorption in the soil column, additional column studies for atrazine and alachlor were conducted with lower and higher pore water velocities. The lower pore water velocity investigated was 5.5 cm/h (CPA5 in Table 11) and the higher pore water velocity was 30.3 cm/h (CPA30 in Table 11). The column results for all three pore water velocities for atrazine are shown in Figure 23 and for alachlor are shown in Figure 24. The breakthrough curves were conducted for additional pore volumes for the latter column runs to determine if the alachlor would reach complete breakthrough ($C/C_0 = 1.0$). Thus, the initiation of desorption occurred at different values of V/V_0 for all of the column runs (as shown in Table 11). For ease of comparison, the elution curves were normalized such that a value for $V/V_0 = 0.0$ indicates the point when desorption was begun for each individual column run. These normalized elution curves are shown for atrazine in Figure 25 and alachlor in Figure 26.

It is observed from Figure 23 that decreasing the pore water velocity from 10.6 to 5.5 cm/h did not affect the appearance of the atrazine breakthrough curve while increasing the pore water velocity from 10.6 to 30.3 cm/h caused the atrazine breakthrough curve to appear within fewer pore volumes. The atrazine r_f values (from $C/C_0 = 0.5$) for pore

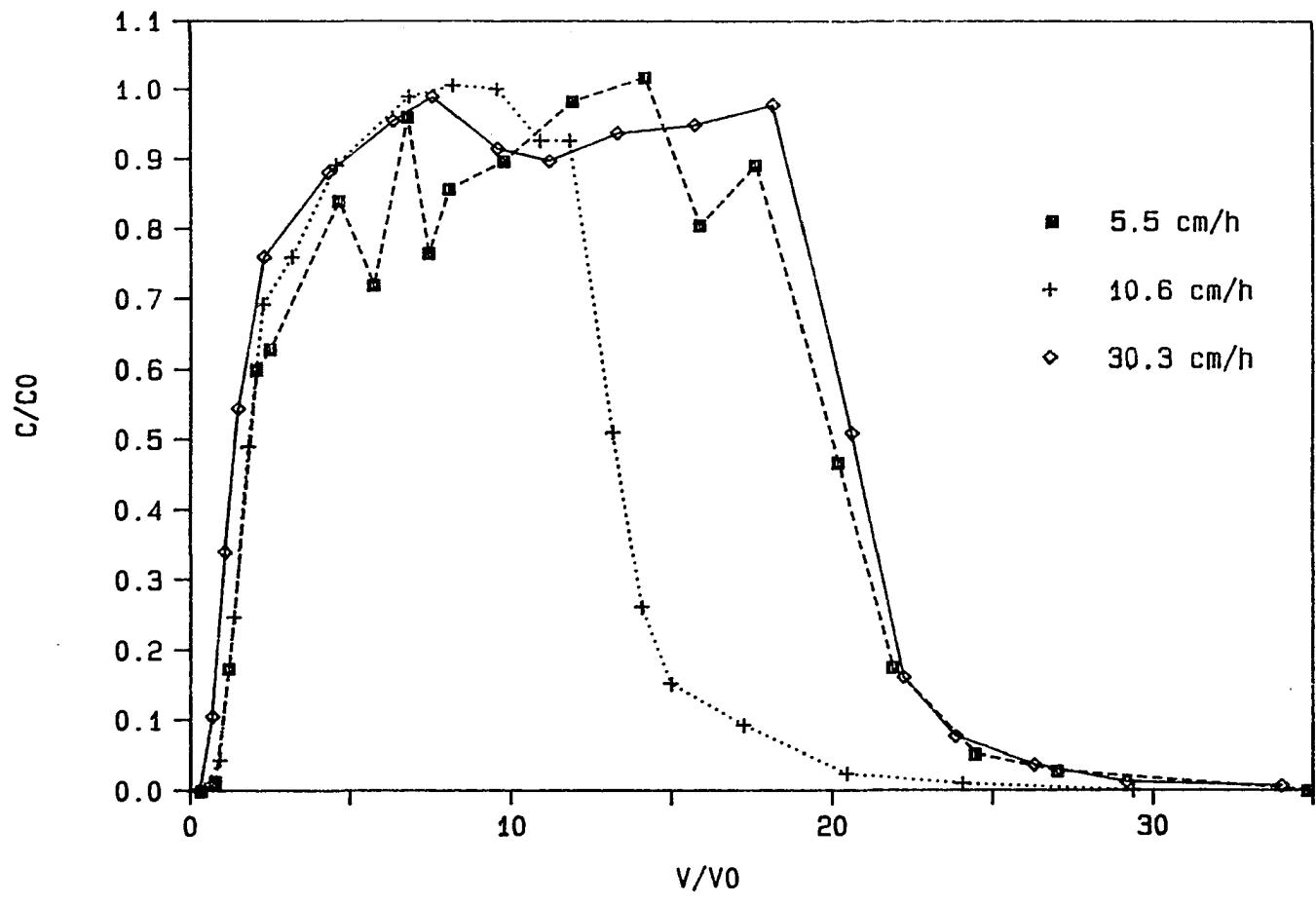


Figure 23: Atrazine breakthrough curves at three pore water velocities

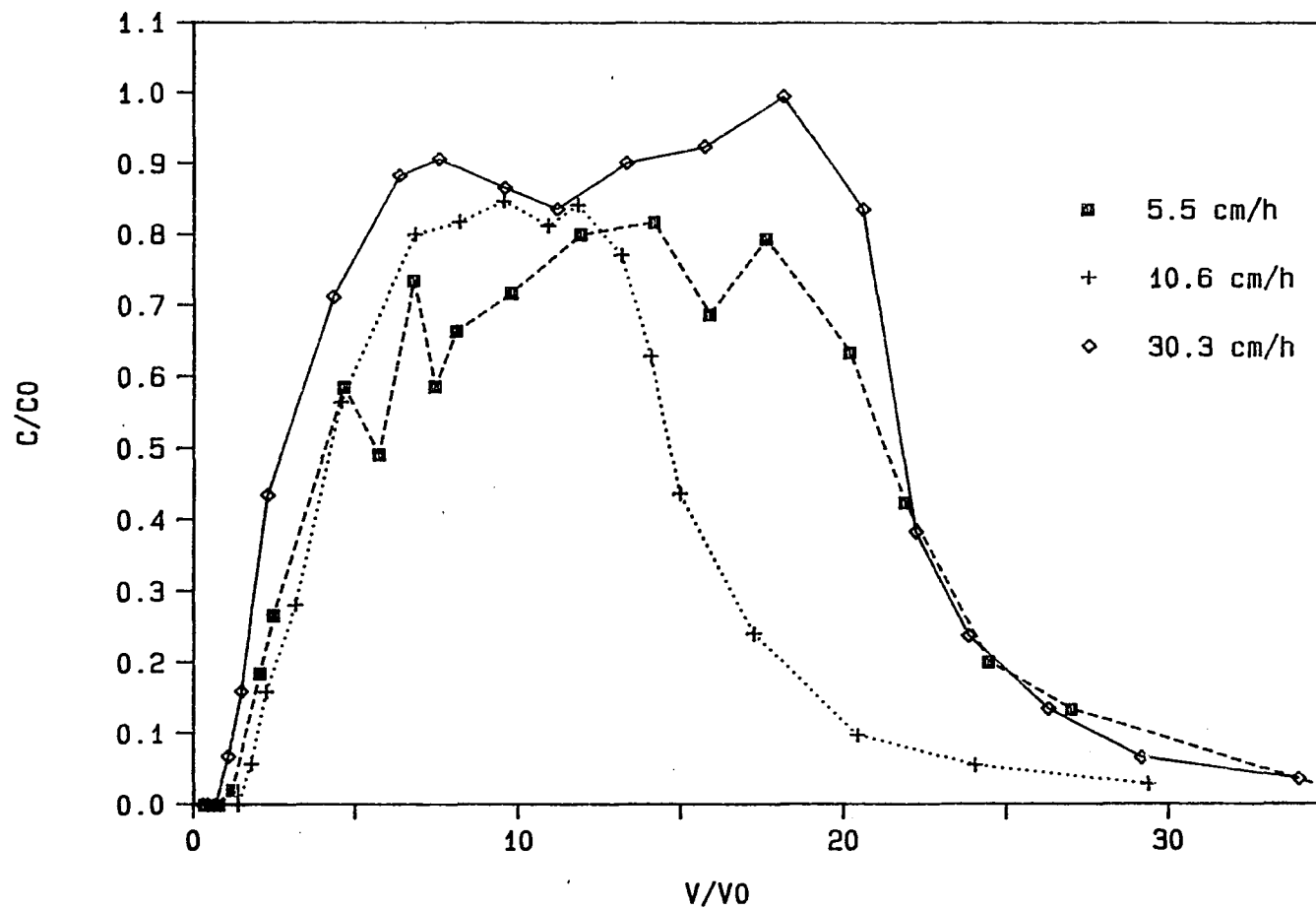


Figure 24: Alachlor breakthrough curves at three pore water velocities

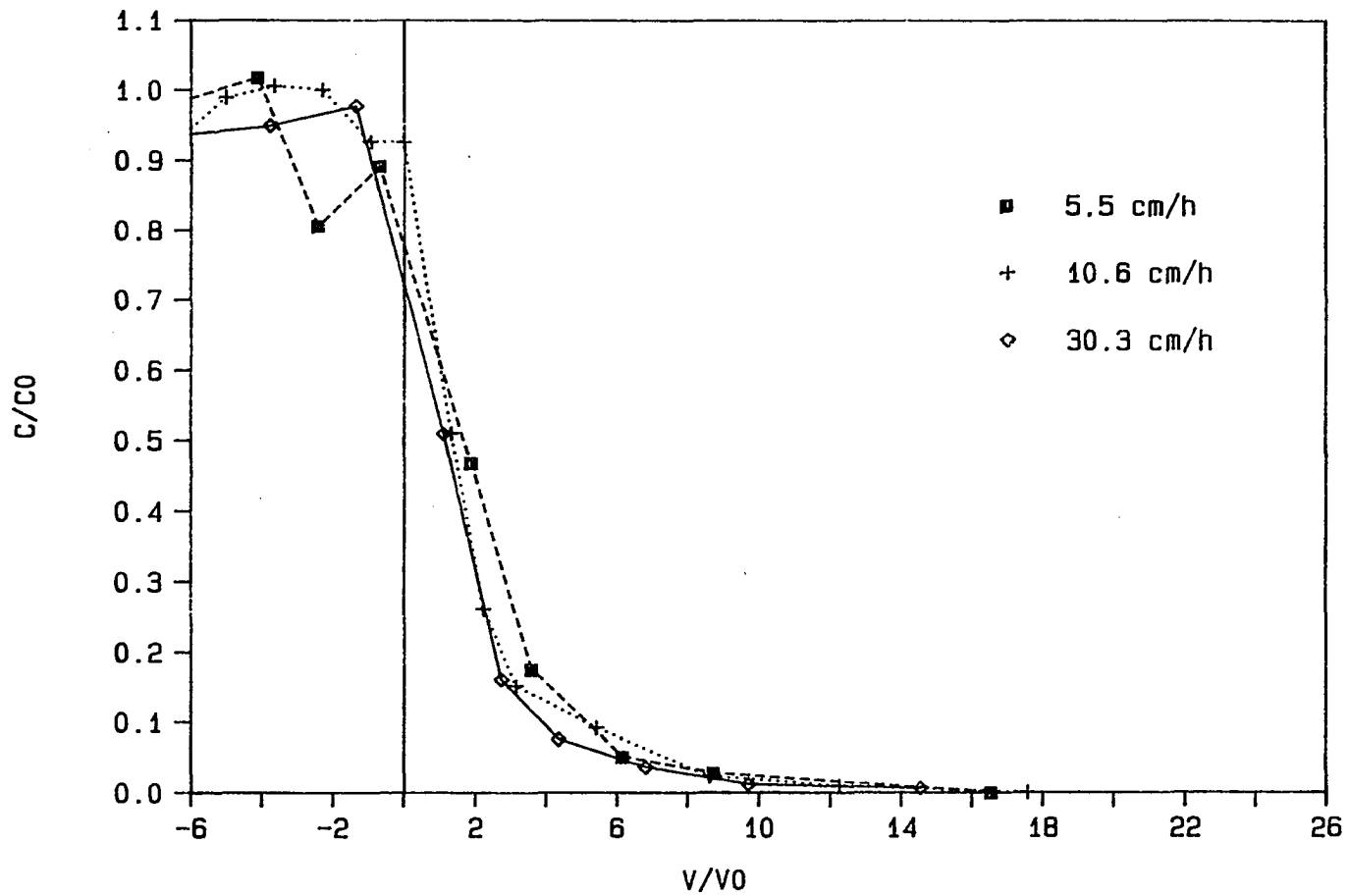


Figure 25: Atrazine elution curves at three pore water velocities (normalized such that $V/V_0 = 0.0$ corresponds to initiation of desorption)

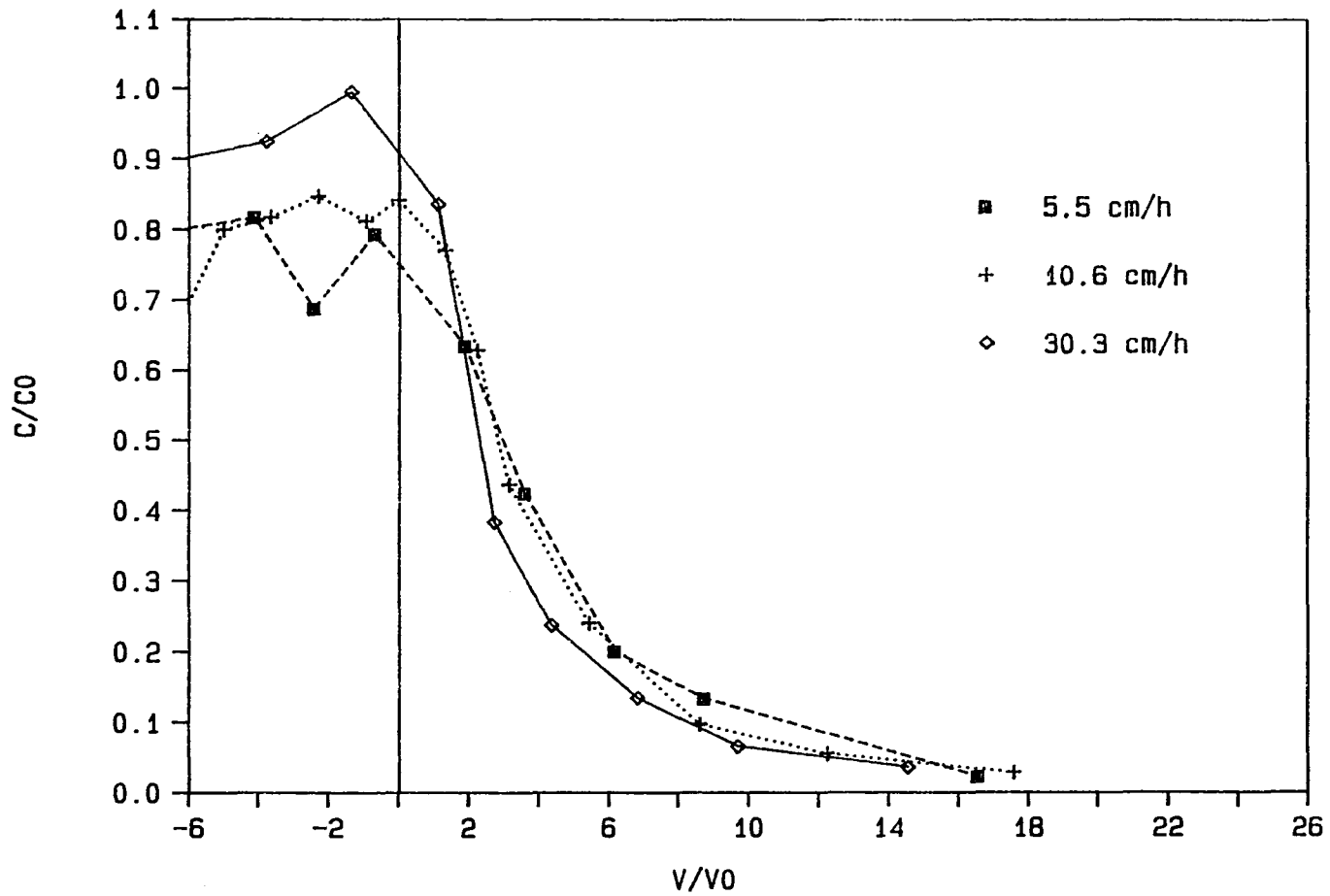


Figure 26: Alachlor elution curves at three pore water velocities (normalized such that $V/V_0 = 0.0$ corresponds to initiation of desorption)

water velocities of 5.5, 10.6 and 30.3 cm/h were 1.9, 1.9 and 1.4, respectively. The chloride breakthrough curves were observed to be relatively independent of pore water velocity (Pe was relatively constant, see Table 11), indicating that the column hydrodynamics were not responsible for the differences in the pesticide breakthrough curves. Some scatter was observed in the pesticide concentrations, as was expected due to the low concentration of pesticides investigated (200 $\mu\text{g/L}$) and the small sample sizes available for extraction. Figure 25 shows the elution curves appearing after fewer pore volumes with increasing pore water velocity.

For alachlor, the increasing pore water velocity was also observed to cause breakthrough at fewer pore volumes, as observed in Figure 24. The alachlor r_f values (from $C/C_0 = 0.5$) for pore water velocities of 5.5, 10.6 and 30.3 cm/h were 4.2, 4.1 and 2.8, respectively. It is observed from Figure 26 that the elution curves appeared after fewer pore volumes with increasing pore water velocities.

Increasing the pore water velocity (decreasing the column detention time) appeared to result in a higher value of C/C_0 for alachlor (Figure 24). This may suggest that the nonadsorption mechanism responsible for alachlor loss was dependent on the detention time in the column. The percent recoveries of alachlor for pore water velocities of 5.5, 10.6 and 30.3 cm/h were 60, 68 and 72%, respectively. Baker and Johnson (1979), utilizing agricultural field plots, determined half lives ($t_{1/2}$) for alachlor in the range of 8 to 17 days. It may be possible that degradation was the cause for the loss of alachlor experienced in this

study, although GC chromatograms showed no evidence of new peaks which would be expected for metabolites.

Fluorescent Dyes

Breakthrough and elution curves were collected for RWT and fluorescein. Experimental variations considered were the result of observations made from the batch results.

Breakthrough curves for rhodamine WT and fluorescein

Breakthrough and elution curves for RWT and fluorescein were compared using the South Ames alluvial aquifer material. The conditions for the column studies are summarized in Table 13 (CRA for RWT and CFA for fluorescein). Figure 27 shows the breakthrough and elution curves for RWT and Figure 28 for fluorescein. Based on results of the batch studies, the concentrations of the fluorescent dyes utilized were in the linear adsorption range. Mass balances of breakthrough and elution curves for the fluorescent dyes indicated virtually complete recovery of the dyes (85 to 110%) for all column runs. This indicates that the adsorption of the fluorescent dyes is reversible (physical adsorption) and that degradation of the fluorescent dyes was not evident in the columns.

The breakthrough curve for RWT (Figure 27) is not the conventional sigmoidal form but instead has a plateau at a value of C/C_0 of 0.5. This plateau was evidenced for approximately 20 pore volumes prior to C/C_0 values increasing again. The second leg of the breakthrough curve was of

Table 13. Column parameters for rhodamine WT and fluorescein column runs

Run	Dye	CO ($\mu\text{g/L}$)	PWV (cm/h)	Soil Type ^a	Length (cm)	Weight (g)	Porosity	Conservative Tracer	D_x (cm^2/h)
CRA	RWT	201	11.7	SA	13.0	388.0	0.42	NaCl	7.6
CFA	Fluorescein	225	13.2	SA	9.0	300.0	0.36	CaCl_2	5.9
CRACA	RWT	195	11.3	SA	12.0	360.0	0.42	CaCl_2	7.9
CRH	RWT	200	30.0	H	13.0	127.9 ^b	0.30	CaCl_2	19.0
CRAHP	RWT	198	34.1	SA	11.0	352.0	0.38	NaCl	15.0
CRAHC	RWT	1950	11.9	SA	11.5	352.0	0.40	NaCl	6.8

^aSoil type: SA = South Ames, H = Halletts.

^bSmaller diameter column (2.5 cm).

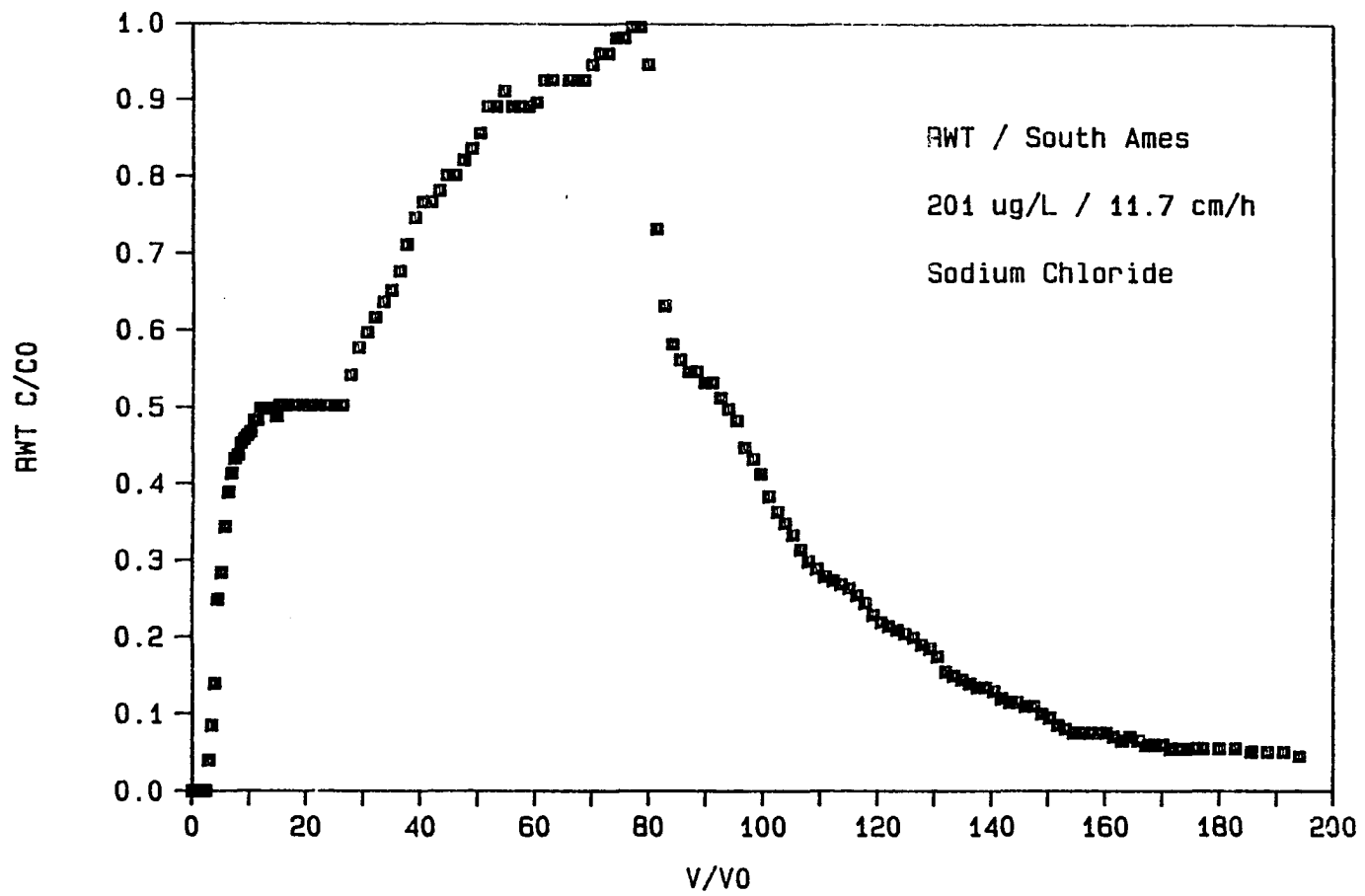


Figure 27: Rhodamine WT breakthrough curve (South Ames, NaCl, 11.7 cm/h, 201 $\mu\text{g/L}$)

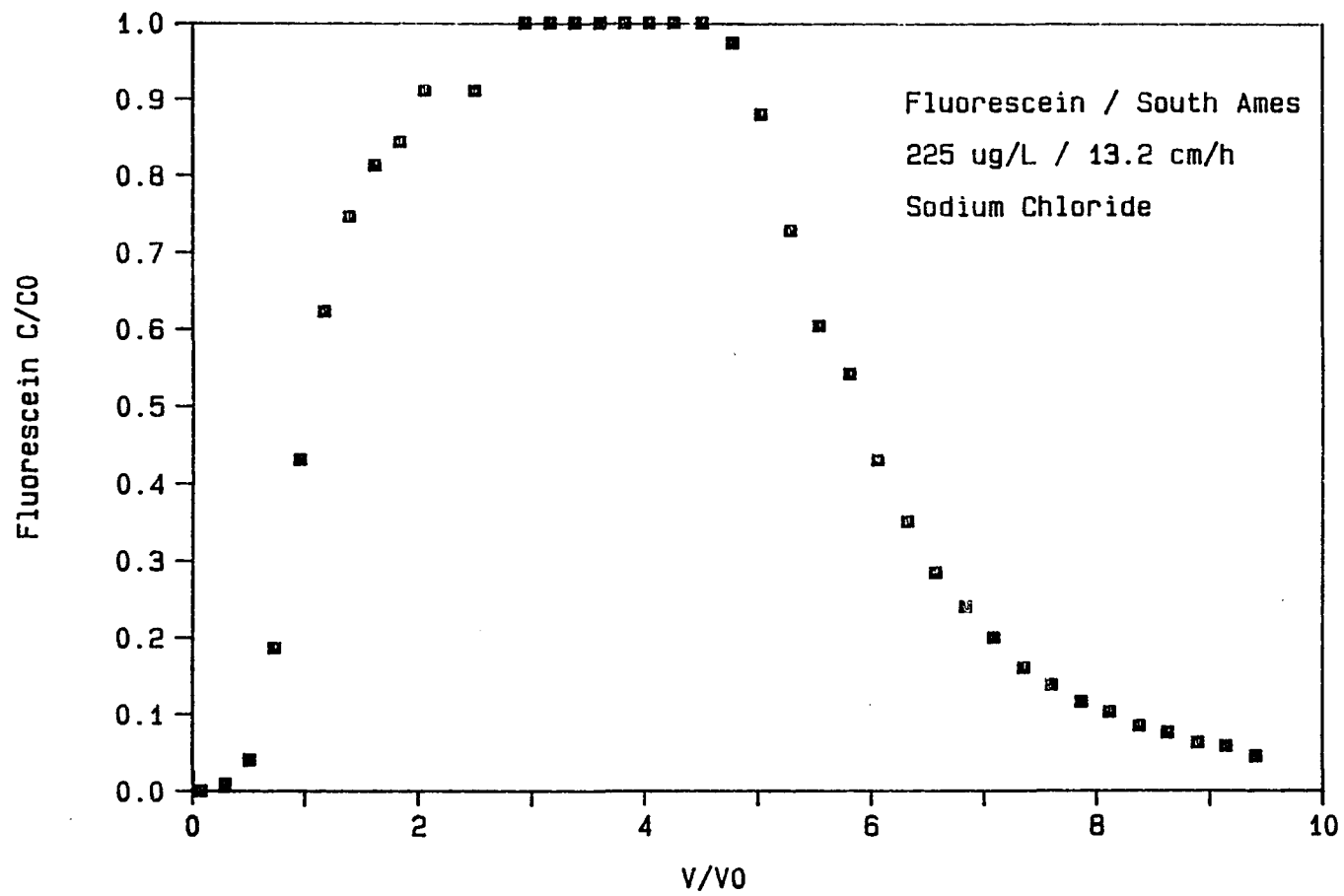


Figure 28: Fluorescein breakthrough curve

a shallower slope than the first leg. This two leg breakthrough curve has also been observed by Everts (1988) for RWT and a surface soil. The elution curve did not demonstrate a plateau but did demonstrate hysteresis of desorption (the elution curve had not reached a value of C/C_0 of 0.0 in the same number of pore volumes required for the breakthrough curve to reach a C/C_0 value of 1.0).

The breakthrough curve for fluorescein (Figure 28) occurred in much fewer pore volumes than for RWT and did not demonstrate the plateau observed for the RWT. Hysteresis of desorption was evidenced for the fluorescein elution curve. A comparison of the column results for fluorescein and RWT is shown in Figure 29.

Values for K_p determined by mass balance from the column runs are shown in Table 14 for RWT (CRA) and fluorescein (CFA). The K_p value determined for RWT from the column run (CRA) is seen to be greater than that measured in the batch test with the ratio of column to batch K_p being 1.5. Typically, K_p values determined in columns are seen to be less than those determined in batch tests due to the kinetic limitations (physical or chemical) of adsorption during porous media flow. Bouchard et al. (1988) reported data that gave ratios of column to batch K_p values in the range of 0.43 to 0.74. Either the nature of the batch system decreased the level of adsorption for RWT or the nature of the column system increased the level of adsorption for RWT. With the data collected in this research, it was not possible to determine the mechanism(s) responsible for this phenomena. The investigation of the mechanism(s) responsible for this phenomena should be the focus of future

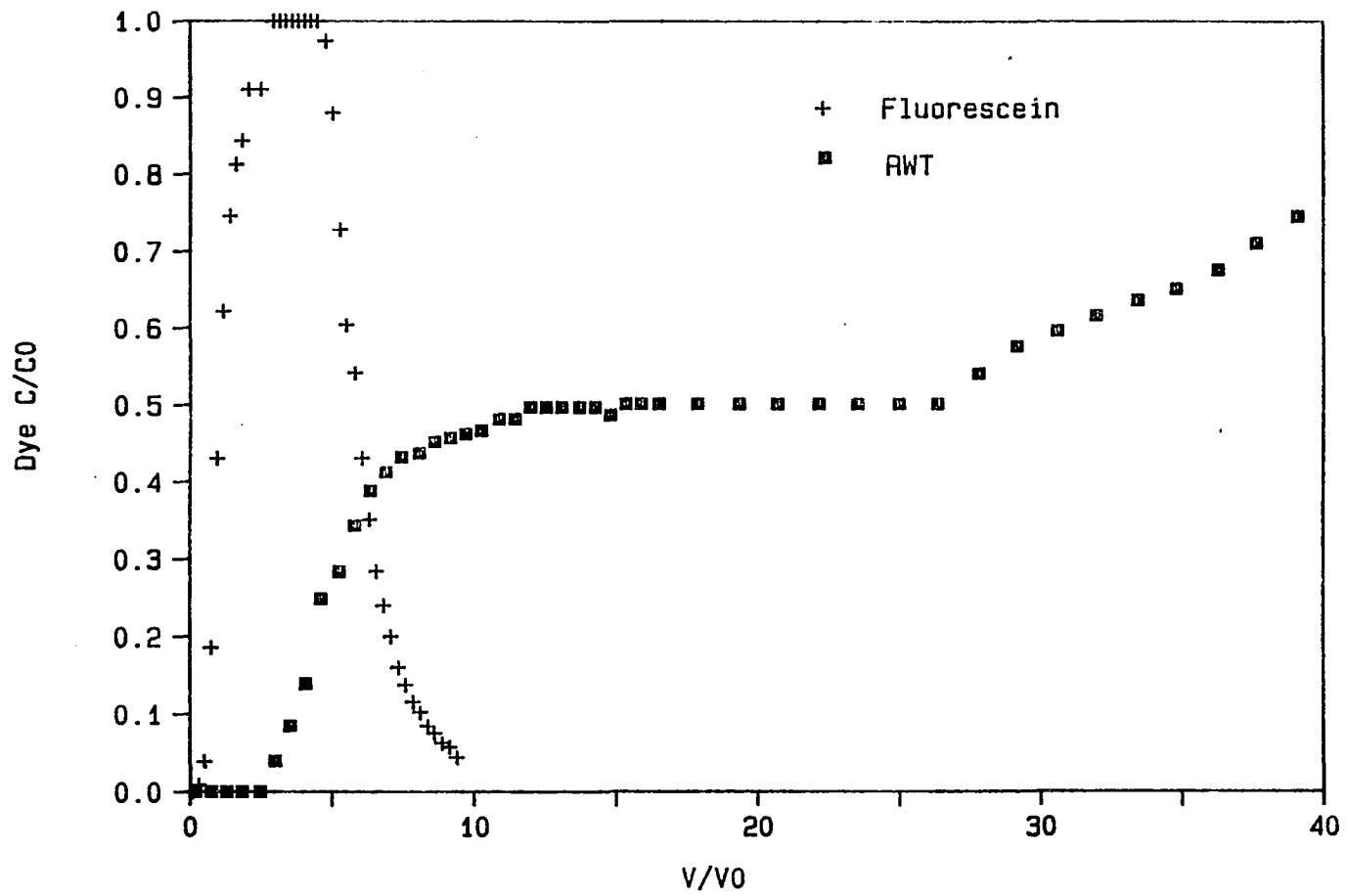


Figure 29: Comparison of rhodamine WT and fluorescein column results

Table 14. Column adsorption results for rhodamine WT and fluorescein column runs

Run	Dye	Soil Type ^a	Conservative Tracer	Mass Soil (g)	Mass Dye Adsorbed ($\times 10^{-4}$ g)	C_e ($\mu\text{g/L}$)	$(K_p)_{\text{column}}$ (cm^3/g)	$(K_p)_{\text{batch}}$ (cm^3/g)
CRA	RWT	SA	NaCl	388.0	5.2	201	6.9	4.5
CFA	Fluorescein	SA	CaCl_2	300.0	0.03	225	0.05	0.33
CRACA	RWT	SA	CaCl_2	360.0	11.0	195	15.7	9.7
CRH	RWT	H	CaCl_2	127.9 ^b	1.7	200	6.6	---
CRAHP	RWT	SA	NaCl	352.0	3.0	198	4.3	4.5
CRAHC	RWT	SA	NaCl	352.0	17.0	1950	2.5	4.5

^aSoil type: SA = South Ames, H = Halletts.

^bSmaller diameter column (2.5 cm).

research.

The K_p value determined for the fluorescein column run (Table 14, CFA) is observed to be less than that observed during the batch test with the ratio of column to batch K_p values being 0.15. This ratio is smaller than typically observed (0.43 to 0.74 after Bouchard et al., 1988). The fluorescein breakthrough curve was not significantly retarded from the chloride breakthrough curve ($C/C_0 = 1.0$ in 3 pore volumes for fluorescein versus 2 pore volumes for chloride). However, for higher organic carbon content surface soils, the fluorescein would be more significantly retarded from the conservative tracer (Omoti and Wild, 1979).

Effect of background ions

The batch studies showed the level of RWT adsorption to be a function of the background ions. The RWT breakthrough curve above (Figure 27 and CRA in Tables 13 and 14) was conducted with sodium chloride as the conservative tracer. The presence of sodium chloride was not observed to significantly affect the level of RWT adsorption during batch tests while the presence of calcium chloride was observed to increase the level of RWT adsorption. For this reason, a column run was conducted with 10^{-2} N CaCl_2 as the conservative tracer in the RWT solution. This breakthrough curve is shown in Figure 30 (CRACA in Tables 13 and 14). Figure 31 shows jointly the RWT column data with CaCl_2 and with NaCl . The increase in K_p values when CaCl_2 was present (Table 14) indicates that the adsorption capacity of the soil for RWT was increased in the presence of CaCl_2 (as observed during the batch studies). From

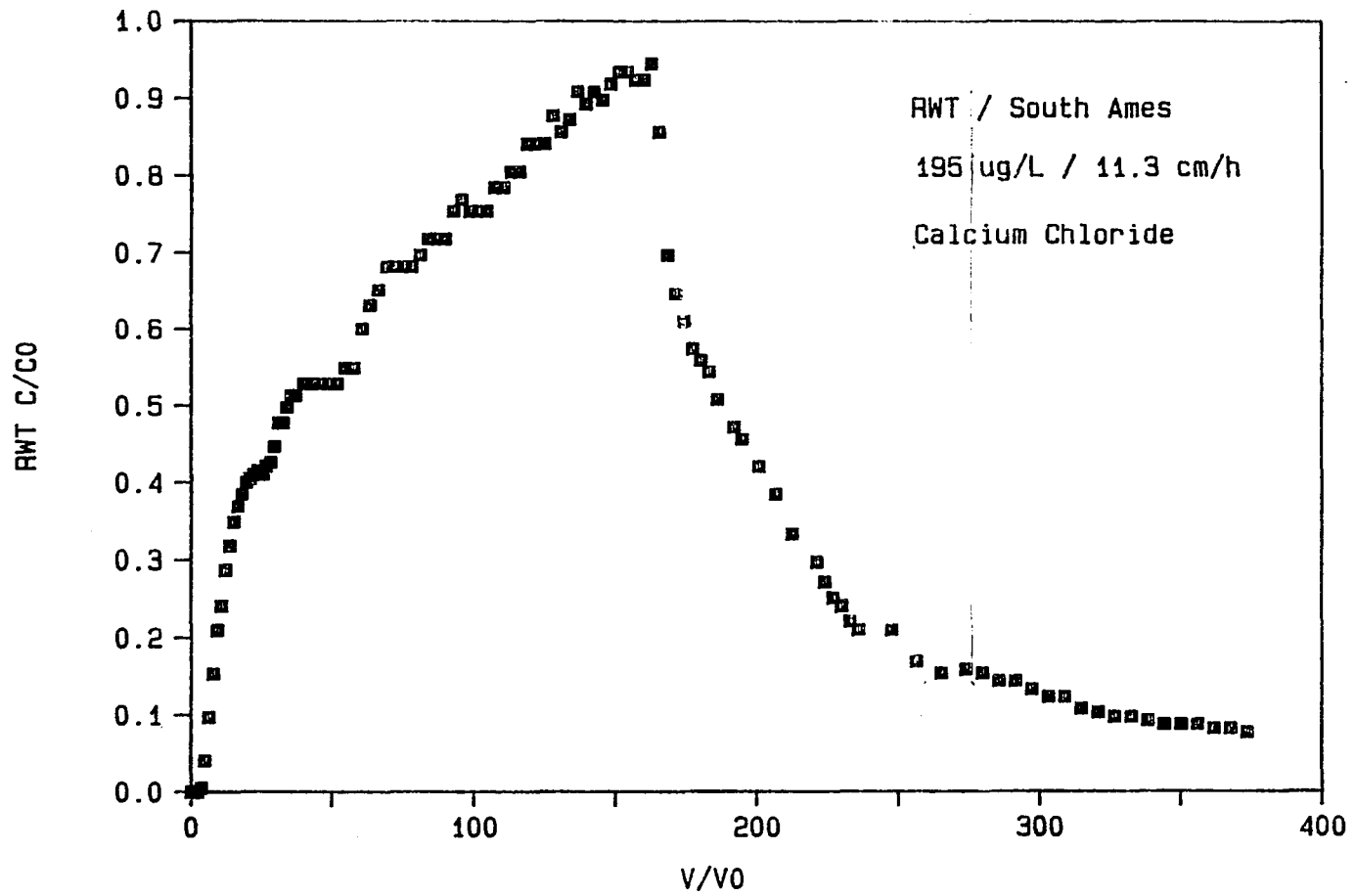


Figure 30: Rhodamine WT breakthrough curve (South Ames, CaCl₂, 11.3 cm/h, 195 μg/L)

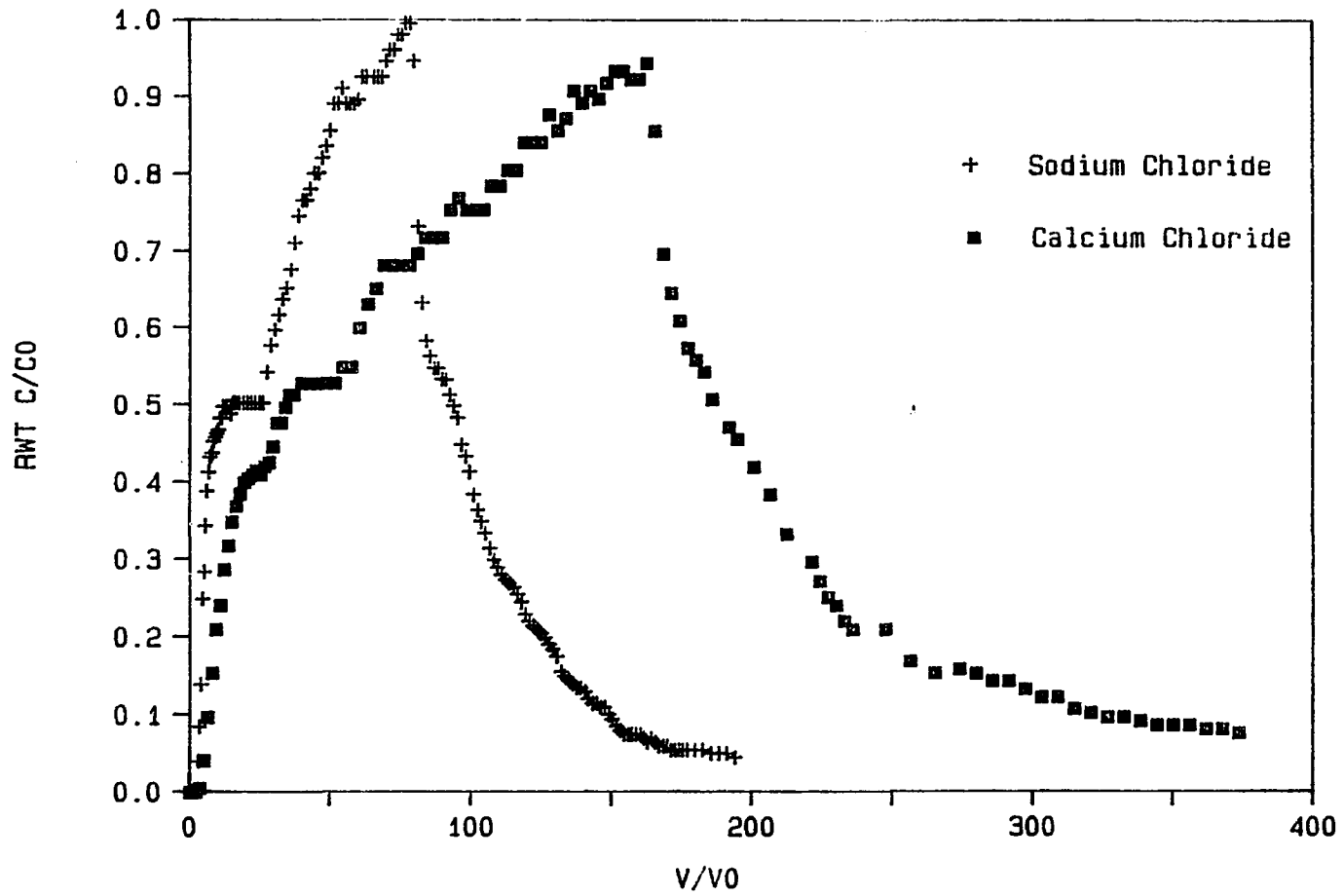


Figure 31: Rhodamine WT breakthrough curves - CaCl₂ versus NaCl

Table 14, it is observed that the ratio of column to batch K_p values (with CaCl_2 as background) was 1.6 while it was 1.5 for RWT without CaCl_2 .

Effect of aquifer material

The breakthrough of RWT with the Halletts alluvial material was investigated to evaluate the occurrence and nature of the two leg breakthrough curve (observed for the South Ames material) with a second alluvial aquifer material. Figure 32 shows the breakthrough curve for RWT with the Halletts alluvial material (CRH in Tables 13 and 14). The conservative tracer used during this column run was CaCl_2 . The breakthrough curve is observed to plateau at a value of C/C_0 of 0.5 and maintain this plateau for approximately ten pore volumes. From the column K_p values (CRACA, Table 14), it is observed that the South Ames material had a higher capacity for adsorbing the RWT than the Halletts material. This is consistent with the batch results and the lower organic carbon content of the Halletts material and may explain why the plateau was evidenced for less pore volumes (10) in this column run than in the column run using the South Ames material (20 pore volumes). Thus, the two leg breakthrough curve has been observed for two aquifer materials in this study and a surface soil by Everts (1988).

Effects of size fractions and organic content

In an effort to better understand the nature of the RWT adsorption and two leg column breakthrough curve, various steps were taken to reduce

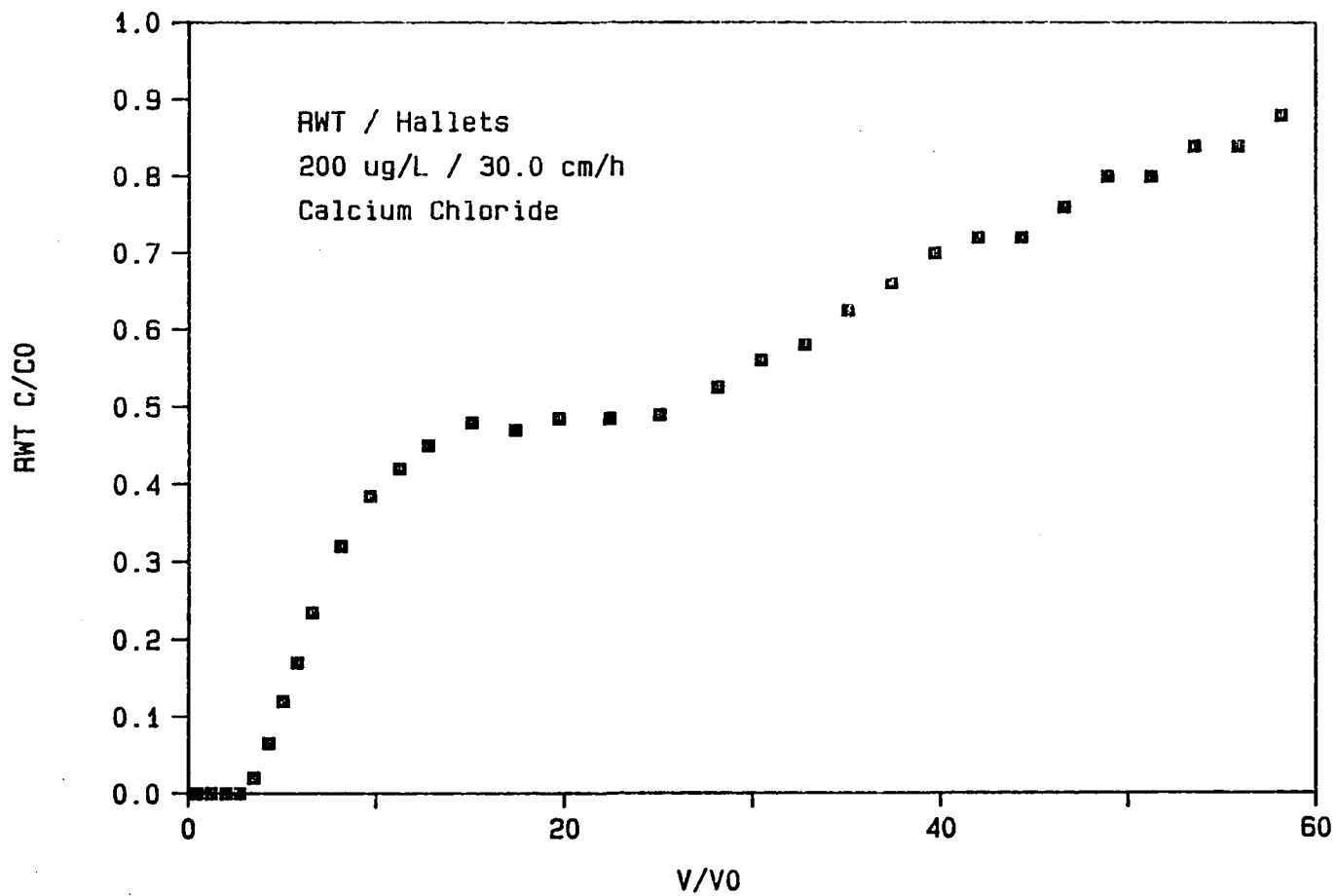


Figure 32: Rhodamine WT breakthrough curve (Hallets, CaCl₂, 30.0 cm/h, 200 μg/L)

the organic content and/or percent fines (clays) in the soil columns. The soil treatments utilized included wet sieving, backwashing and heating at 550 or 850 °C.

Figure 33 shows four column runs which utilized samples of the South Ames alluvial aquifer material subjected to four different treatments with Figure 34 providing increased resolution of the data at the lower pore volumes. Table 15 shows the treatments utilized in each of the four column runs and the adsorption realized. Calcium chloride was utilized as the conservative tracer in all of these column runs. The plot labeled CRACA corresponds to an unaltered sample, as shown previously in Figure 30. The plot labeled BW corresponds to a sample which was retained during wet sieving on a number 200 sieve (75 μm) and then backwashed in a column overnight to assure the removal of the clays. It should be noted that in this process the f_{oc} of the soil was decreased from 0.0027 to 0.0010. The plot labelled HT/850 corresponds to a soil sample heated at 850 °C. This temperature will not only affect the organic carbon content but will also affect some of the clays. Analysis of the clay fraction by x-ray diffraction indicated the presence of kaolinite, illite and sodium and calcium montmorillonite with kaolinite and illite the most likely to be affected at the temperature considered here (Deer et al., 1966). The plot labelled BW-HT/850 corresponds to the backwashed sample from above being heated at 850 °C. This corresponds to the alluvial material minus the fines and the organic content.

The shift from the whole soil curve (CRACA) to the backwashed curve may be attributed to the loss of the clays and/or the loss of the organic

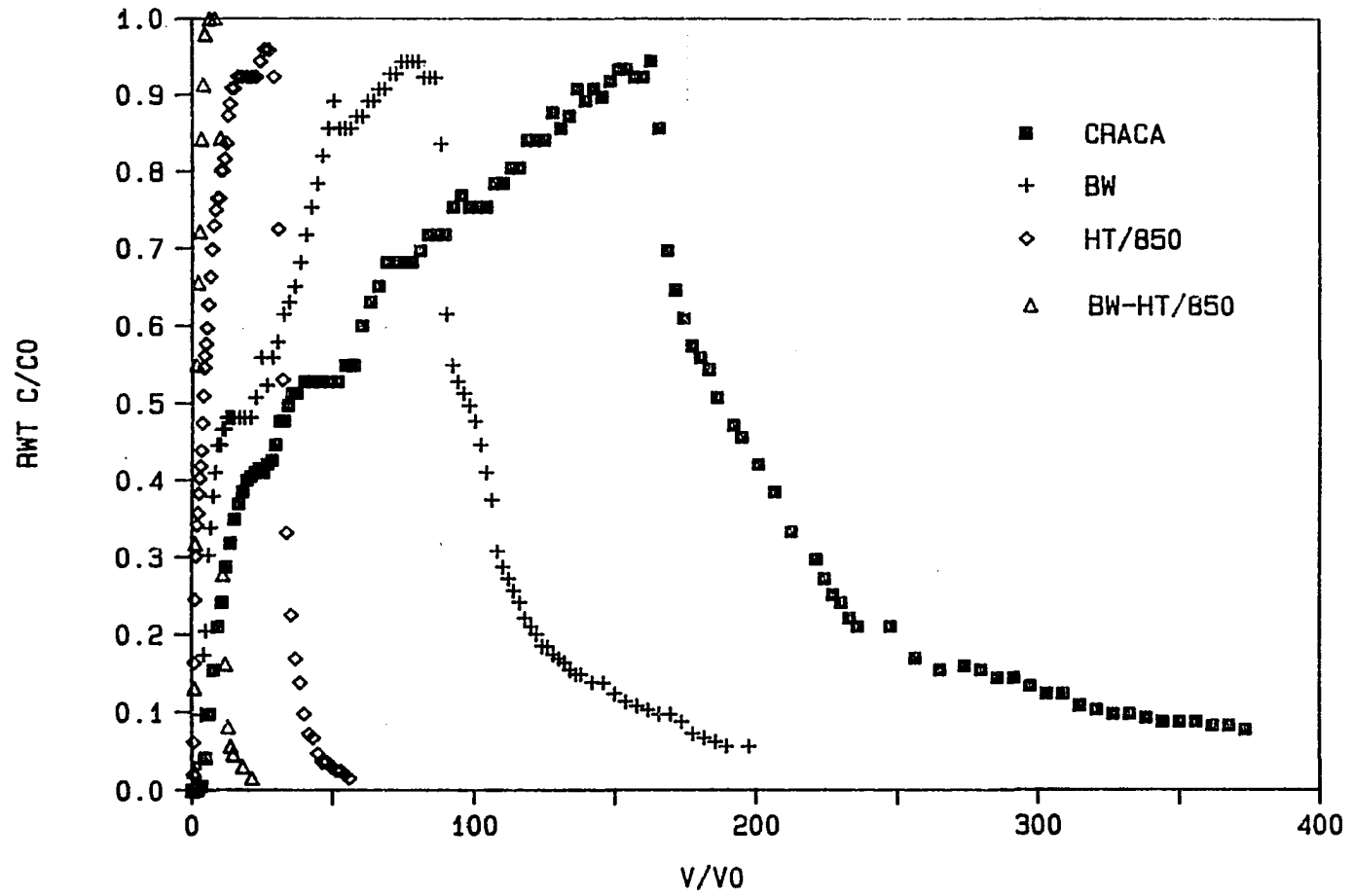


Figure 33: Rhodamine WT column runs with treated soils (0 - 400 pore volumes)

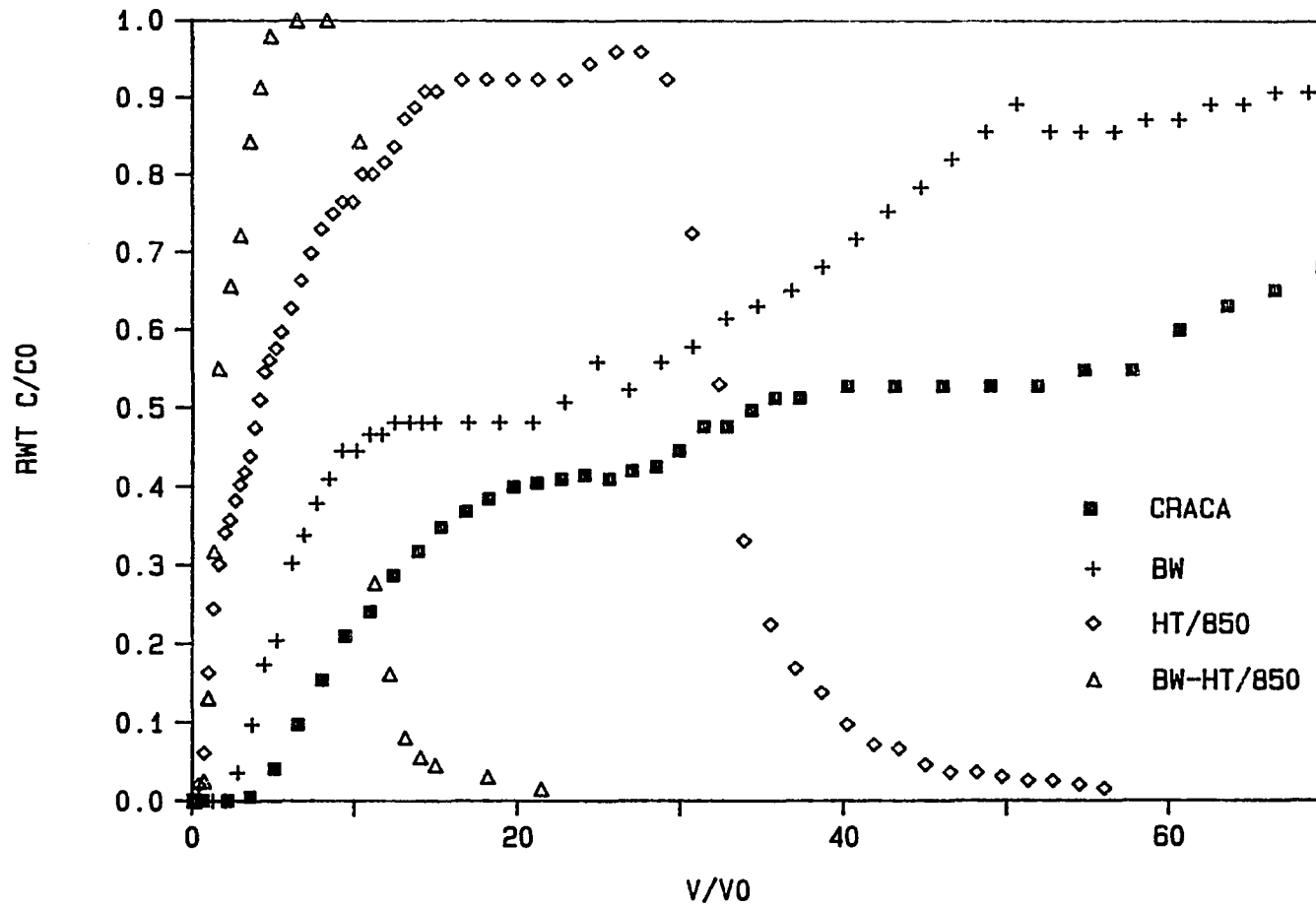


Figure 34: Rhodamine WT column runs with treated soils (0 - 70 pore volumes)

Table 15. Column adsorption results for rhodamine WT and treated materials

Curve	Soil Treatment	Mass Soil (g)	Mass Dye Adsorbed ($\times 10^{-4}$ g)	C_e ($\mu\text{g/L}$)	$(K_p)_{\text{column}}$ (cm^3/g)
-------	----------------	------------------	--	------------------------------	---

Figure 33 and 34

CRACA	whole soil	360.0	11.0	195	15.7
BW	backwashed	301.4	3.7	195	6.3
HT/850	heated @ 850 °C	356.9	1.0	196	1.4
BW-HT/850	backwashed and heated @ 850 °C	283.6	0.10	196	0.25

Figure 35

BW-HT/550	backwashed and heated @ 550 °C	298.6	1.2	195	2.1
HT/850	heated @ 850 °C	356.9	1.0	196	1.4
BW-HT/850	backwashed and heated @ 850 °C	283.6	0.10	196	0.25
GLBDS	glass beads	325.0	0.02	194	0.03

content. The adsorption of RWT has been shown in batch and column studies discussed above to be a function of the organic carbon content. The ratio of f_{oc} values for the whole soil and the backwashed soil is 2.7 and from Table 15 it is observed that the ratio of K_p values is 2.5. It could be hypothesized that the decrease in the adsorption observed was caused largely by the loss of the organic carbon content. Comparison of the breakthrough curves for alluvial materials heated at 850 °C with and without backwashing (BW-HT/850 and HT/850, respectively) indicates that the clays provide adsorption sites for the RWT even upon heating at 850 °C. While no distinct plateau is observed for the heat treated alluvial materials, the change in slope observed for the HT/850 plot could represent the same phenomena.

Figure 35 shows the results of three column runs which used treated alluvial materials and one column run which used glass beads. Two of the column runs (treated materials) were shown in Figure 34 (BW-HT/850 and HT/850) and correspond to materials heated at 850 °C with and without backwashing, respectively. Figure 35 also includes column results from a South Ames sample backwashed and heated at 550 °C (BW-HT/550) and from a column packed with 18/20 mesh glass beads (GLBDS). The treatments and adsorption results for the plots shown in Figure 35 are summarized in Table 15. Inspection of K_p values indicates that the backwashed material heated at 550 °C experienced more RWT adsorption than the backwashed material heated at 850 °C (BW-HT/850). This suggests that further decomposition of recalcitrant organics or further collapse of clays occurred between 550 and 850 °C, causing the observed decrease in the

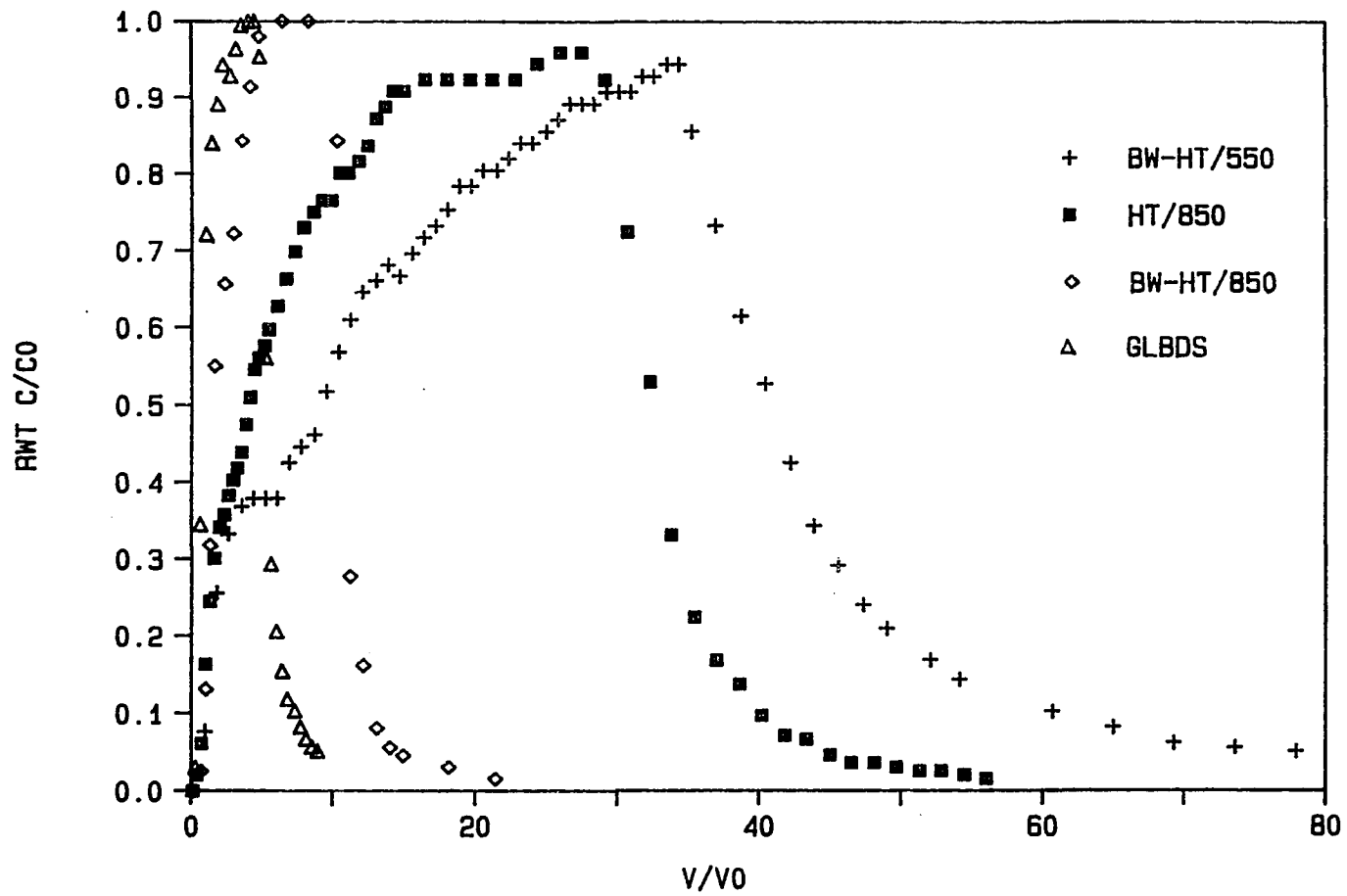


Figure 35: Rhodamine WT column runs with treated soils and glass beads

level of adsorption. The column run utilizing glass beads resulted in negligible adsorption and the breakthrough curve was very close to that for the conservative chloride (as indicated by observing the K_p value in Table 15 and noting that a conservative chemical has a K_p value of 0.0).

In an effort to determine if the organic content was preferentially distributed among sand size fractions, a portion of the South Ames material was wet sieved through a number fifty sieve ($300 \mu\text{m}$). The material retained on this sieve was used to pack a column and a RWT breakthrough curve was run. Figure 36 compares this run, WS ($> 300 \mu\text{m}$), with a run previously shown (BW in Figures 33 and 34 and Table 15 above) in which the material was wet sieved through a number 200 sieve ($75 \mu\text{m}$) and subsequently backwashed (BW ($>75 \mu\text{m}$) in Figure 36). It is observed that the two curves are virtually the same. Comparing the organic contents for the two materials reveals that the coarser media ($> 300 \mu\text{m}$) had a slightly higher f_{oc} (0.0013 ± 0.00017) than the finer media ($> 75 \mu\text{m}$, 0.0010 ± 0.00017). Theoretically, it would seem that the finer material, having a greater surface area, would have the higher organic content. The differences observed could be the result of a slight variation in the treatments used to obtain the two medias. Backwashing was used to help assure that the clays were removed from the $> 75 \mu\text{m}$ sample while backwashing was not used for the $> 300 \mu\text{m}$ media. It could be that this overnight backwashing removed a portion of the organic content from the media remaining in the column, thus explaining the lower organic content for the finer material. The significant thing to note is that the coarser media still had a relatively significant organic

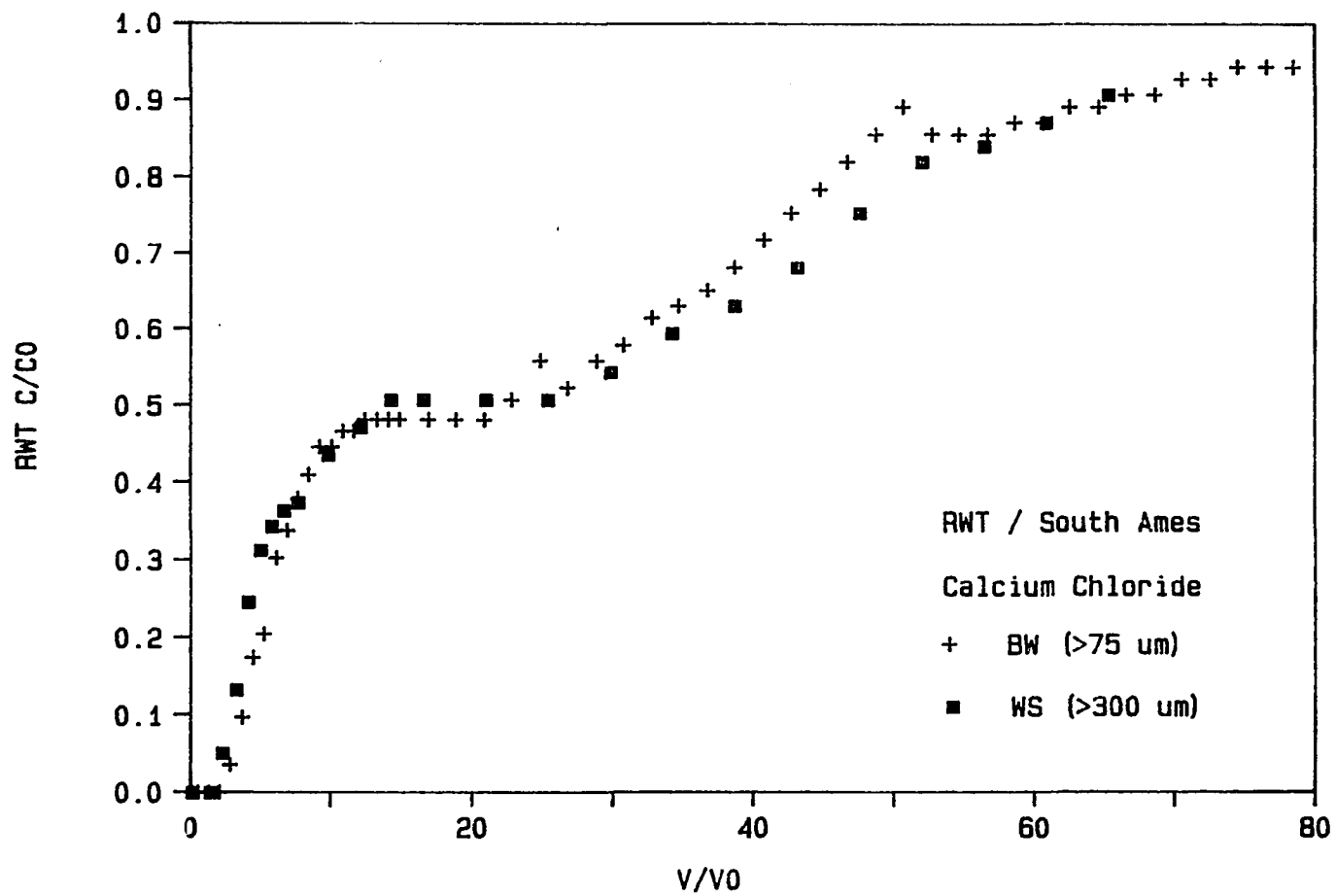


Figure 36: Rhodamine WT breakthrough as function of sand size fractions

content. It thus appears that the organic content is distributed throughout the soil size fractions and are attached to the particles strongly enough to resist their loss during wet sieving and backwashing. Observations of several sand sizes using scanning electron microscopy (SEM) showed micron and submicron sized particles attached to the surface of the sand grains at each sand size range. This may support the hypothesis of distribution of organic content throughout the sand size ranges, although it was not possible to identify the micron and submicron particles as organic content in the SEM analysis.

Effect of pore water velocity / concentration

To evaluate the kinetics of adsorption in the soil column, a column run was conducted with a pore water velocity of 34.1 cm/h (CRAHP in Tables 13 and 14). These results are compared with a similar column run conducted at a pore water velocity of 11.7 cm/h (CRA in Tables 13 and 14) with other parameters being the same. These runs were both conducted with sodium chloride as the conservative tracer. The column results for these two runs are shown jointly in Figure 37 with Figure 38 providing increased resolution at the lower pore volumes. It is seen that the two curves (with pore water velocity as the variable) are virtually the same for the first leg of the breakthrough and that the plateau occurs at about 0.5 for both cases and at about the same relative pore volume. However, in the case of the higher pore water velocity the second leg of the breakthrough occurs sooner and has a steeper slope. It thus appears that the first adsorption mechanism (first leg) is not significantly

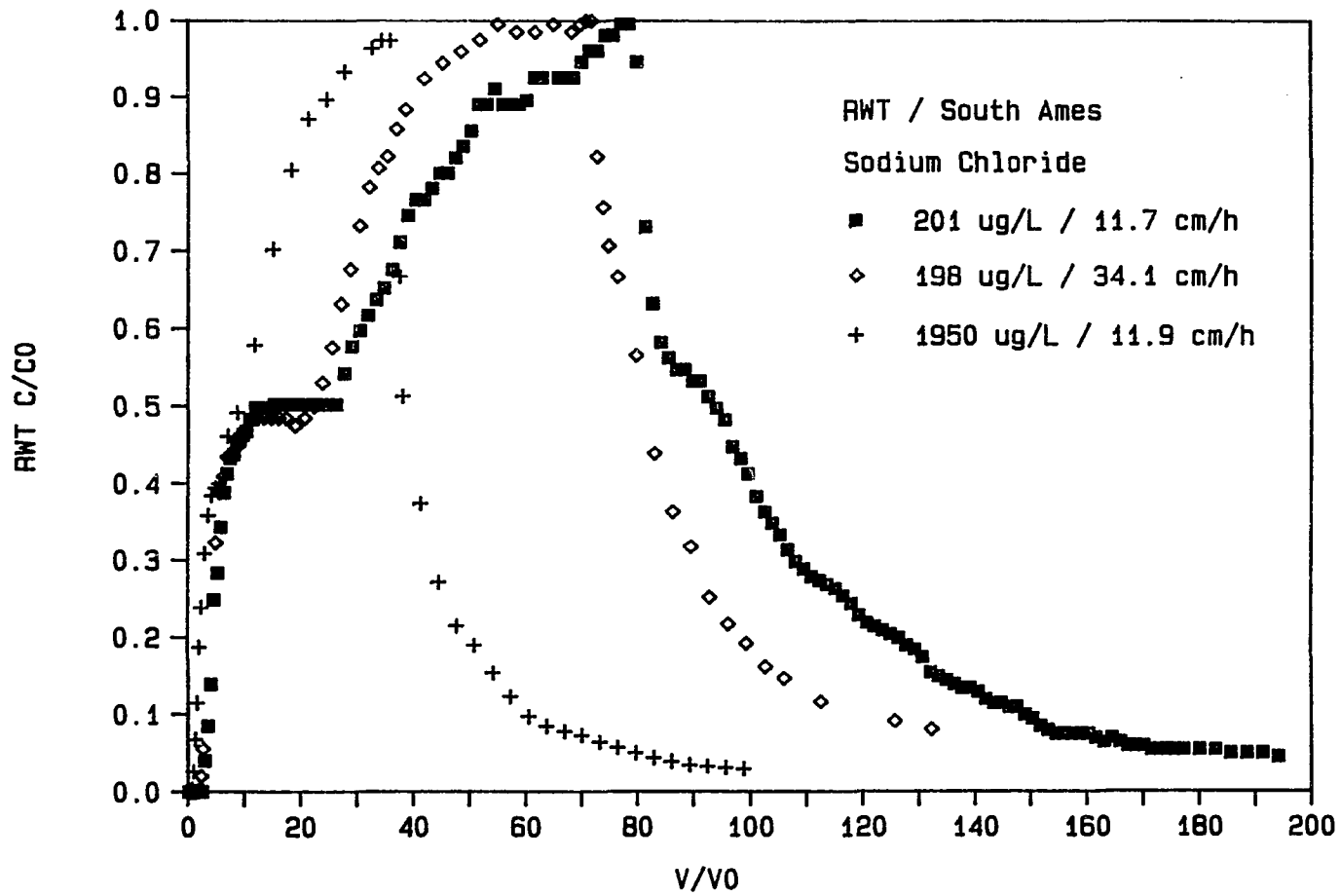


Figure 37: Rhodamine WT breakthrough - effects of pore water velocity and concentration (0 - 200 pore volumes)

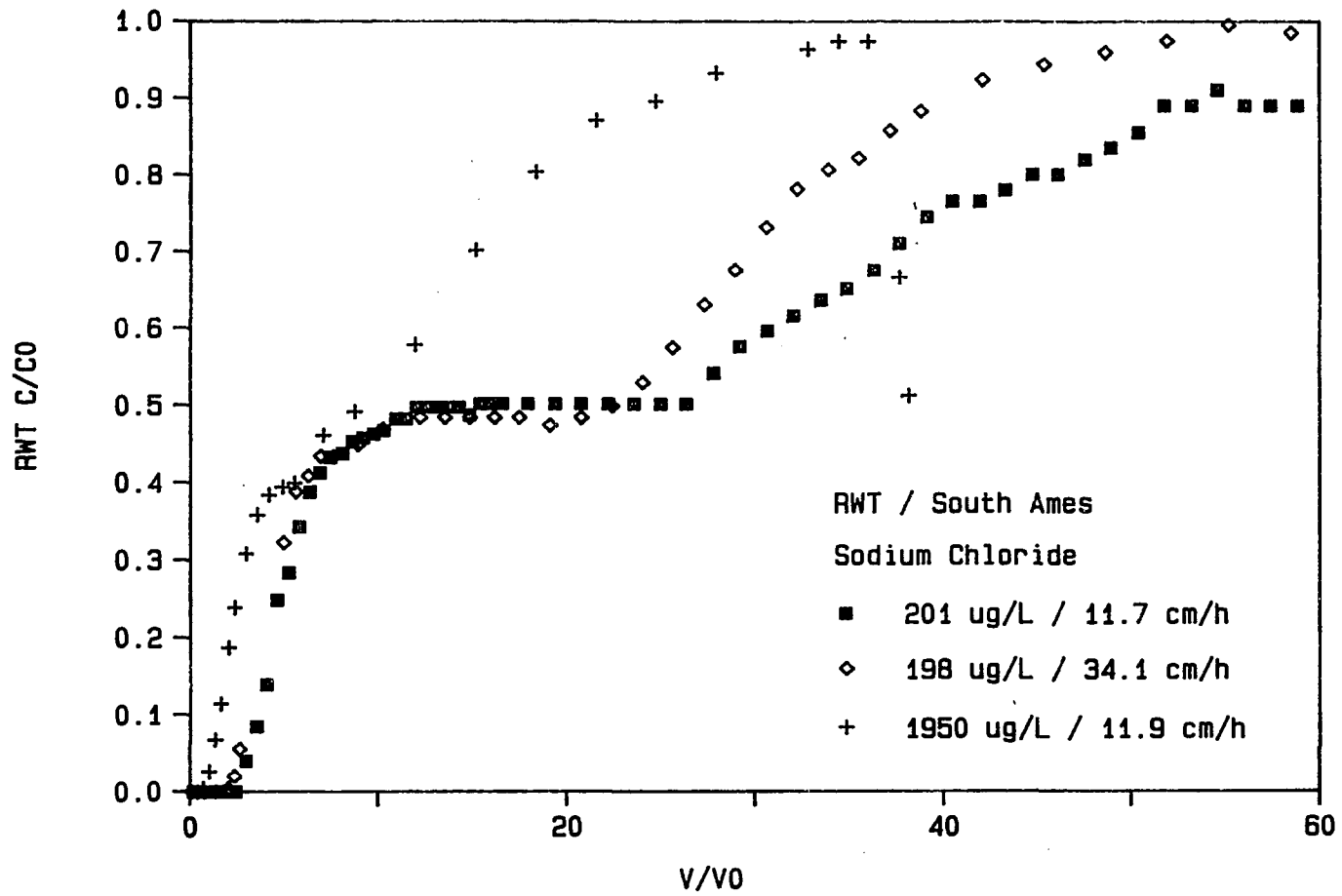


Figure 38: Rhodamine WT breakthrough - effects of pore water velocity and concentration (0 - 60 pore volumes)

affected by the reduced reaction time (is not kinetically limited) while the second adsorption mechanism (second leg) is kinetically limited. This may support the hypothesis that the first leg of the breakthrough curve corresponds to the development of a monolayer of adsorption and the second leg of the breakthrough curve corresponds to the development of multilayers of adsorption.

To evaluate the impacts of the nonlinear adsorption of RWT (as observed in the batch studies) on the column data, a column run was conducted with an order of magnitude higher RWT concentration (1950 $\mu\text{g}/\text{l}$ versus 201 $\mu\text{g}/\text{l}$) using the same soil and porewater velocity (CRAHC and CRA, respectively, in Tables 13 and 14). This comparison is also illustrated in Figures 37 and 38. It is observed that the higher concentration resulted in breakthrough at fewer pore volumes. While the amount of adsorption had increased with the higher concentration (q is larger), the ratio of the increase in adsorption to the increase of the concentration is less than one (which is indicated by the deviation from linearity in the isotherm test at C_e values for RWT greater than approximately 250 $\mu\text{g}/\text{l}$). The nonlinear ($N < 1.0$) adsorption results in the adsorption occurring with fewer pore volumes passed for the higher concentration, as observed in this run. These results point out the danger of conducting isotherm tests at lower concentrations (which will typically result in a linear isotherm) and extrapolating the data to higher concentrations (where linearity may be violated). The time of first appearance for the RWT and the time till complete breakthrough will be overestimated if the nonlinear adsorption ($N < 1.0$) is not considered.

MODELING RESULTS

The abilities of two existing solute transport with adsorption models to describe and predict the breakthrough curves observed for atrazine and alachlor were evaluated. A simple equilibrium adsorption model and a more sophisticated physical nonequilibrium model were utilized. Data from pesticide column runs at two pore water velocities were utilized to determine the ability of the models to predict breakthrough data with variations in experimental conditions.

Equilibrium Adsorption Modeling

The equilibrium adsorption models are the easiest to solve with analytical solutions being available for certain boundary conditions. For purposes of this study, the analytical solution outlined in Equations 15 through 18 was utilized. Nonequilibrium breakthrough curves have been observed to contain more spreading (dispersion) than predicted by equilibrium models. Some researchers have suggested incorporating this additional spreading into a fitted dispersion coefficient (or P_e number) which would account for both hydrodynamic and nonequilibrium dispersion (Parker and Valocchi, 1986; Hutzler et al., 1986; Lee et al., 1988). The use of fitted values for D_x will be evaluated.

The parameters determined during the column studies for atrazine and alachlor (Tables 11 and 12) were utilized as input to the equilibrium adsorption model. The $(K_p)_{\text{column}}$ values for atrazine and alachlor were utilized to allow better comparison of the shapes of breakthrough curves

predicted and observed. Had the $(K_p)_{\text{batch}}$ values (which were greater than the $(K_p)_{\text{column}}$ values - see Table 12) been utilized for atrazine and alachlor, the predicted breakthrough curves would have been shifted to the right (more adsorption was experienced during batch studies than during column studies). Data for column runs at pore water velocities of 10.6 and 30.3 cm/h were utilized for this analysis.

Atrazine

The atrazine data and equilibrium adsorption curves are shown in Figures 39 and 40 for pore water velocities of 10.6 cm/h and 30.3 cm/h, respectively. The deviations between the equilibrium adsorption model and the atrazine data are observed to be greater for the higher pore water velocity (lower detention time), as would be expected. The equilibrium model would overestimate the time till first appearance of the atrazine and underestimate the time necessary for the atrazine concentration to return to zero during elution (desorption).

As observed in Figures 39 and 40, use of fitted dispersion coefficients provided improved description of the atrazine column data. The fitted dispersion coefficient ($D_{x,\text{fitted}}$), the hydrodynamic dispersion coefficient (D_x - from Table 11) and the ratio of the two are shown in Table 16. Values for $D_{x,\text{fitted}}$ were determined by adjusting the value of D_x to minimize the sum of squared errors between the data and the model predictions. The ratio of $D_{x,\text{fitted}}$ to D_x is observed to increase from 2.4 to 5.9 for atrazine with increasing pore water velocity, which is necessary to account for the increased nonequilibrium

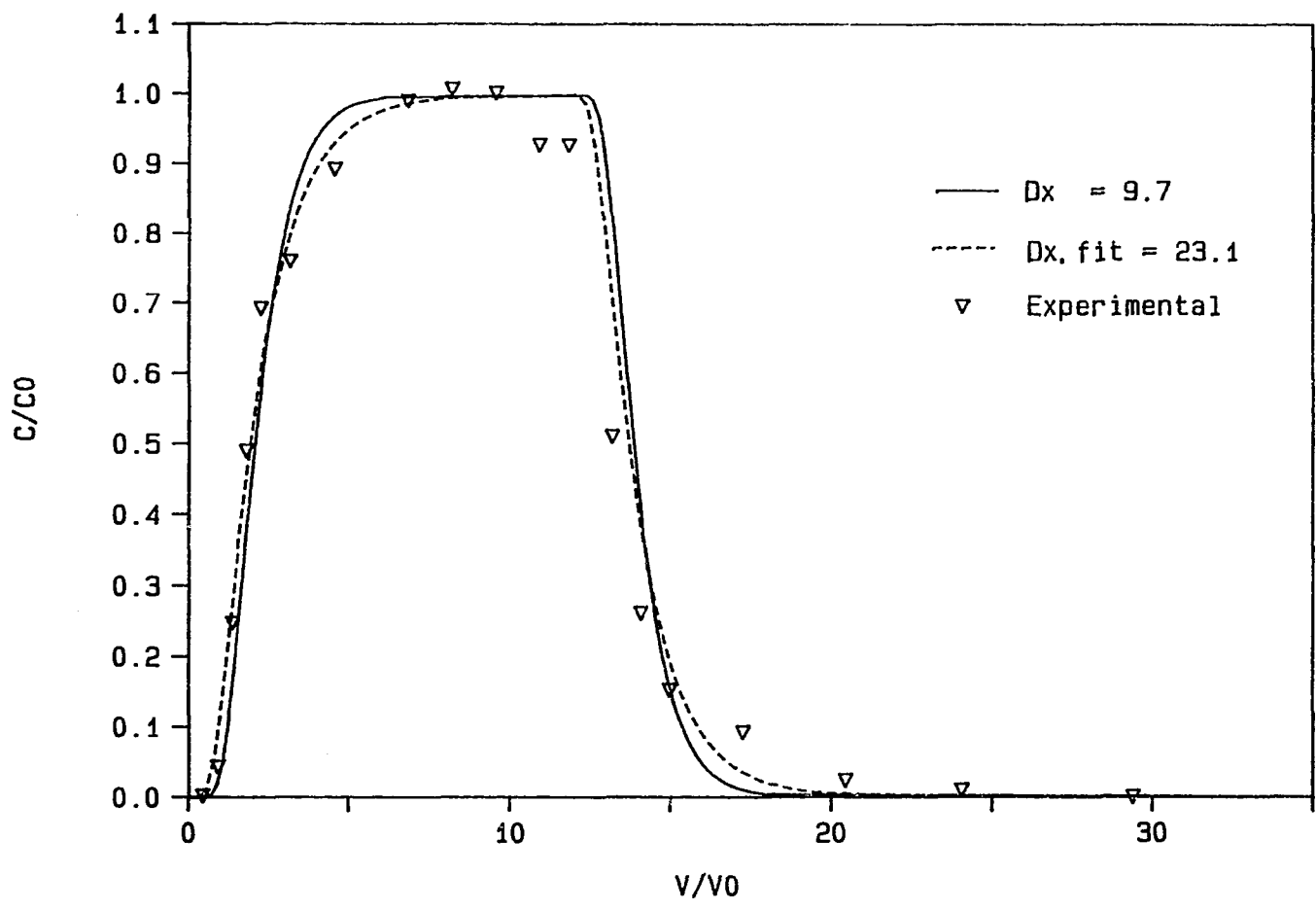


Figure 39: Atrazine equilibrium modeling (10.6 cm/h)

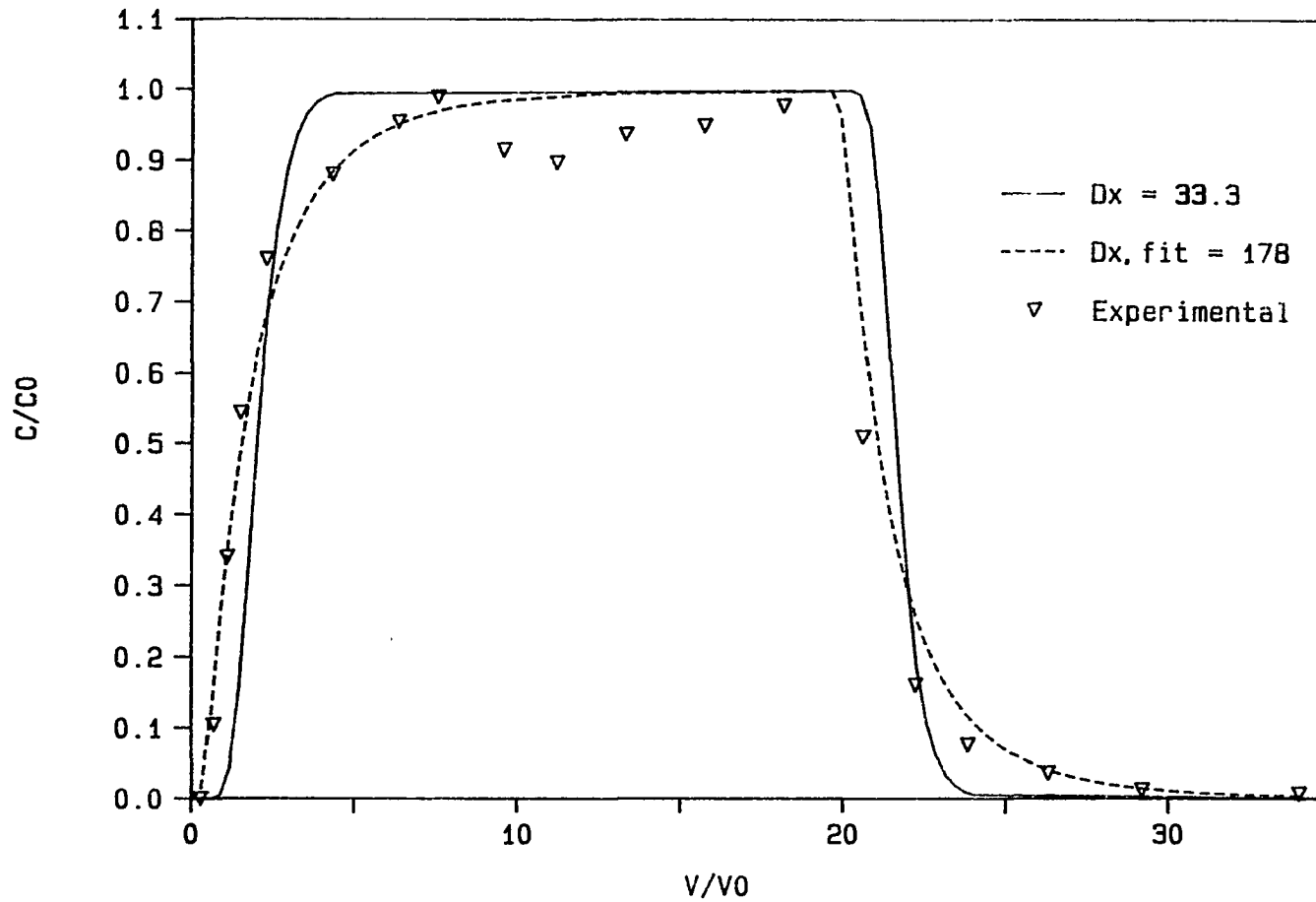


Figure 40: Atrazine equilibrium modeling (30.3 cm/h)

Table 16. Dispersion coefficients - hydrodynamic and fitted

Pesticide	Pore Water Velocity (cm/h)	$D_{x,\text{fitted}}$ cm^2/h	D_x cm^2/h	$D_{x,\text{fitted}}/D_x$
Atrazine	10.6	23.1	9.7	2.4
Atrazine	30.3	178	33.3	5.3
Alachlor	10.6	25.2	9.7	2.6
Alachlor	30.3	213	33.3	6.4

experienced with the higher pore water velocity. This points out that while the use of the $D_{x,\text{fitted}}$ parameter fits the experimental data well, this parameter is dependent on the pore water velocity and may not be utilized for prediction purposes at a different pore water velocity. It is observed that hysteresis of desorption needs to be incorporated to improve the description of the elution data using $D_{x,\text{fitted}}$.

Lee et al. (1988) utilized a method proposed by Parker and Valocchi (1986) for determining $D_{x,\text{fitted}}$ ($P_{e,\text{eff}}$) values. This method involves utilizing modeling parameters determined for a given set of experimental conditions and results in $P_{e,\text{eff}}$ parameters that are a function of pore water velocity. Lee et al. (1988) found this method fairly successful for predicting breakthrough data at a pore water velocity different from that used to determine the model parameters. The necessary model parameters were not determined in this study, so this method could not be evaluated.

Alachlor

The alachlor data and the predictions utilizing the equilibrium adsorption model are shown in Figure 41 and 42 for pore water velocities of 10.6 and 30.3 cm/h, respectively. The variance of the equilibrium predictions from the alachlor data are observed to be greater at the higher pore water velocity. The deviations between the data and the equilibrium predictions appear to be greater than that observed for atrazine data. The ratio of $D_{x,\text{fitted}}$ to D_x (as shown in Table 16) is observed to be greater for alachlor (at a given pore water velocity) than

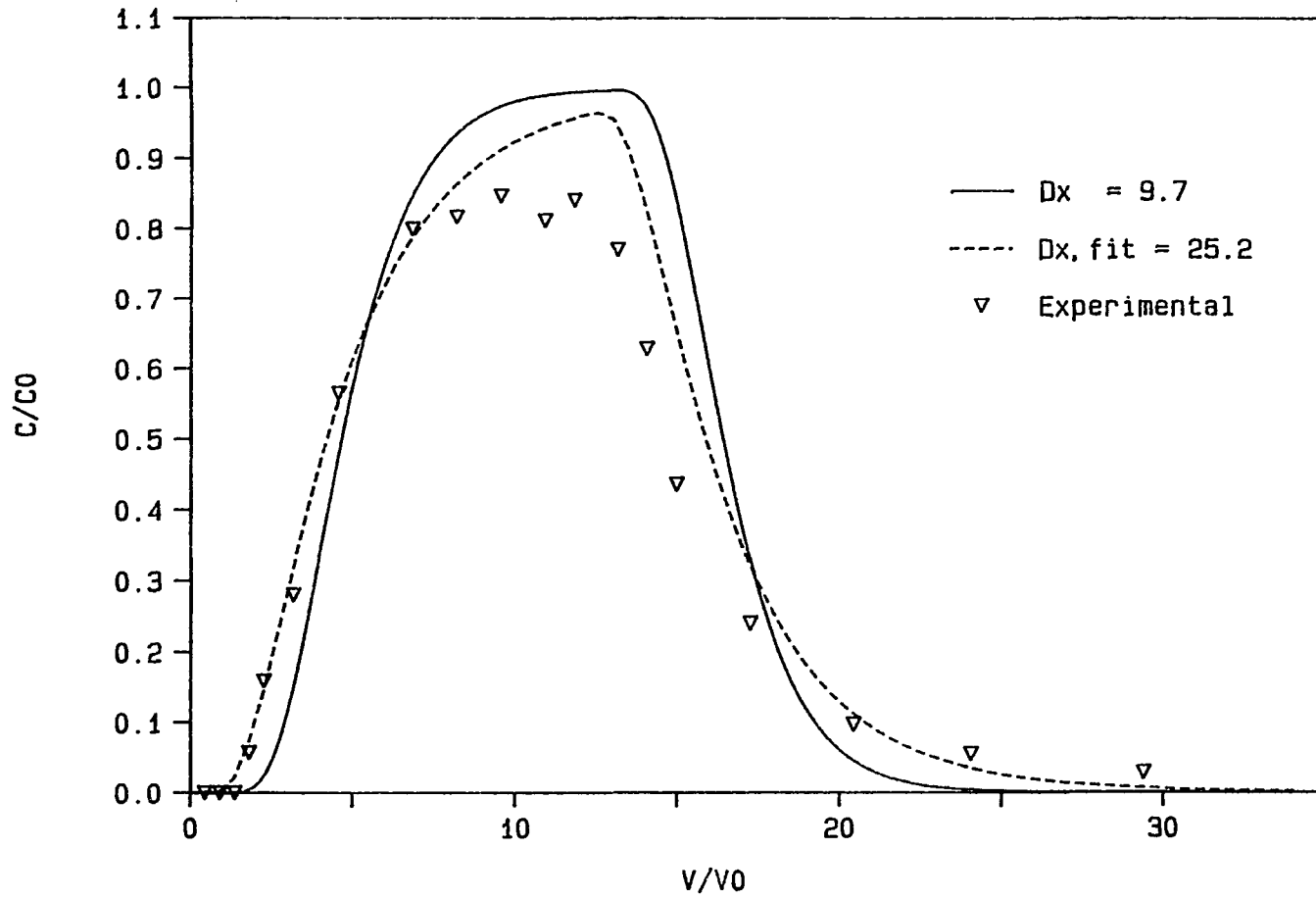


Figure 41: Alachlor equilibrium modeling (10.6 cm/h)

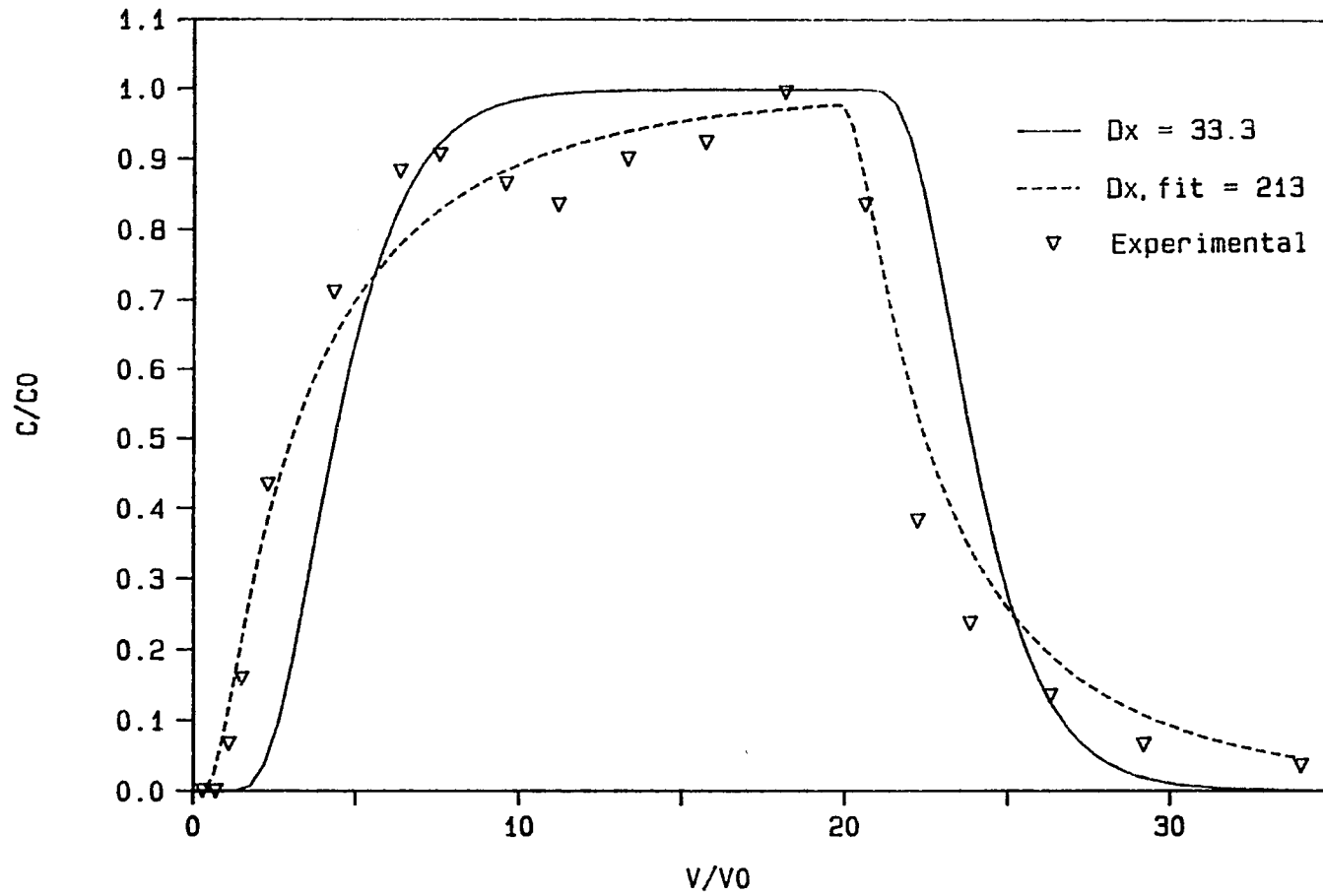


Figure 42: Alachlor equilibrium modeling (30.3 cm/h)

for atrazine, which supports the visual observation that the alachlor experienced greater deviations than atrazine from equilibrium adsorption. Once again, the ratio of $D_{x,\text{fitted}}$ to D_x for alachlor was greater at higher pore water velocities, indicating that value of $D_{x,\text{fitted}}$ (as determined in this study) may not be used for predictive purposes at other pore water velocities. It is observed that inclusion of hysteresis of desorption would improve the description of the alachlor elution data using $D_{x,\text{fitted}}$.

Nonequilibrium Adsorption Modeling

The model of Crittenden et al. (1986) was utilized to investigate the ability of a physical nonequilibrium model to describe / predict the atrazine and alachlor column data. This model has been utilized by several researchers to investigate nonequilibrium breakthrough data (Crittenden et al., 1986; Hutzler et al., 1986; Roberts et al., 1987). The model of Crittenden et al. (1986) assumes that preferential flow paths occur within the soil due to the presence of physical aggregates or aggregate type (diffusion limited) regions in the soil, with the intraaggregate diffusion causing the nonequilibrium shapes of the predicted breakthrough curves. For a general conceptualization of this diffusion limited physical nonequilibrium modeling approach see Figure 6.

The model of Crittenden et al. (1986) requires input of an aggregate radius for the soil column. In the absence of physical aggregates, this becomes a difficult parameter to measure and it has been used as a fitting parameter. Hutzler et al. (1986) adjusted the aggregate radius

parameter to determine a best fit to column data which resulted in aggregate radii 7 to 20 times greater than the radii of the d_{50} particle. Crittenden et al. (1986) utilized an aggregate radius 13 times greater than the $d_{50}/2$ of the soil.

Other parameters necessary for input into the model include the film transfer coefficient (k_f) and the intraaggregate diffusion coefficient (D_p). The value of D_p is determined by dividing the free solution liquid diffusion coefficient (D_1) by the tortuosity factor (τ_p). The value of D_1 for atrazine and alachlor was estimated by the method of Hayduk and Laudie as outlined by Tucker and Nelken (1982). The value of τ_p utilized was 2 (Bear, 1972; Perkins and Johnston, 1963; Crittenden et al., 1986). The method for estimating the k_f parameter was outlined by Hutzler et al. (1986) and will not be repeated here. Sensitivity analyses for specific column conditions by Crittenden et al. (1986), Roberts et al. (1987) and in this study showed the breakthrough curves to be relatively insensitive to the value for k_f but more significantly affected by values used for aggregate radius and D_p .

The D_p parameter, as outlined by Crittenden et al. (1986), was intended to account for diffusion in intraaggregate pore water (or aggregate type regions in the absence of physical aggregates). Several researchers have suggested that the rate limiting diffusion causing nonequilibrium solute transport (especially in the absence of physical aggregates) is diffusion into organic carbon content (Miller, 1984; Hutzler et al., 1986; Bouchard et al., 1988). Miller (1984) utilized completely mixed batch reactor data for sand aquifer material ($f_{oc} =$

0.014) and lindane to determine a value for D_s (diffusion into organic carbon content, as defined by Miller (1984)). The value of D_s determined was $4.8 \times 10^{-11} \text{ cm}^2/\text{s}$, which is several orders of magnitude lower than what would be predicted based on D_1/τ_p . This appears to support the hypothesis of diffusion into organic carbon content as the diffusion limiting case in the absence of physical aggregates. Fundamentally, this may be a more acceptable explanation for nonequilibrium solute transport than assuming aggregate type regions in the absence of physical aggregates.

Complete coverage of the Crittenden et al. (1986) model is beyond the scope of this effort. For additional information on the model, model parameters and estimation techniques, the reader is referenced to thorough treatments by Crittenden et al. (1986), Hutzler et al. (1986) and Roberts et al. (1987). For these modeling runs, 4 radial and 12 axial collocation points were utilized.

Model sensitivity analyses

Sensitivity analyses of the nonequilibrium model for the aggregate radius and D_p were conducted. Major parameters utilized during the model runs are shown in Table 17. The model sensitivity analyses were conducted utilizing the atrazine column data for a pore water velocity of 10.6 cm/h and the South Ames alluvial material (see Tables 11 and 12).

A sensitivity analysis of the aggregate radius was evaluated by conducting model runs with ratios of aggregate radius to $d_{50}/2$ of 10, 4 and 1. The column parameters for these model runs are shown in Table 17

Table 17. Input parameters for nonequilibrium model runs

Model Run	Pesticide	Pore Water Velocity (cm/h)	Water Flow (cm ³ /s)	Aggregate Radius (cm)	k _f (cm/s)	D _p (cm ² /s)
ATL10D	atrazine	10.6	0.022	0.29	1.79 x 10 ⁻⁴	2.58 x 10 ⁻⁶
ATL4D	atrazine	10.6	0.022	0.12	3.22 x 10 ⁻⁴	2.58 x 10 ⁻⁶
ATL1D	atrazine	10.6	0.022	0.03	8.10 x 10 ⁻⁴	2.58 x 10 ⁻⁶
ATLDP2	atrazine	10.6	0.022	0.03	8.10 x 10 ⁻⁴	1.60 x 10 ⁻⁷
ATLDP3	atrazine	10.6	0.022	0.03	8.10 x 10 ⁻⁴	2.58 x 10 ⁻⁸
ATH4D	atrazine	30.3	0.063	0.12	4.56 x 10 ⁻⁴	2.58 x 10 ⁻⁶
ATHDP	atrazine	30.3	0.063	0.03	1.15 x 10 ⁻³	1.60 x 10 ⁻⁷
ALL4D	alachlor	10.6	0.022	0.12	2.85 x 10 ⁻⁴	2.16 x 10 ⁻⁶
ALLDP	alachlor	10.6	0.022	0.03	7.20 x 10 ⁻⁴	1.30 x 10 ⁻⁷
ALH4D	alachlor	30.3	0.063	0.12	4.06 x 10 ⁻⁴	2.16 x 10 ⁻⁶
ALHDP	alachlor	30.3	0.063	0.03	1.02 x 10 ⁻³	1.30 x 10 ⁻⁷

as ATLL0D, ATLL4D and ATLL1D, respectively. The d_{50} of the South Ames alluvial material was 0.058 cm. The results of these model runs and the experimental atrazine data are shown in Figure 43. It is observed that an aggregate radius of 4 times $d_{50}/2$ provides a good fit to the data. This ratio is low relative to values reported by Crittenden et al. (1986) and Hutzler et al. (1986) (7 to 20). However, no visual aggregates were observed for the column runs and the low silt and clay contents (< 3%) and high sand content (97%) would not suggest the presence of aggregate type regions in the soil column. The absence of aggregate type regions in this study was supported by the chloride breakthrough data which was not significantly affected by increases in pore water velocity (see P_e values in Table 11).

A sensitivity analysis was conducted on the D_p value utilizing the atrazine column data at 10.6 cm/h. Throughout this sensitivity analysis the value of the aggregate radius was assumed to be equal to $d_{50}/2$. The D_p value determined based on intraaggregate diffusion with a value of r_p of 2 was $2.58 \times 10^{-6} \text{ cm}^2/\text{s}$. Assuming that D_p was rate limiting and the cause of the nonequilibrium breakthrough, the value of D_p was decreased (increasing the resistance to diffusion) by 2 orders of magnitude (1.6×10^{-7} and 2.58×10^{-8}). This analysis assumes the absence of significant aggregation in the soil and suggests diffusion occurs into aggregates (particles) with much greater resistance to diffusion than pore water (more than predicted by r_p alone). This scenario would be consistent with the conclusions of Miller (1984), Hutzler et al. (1986) and Bouchard et al. (1988) that, with no significant aggregation present, diffusion

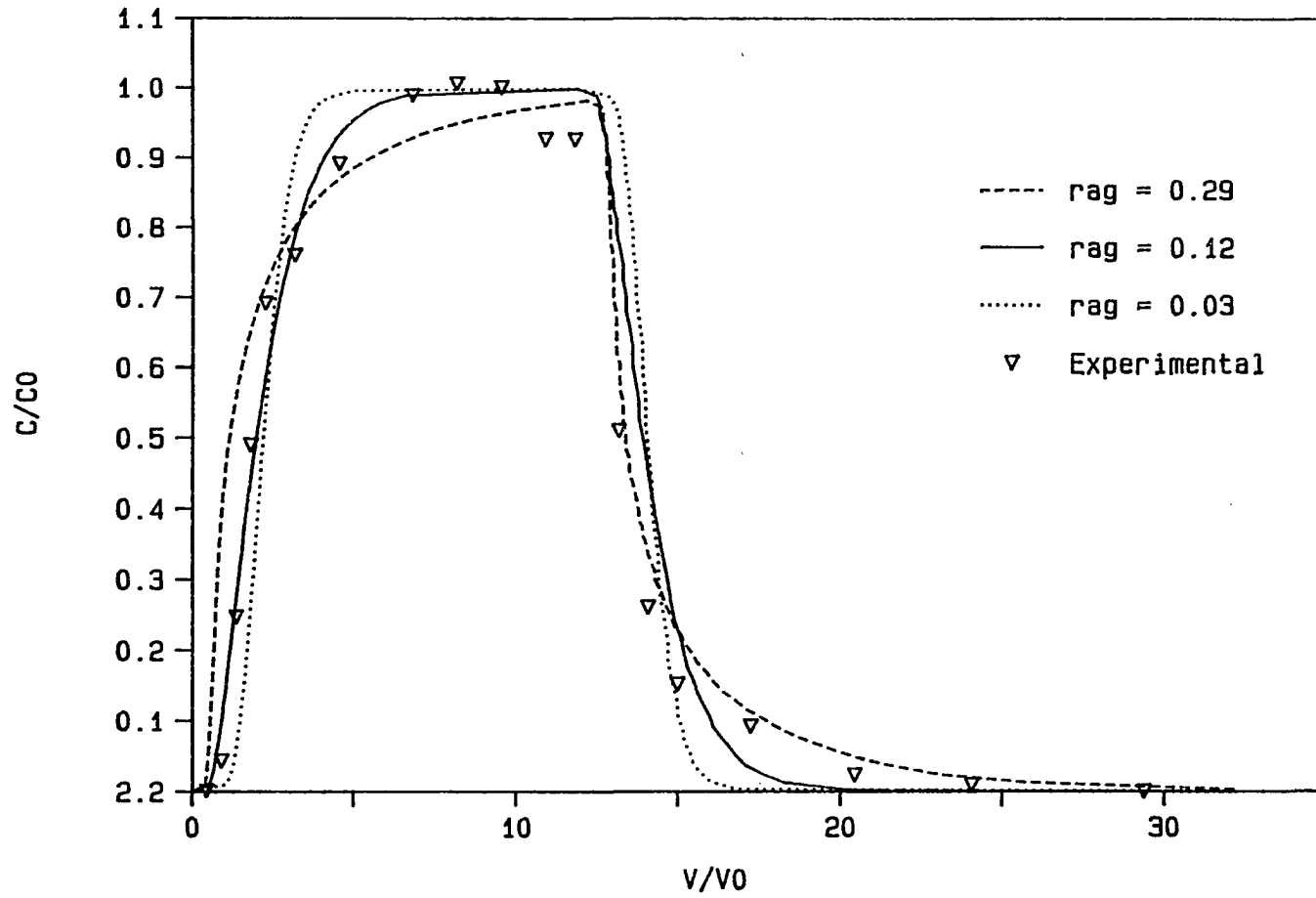


Figure 43: Nonequilibrium model sensitivity analysis - radius of aggregate (rag, cm)

into organic carbon content caused the nonequilibrium breakthrough curves observed and that the diffusion into the organic carbon content is significantly less than that predicted by D_1/τ_p . Input parameters for the three model runs of this sensitivity analysis are shown in Table 17 as ATL1D, ATLDP2 and ATLDP3, respectively, and the results are shown in Figure 44. It was found that by utilizing a D_p value of $1.6 \times 10^{-7} \text{ cm}^2/\text{s}$ and an aggregate radius equal to $d_{50}/2$ that a good fit of the atrazine data was obtained. It is also observed that adjusting the aggregate radius over an order of magnitude provided similar column predictions as adjusting the D_p over 2 orders of magnitude.

Atrazine

The atrazine column data for a pore water velocity of 10.6 cm/h was evaluated during the model sensitivity analysis and good fits were found for two combinations of aggregate radius and D_p . For an aggregate radius of 0.03 cm (aggregate diameter equal to d_{50}) the optimal value of D_p was found to be $1.6 \times 10^{-7} \text{ cm}^2/\text{s}$ (ATLDP2 in Table 17). For a D_p value of $2.58 \times 10^{-6} \text{ cm}^2/\text{s}$ (estimated using τ_p of 2), the optimal value of aggregate radius was observed to be 4 times the radius of the d_{50} particle (ATL4D in Table 17). These two model runs and the atrazine column data are shown jointly in Figure 45. It is observed that these two model runs produced virtually identical results. The model predictions of the elution data were not as good as those for the breakthrough data, suggesting the need to include hysteresis of desorption into the modeling effort.

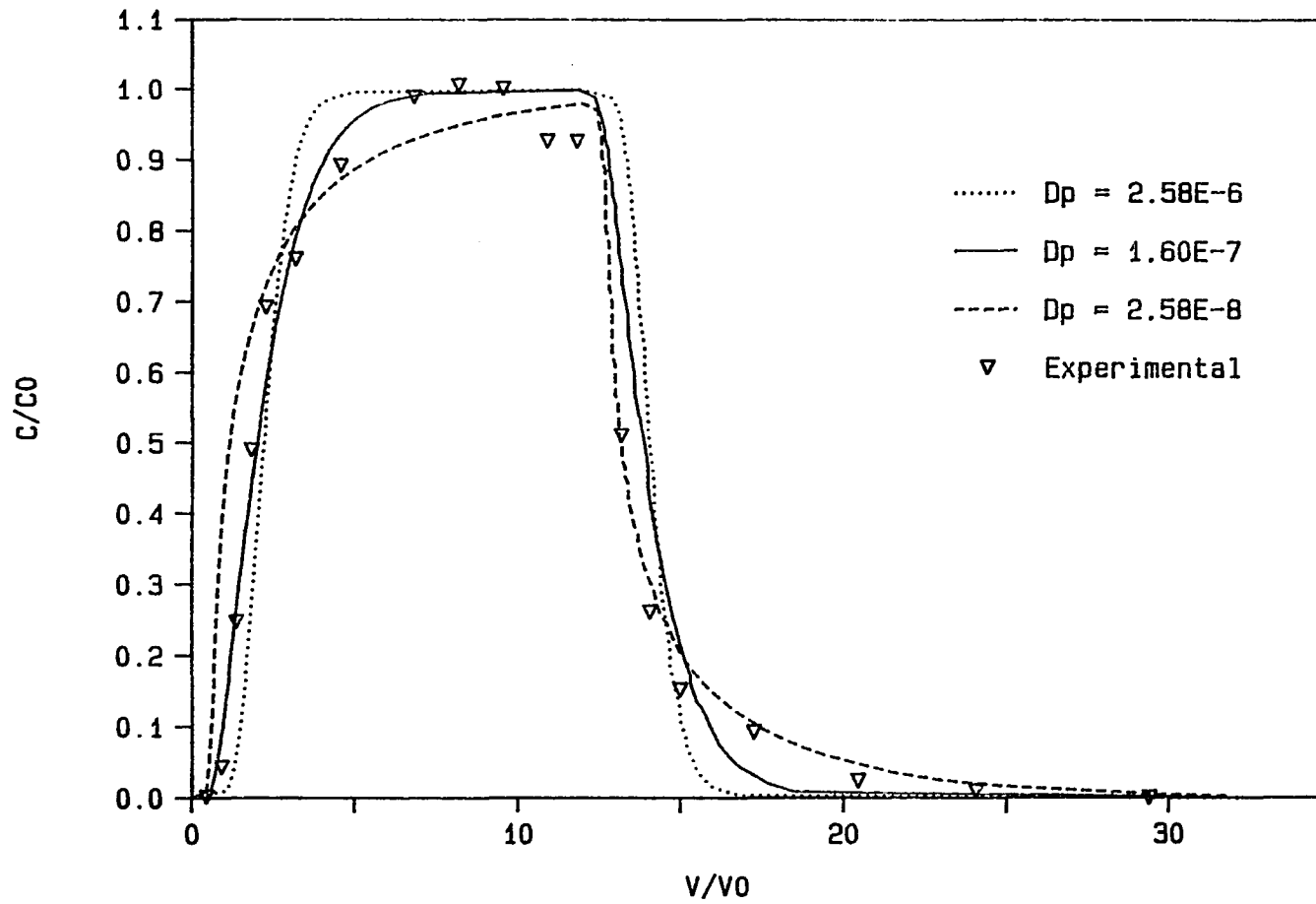


Figure 44: Nonequilibrium model sensitivity analysis - D_p (cm^2/s)

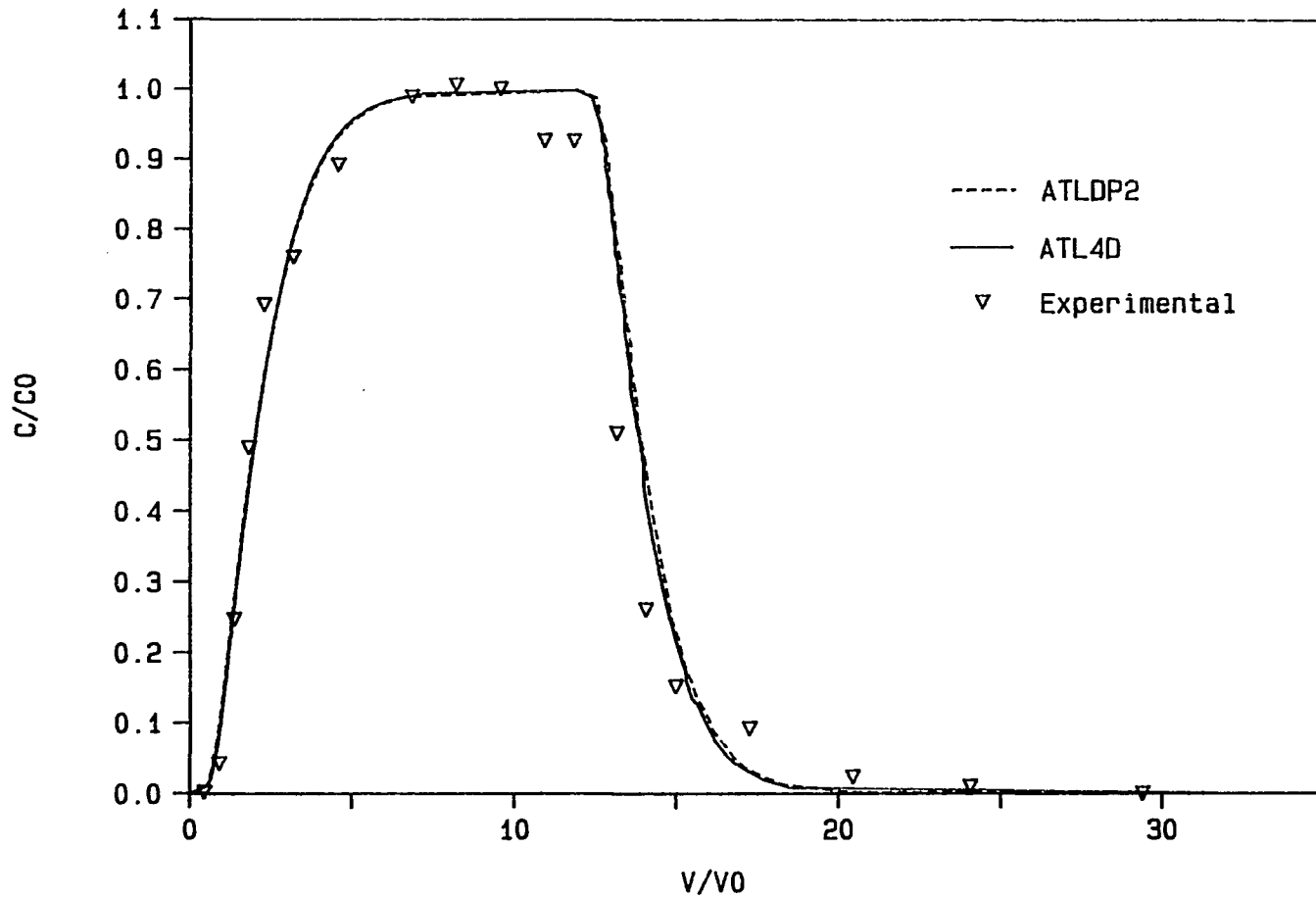


Figure 45: Atrazine nonequilibrium modeling (10.6 cm/h)

The optimal aggregate radius and optimal D_p value were utilized in an attempt to predict atrazine column data from a higher pore water velocity (30.3 cm/h). Inspection of the atrazine column data for these two pore water velocities (Figure 23) shows a leftward shift (earlier appearance) of the atrazine breakthrough curve with increased pore water velocity. The input parameters for these model runs are shown in Table 17 as ATH4D and ATHDP for optimal aggregate radius and optimal D_p , respectively. The model results and the atrazine data are shown jointly in Figure 46. It is observed that the predicted values are very similar to the experimentally observed values. The ability of the model to utilize parameters determined at a lower pore water velocity to satisfactorily predict the breakthrough at a higher pore water velocity (including the leftward shift) is encouraging.

Alachlor

Modeling results for alachlor were conducted without fitting model parameters to the alachlor data. Instead, the optimal value for aggregate radius determined in the previous analysis (4 times $d_{50}/2$) was utilized and the D_p value was determined for alachlor utilizing an estimated value for D_1 and a value for τ_p of 2. When utilizing an aggregate radius equal to $d_{50}/2$, the D_p value for alachlor was decreased from $(D_1)_{alachlor}/\tau_p$ by the same ratio as that determined to be optimal for atrazine. The input parameters utilized to predict the alachlor data at a pore water velocity of 10.6 cm/h are shown in Table 17 as ALL4D and ALLDP, respectively. The model predictions and the alachlor column data

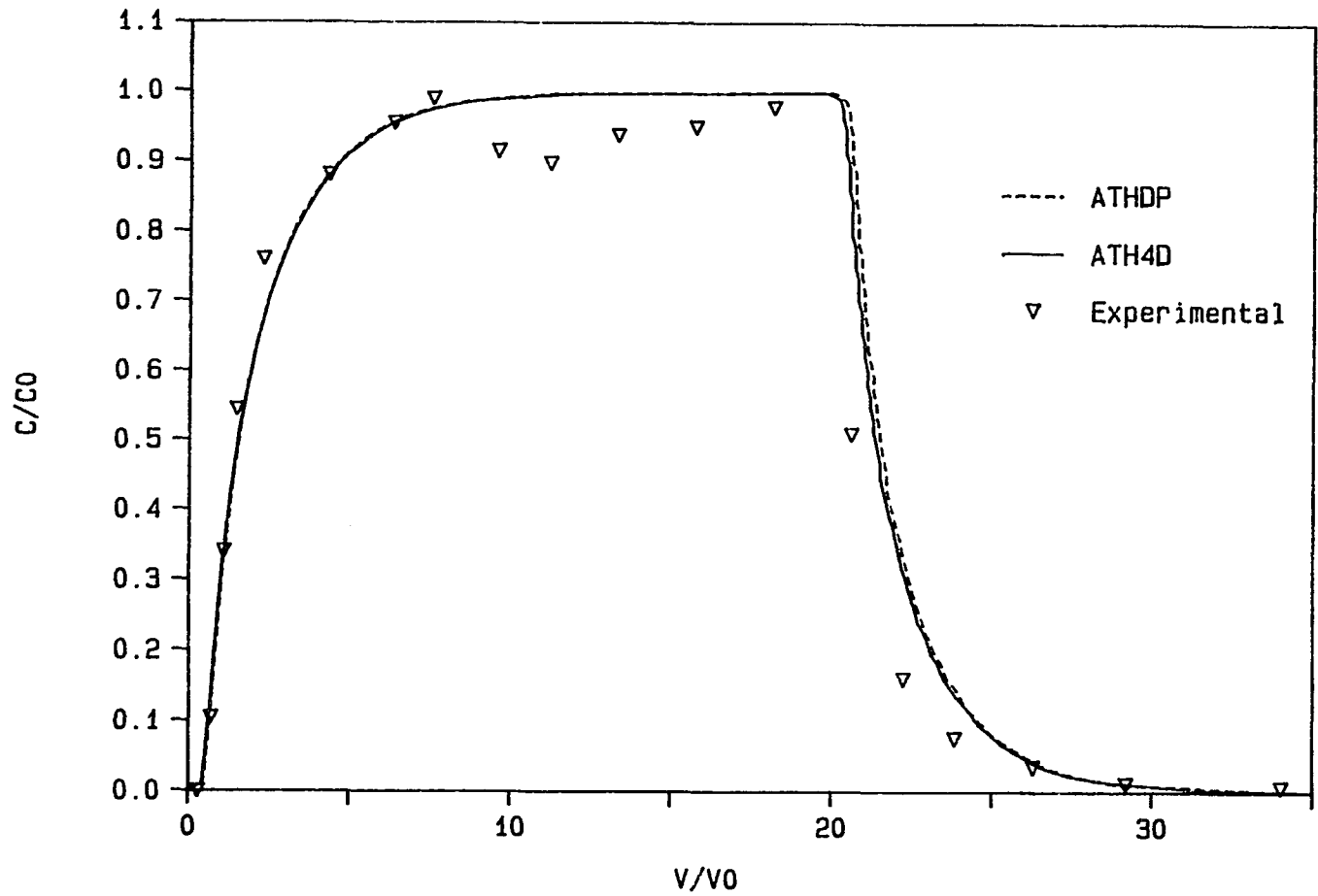


Figure 46: Atrazine nonequilibrium modeling (30.3 cm/h)

are shown jointly in Figure 47. Based on the fact that the model parameters were determined separate from the column data, the agreement between the predicted and observed data is quite good. The model results and alachlor data at the higher pore water velocity of 30.3 cm/h (ALH4D and ALHDP in Table 17) are shown jointly in Figure 48. As with the atrazine, the model was able to predict the leftward shift in the alachlor column data with increasing pore water velocity fairly successfully. For both pore water velocities, inclusion of hysteresis of desorption would have improved the model predictions of the elution data.

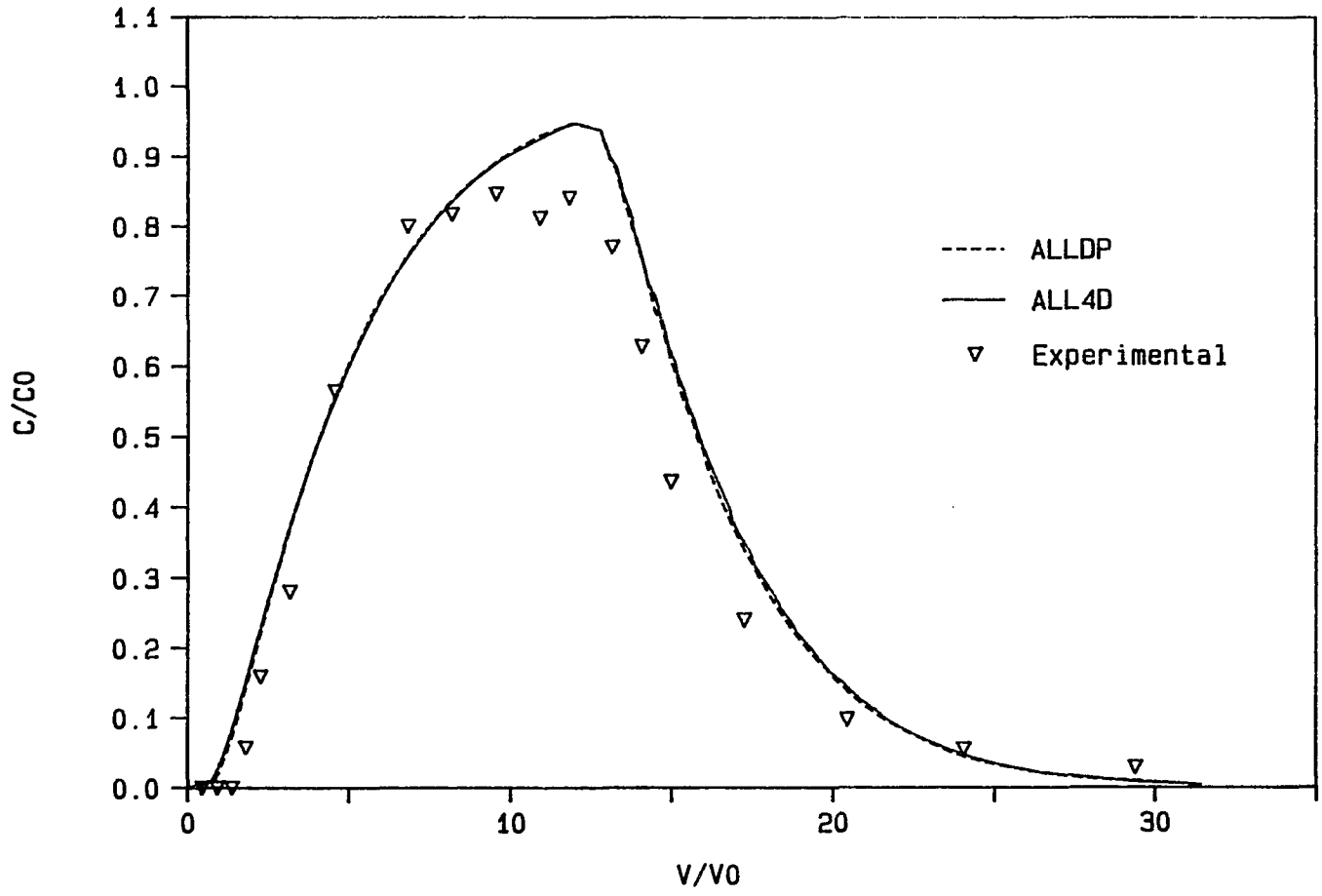


Figure 47: Alachlor nonequilibrium modeling (10.6 cm/h)

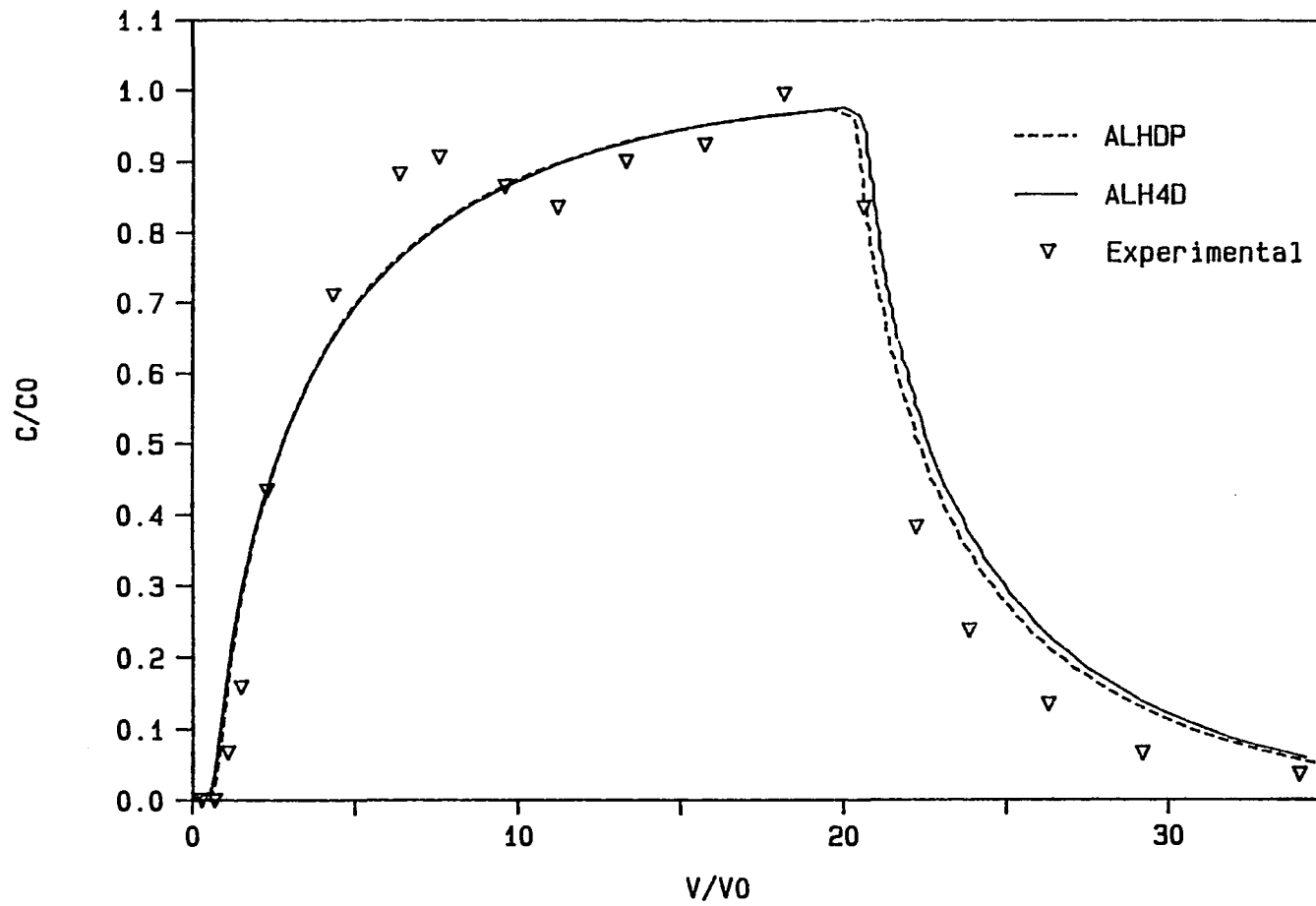


Figure 48: Alachlor nonequilibrium modeling (30.3 cm/h)

CONCLUSIONS AND RECOMMENDATIONS

Batch and column studies were utilized to investigate the transport of atrazine and alachlor in an alluvial sand aquifer material. The ability of existing models to describe / predict the column data was investigated. The use of fluorescent dyes as surrogates (adsorbing tracers) for the pesticides was evaluated. The following conclusions were established during this research.

Conclusions

Adsorption isotherms were observed to be linear for atrazine ($C_e < 900 \mu\text{g/L}$) and alachlor ($C_e < 700 \mu\text{g/L}$). Alachlor was observed to be more highly adsorbed than atrazine with batch K_p values of $1.08 \text{ cm}^3/\text{g}$ and $0.40 \text{ cm}^3/\text{g}$, respectively. The column K_p values (determined by mass balance) were less than those determined in the batch studies ($0.93 \text{ cm}^3/\text{g}$ for alachlor and $0.30 \text{ cm}^3/\text{g}$ for atrazine).

The estimation techniques based on values of K_{ow} (Equations 25 and 26) to predict K_{oc} values for the pesticides and the low organic content alluvial sand were fairly accurate. For atrazine, the predicted K_{oc} values were within 9% of batch K_{oc} values and within 38% of the column K_{oc} values. For alachlor, the predicted K_{oc} values were within 52% of the batch K_{oc} values and within 44% of the column K_{oc} values.

No competitive adsorption was evidenced in batch studies for atrazine and alachlor for the concentrations and soils investigated. No effect of background ions on the level of adsorption was observed for

atrazine or alachlor in this study.

Adsorption isotherms and column runs for the fluorescent dyes showed that rhodamine WT (RWT) experienced significantly more adsorption by the alluvial sand than fluorescein. Batch values of K_p (with no background ions added) for fluorescein and RWT were $0.33 \text{ cm}^3/\text{g}$ and $4.5 \text{ cm}^3/\text{g}$, respectively. The isotherms for the dyes were observed to be linear at low concentrations ($\mu\text{g}/\text{L}$) with nonlinearity evidenced at higher concentrations (mg/L).

Analysis of fluorescein batch tests was complicated by the presence of natural background fluorescence for the alluvial aquifer material. During column runs the problem of background fluorescence was not as significant.

For the dyes, measured K_{oc} values were several orders of magnitude greater than predicted using estimation techniques (based on K_{ow} and f_{oc}). This indicates that the polar and ionizable nature of the dyes violates the premise of nonpolar chemicals which were utilized in developing the empirical estimation techniques. The estimation techniques predicted that fluorescein would be more highly adsorbed than RWT (fluorescein has a higher K_{ow} than RWT), while the batch and column studies showed RWT to be more highly adsorbed than fluorescein. These results point out the need to apply estimation techniques with care.

Background ions were observed to affect the level of RWT adsorption. Increasing valency and increasing concentration of cations were observed to most significantly affect the level of RWT adsorption. Batch tests and column runs for RWT with 10^{-2} N CaCl_2 present resulted in K_{oc} values

greater by more than a factor of 2 than without CaCl_2 added. It is hypothesized that increasing cation valency and concentration reduced the diffuse double layers about the alluvial aquifer particles and caused the increased adsorption observed.

Comparison of K_p values (batch or column) for the pesticides and the dyes shows the following order of increasing adsorption on the alluvial aquifer material: fluorescein, atrazine, alachlor and RWT. This hierarchy suggests that if both dyes were utilized as adsorbing tracers in a solute transport study, atrazine and alachlor would be expected to appear after the fluorescein and before the RWT.

The atrazine and alachlor breakthrough curves demonstrated a nonequilibrium shape (as observed visually and numerically). Increasing the pore water velocity from 10.6 to 30.3 cm/h resulted in earlier appearance (leftward shift) of the breakthrough curves for both pesticides. Decreasing the pore water velocity from 10.6 to 5.5 cm/h was not observed to significantly affect the appearance of the breakthrough curve for either pesticide. The chloride breakthrough curve was observed to be relatively independent of changes in pore water velocity, indicating that the changes in the breakthrough curves observed for the pesticides were not due to the hydrodynamics of pore water flow.

Elution studies showed desorption to occur for both pesticides and both dyes. This indicates that physical adsorption was the dominant adsorption mechanism. More pore volumes were required to return to $C/C_0 = 0.0$ than to reach $C/C_0 = 1.0$ for all column runs. Thus, hysteresis of desorption was evidenced for both pesticides and both dyes.

The RWT breakthrough curves were not the conventional sigmoidal breakthrough curve but instead leveled off at a C/C₀ value of 0.5 for a number of pore volumes prior to increasing C/C₀ values again. Mass balances of breakthrough and elution data showed conservation of mass, indicating that degradation was not the mechanism responsible for this two leg breakthrough curve. Treatment of the alluvial aquifer material to reduce the organic carbon content and/or the clay content resulted in decreases in RWT adsorption, but the two leg breakthrough curve was still evident. This suggests that both organic carbon content and clays are involved in adsorbing RWT and responsible for the two leg breakthrough curve. Additional study will be required to determine the mechanisms responsible for the two leg breakthrough curve observed for RWT.

The batch K_p values for atrazine, alachlor and fluorescein were observed to be greater than K_p values determined from column runs. For RWT, however, the batch K_p values were lower than those determined from column runs. It was beyond the scope of this research to determine the mechanism(s) responsible for greater RWT adsorption in the column runs than in the batch studies. The same mechanism(s) may be responsible for the two leg breakthrough curves observed during column runs for RWT. One plausible mechanism that may account for the two leg breakthrough curve for RWT is the development of multiple layers of RWT during adsorption.

Column studies (using RWT) indicated that the organic content was distributed throughout the sand size fractions and was attached to the sand particles in a sufficient manner to withstand complete removal by wet sieving or backwashing. The appearance of micron and submicron size

particles attached to various size fractions of sand particles was observed during SEM analysis.

For RWT, increasing the pore water velocity from 11.7 cm/h to 34.1 cm/h was not observed to affect the first leg of the breakthrough curve but resulted in earlier rise and steeper slope of the second leg of the breakthrough curve. This suggests that the mechanism responsible for the first leg of the RWT breakthrough curve was not rate limited but that the mechanism responsible for the second leg of the breakthrough curve was rate limited.

Increasing the influent RWT concentration from 201 $\mu\text{g/L}$ to 1950 $\mu\text{g/L}$ resulted in earlier breakthrough of the RWT. This is consistent with the nonlinear isotherm ($N < 1.0$) observed for RWT for the higher concentrations.

Equilibrium models were not able to predict the exact shapes of breakthrough curves observed for atrazine or alachlor with increased deviations between the model results and the data observed at higher pore water velocities. Use of dispersion coefficients fitted to the column data improved the agreement between model results and experimental data, but the fitted dispersion coefficients were a function of the pore water velocity. Improved description of elution data could be obtained by incorporating hysteresis of desorption in the modeling efforts.

Sensitivity analyses of the Crittenden et al. (1986) model showed that adjustment of either the aggregate radius or the intraaggregate (intraparticle) diffusion coefficient (D_p) could be utilized to fit the atrazine column data. In the absence of physical aggregates or

significant diffusion limited agglomerates of particles (as in this study), the concept of diffusion into organic carbon content (with increased diffusion resistance) as the cause of nonequilibrium solute transport is more fundamentally appealing. The results of this research appear to support the hypothesis of organic carbon content motivated nonequilibrium solute transport.

Utilizing the model of Crittenden et al. (1986) and either the aggregate radius or the D_p values fitted for the atrazine column run at 10.6 cm/h, good predictions of the experimental breakthrough curves for atrazine at 30.3 cm/h and for alachlor at 10.6 and 30.3 cm/h were achieved. The ability of the model to predict breakthrough curves (including the leftward shift for both pesticides at 30.3 cm/h) under different conditions than utilized for calibration is significant. Improved predictions of the elution curves could be obtained by incorporating hysteresis of desorption in the model.

From a fundamental standpoint, the physical nonequilibrium model of Crittenden et al. (1986) showed improved description and prediction capabilities over the simple equilibrium model. From an applied standpoint, other uncertainties inherent in modeling solute transport at the field scale need to be considered (e.g., heterogeneities in hydraulic conductivity and organic carbon content, macropores, other reactions, etc.). The modeler must evaluate the relative uncertainty introduced by each of these elements and decide what level of sophistication is merited for modeling each element for the given set of conditions.

Recommendations for Future Research

Based on the results of this research, the following elements are enumerated as requiring further research.

1. Investigation of these pesticides and dyes with other soils and at the field scale.
2. Investigation of other pesticides and aquifer materials.
3. Investigation of other fluorescent dyes as adsorbing tracers.
4. Further investigation of the mechanism(s) responsible for the two leg breakthrough curve for RWT and the greater adsorption in the column runs than in the batch tests for RWT.
5. Investigation of desorption and hysteresis of desorption.
6. Investigation of intraparticle diffusion into organic carbon content as it affects nonequilibrium solute transport.
7. Further evaluation of adsorption models and their predictive ability.

REFERENCES

- Abdul, A. S. and T. L. Gibson. (1986). "Equilibrium Batch Experiments with Six Polycyclic Aromatic Hydrocarbons and Two Aquifer Materials." Hazardous Wastes and Hazardous Materials 3(2): 125-137.
- Abdul, A. S., T. L. Gibson and D. N. Rai. (1986). "The Effect of Organic Carbon on the Adsorption of Fluorene by Aquifer Materials." Hazardous Wastes and Hazardous Materials 3(4): 429-440.
- American Society for Testing and Materials. (1988) 1988 Annual Book of American Society for Testing and Materials. Philadelphia, PA: American Society for Testing and Materials.
- American Water Works Association. (1988). "Draft Proposes MCLs for Organic, Inorganic Chemicals." Mainstream - American Water Works Association 32(7): 1.
- Anderson, M. P. (1984). "Movement of Contaminants in Groundwater: Groundwater Transport - Advection and Dispersion." In Studies in Geophysics: Groundwater Contamination. New York: National Academy Press. 37-45.
- Bailey, G. W. and J. L. White. (1970). "Factors Influencing the Adsorption, Desorption and Movement of Pesticides in Soil." In Residue Reviews, vol. 32. Ed. F. A. Gunther and J. D. Gunther. New York: Springer-Verlag. 29-92.
- Baker, J. L. and Johnson, H. P. (1979). "The Effect of Tillage Systems on Pesticides in Runoff from Small Watersheds." Transactions of American Society of Agricultural Engineers 22(3): 554-559.
- Banerjee, P., M. D. Pivoni and K. Ebeid. (1985). "Sorption of Organic Contaminants to a Low Carbon Subsurface Core." Chemosphere 14(8): 1057-1067.
- Bear, J. (1972). Dynamics of Fluids in Porous Media. New York: American Elsevier.
- Bencala, K. E., R. E. Rathbun, A. P. Jackman, V. C. Kennedy, G. W. Zellweger and R. J. Avanzino. (1983). "Rhodamine WT Dye Losses in a Mountain Stream Environment." Water Resources Bulletin, vol. 19 (6): 943-950.
- Benfield, L. D., J. F. Judkins and B. L. Weand. (1982). Process Chemistry for Water and Wastewater Treatment. Englewood Cliffs, NJ: Prentice-Hall.

- Beven, K. and P. Germann. (1982). "Macropores and Water Flow in Soils." Water Resources Research 18(5): 1311-1325.
- Bouchard, D. C. and A. L. Wood. (1988). "Pesticide Sorption on Geologic Material of Varying Organic Carbon Content." Toxicology and Industrial Health 4(3): 341-349.
- Bouchard, D. L., A. L. Wood, M. L. Campbell, P. Nkedi-Kizza and P. S. C. Rao. (1988). "Sorption Nonequilibrium During Solute Transport." Journal of Contaminant Hydrology 2: 209-223.
- Brown, D. S. and G. Combs. (1985). "A Modified Langmuir Equation for Predicting Sorption of Methyl-acridinium Ion in Soils and Sediments." Journal of Environmental Quality 14: 195-199.
- Brown, D. S. and E. W. Flagg. (1981). "Empirical Prediction of Organic Pollutant Sorption in Natural Sediments." Journal of Environmental Quality 10(3): 382-386.
- Brunauer, S., P. H. Emmett and E. Teller. (1938). "Adsorption of Gases in Multimolecular Layers." Journal of the American Chemistry Society 60: 309.
- Calvet, R. (1980). "Adsorption - Desorption Phenomena." Interactions between Herbicides and the Soil. Ed. R. J. Hance. New York: Academic Press. 1-30.
- Cameron, D. R. and A. Klute. (1977). "Convective-Dispersive Solute Transport With a Combined Equilibrium and Kinetic Adsorption Model." Water Resources Research 13(1): 183-188.
- Chiou, C. T., P. E. Porter and D. W. Schmedding. (1983). "Partition Equilibria of Nonionic Organic Compounds between Soil Organic Matter and Water." Environmental Science and Technology 17(4): 227-231.
- Crittenden, J. C., N. J. Hutzler, D. G. Geyer, J. L. Oravitz and G. Friedman. (1986). "Transport of Organic Compounds with Saturated Groundwater Flow: Model Development and Parameter Sensitivity." Water Resources Research 22(3): 271-284.
- Davidson, J. M. and J. R. McDougal. (1973). "Experimental and Predicted Movement of Three Herbicides in a Water-Saturated Soil." Journal of Environmental Quality 2(4): 428-433.
- Deer, W. A., R. A. Howie and J. Zussman. (1966). An Introduction to the Rock-Forming Minerals. London: Longman.
- De Smedt, F. and P. J. Wierenga. (1984). "Solute Transfer Through Columns of Glass Beads." Water Resources Research 20(2): 225-232.

- Elrick, D. E., K. T. Erh and H. K. Krupp. (1966). "Applications of Miscible Displacement Techniques to Soils." Water Resources Research 2(4): 717-727.
- Everts, C. J. (1988). Unpublished data, Department of Agricultural Engineering, Iowa State University, Ames.
- Farmer, W. J. and Y. Aochi. (1974). "Picloram Sorption by Soils." Proceedings of the Soil Science Society of America 38: 418-423.
- Fava, A. and H. Eyring. (1956). "Equilibrium and Kinetics of Detergent Adsorption - A Generalized Equilibration Theory." Journal of Physical Chemistry 60: 890-898.
- Feuerstein, D. W. and R. E. Selleck. (1963). "Fluorescent Tracers for Dispersion Measurements." Proceedings of the American Society of Civil Engineers, Journal of Sanitary Engineering Division 89(SA4): 1-21.
- Freeze, R. A. and J. A. Cherry. (1979). Groundwater. New York: John Wiley and Sons, Inc.
- Freundlich, Herbert. (1926). Colloid and Capillary Chemistry. New York: E. P. Dutton and Company Publishers.
- Fusi, P. and R. Corsi. (1968). "Influenza di alcuni elettroliti e tensioattivi sull' adsorbimento e sul rilascio di atrazina da parte di terreni tipici." Quimica 13(1): 44-55.
- Germann, P. F. and K. Beven. (1985). "Kinematic Wave Approximation to Infiltration into Soils with Sorbing Micropores." Water Resources Research 21(7): 990-996.
- Gillham, R. W. and J. A. Cherry. (1982). "Contaminant Migration in Saturated Unconsolidated Geologic Deposits." Recent Trends in Hydrogeology. Ed. T. N. Narasimhan. Boulder, CO: The Geological Society of America. 31-61.
- Hallberg, G. R. (1985a). "Agricultural Chemicals and Groundwater Quality in Iowa: Status Report 1985." Iowa State University, Cooperative Extension Service, Ames, IA, CE-2158q.
- Hallberg, G. R. (1985b). "Groundwater Quality and Agricultural Chemicals: A Perspective from Iowa." North Central Weed Control Conference 40: 130-147.
- Hamaker, J. W. and J. M. Thompson. (1972). "Adsorption." In Organic Chemicals in the Soil Environment, vol. 6. Ed. C. A. Goring and J. W. Hamaker. New York: Marcel Dekker, Inc. 49-143.

- Hansch, C. and A. Leo. (1979). Substituent Constants for Correlation Analysis in Chemistry and Biology. New York: John Wiley and Sons, Inc.
- Harris, C. I. and G. F. Warren. (1964). "Adsorption and Desorption of Herbicides by Soil." Weeds 12: 120-126.
- Harter, R. D. and D. E. Baker. (1977) "Applications and Misapplications of the Langmuir Equation to Soil Adsorption Phenomena." Soil Science Society of America Journal 41: 1077-1080.
- Holden, P. W. (1986). Pesticides and Groundwater Quality Issues and Problems in Four States. Washington, DC: National Academy Press.
- Hornsby, A. G. and J. M. Davidson. (1973). "Solution and Adsorbed Fluometuron Concentration Distribution in a Water-Saturated Soil: Experimental and Predicted Evaluation." Proceedings of the Soil Science Society of America 37: 823-828.
- Hutzler, N. J., J. C. Crittenden, J. S. Gierke and A. S. Johnson. (1986). "Transport of Organic Compounds with Saturated Groundwater Flow: Experimental Results." Water Resources Research 22(3): 285-295.
- Israelachvili, J. N. (1985). Intermolecular and Surface Forces. London: Academic Press.
- Jury, W. A. (1983). "Chemical Transport Modeling: Current Approaches and Unresolved Problems." In Chemical Mobility and Reactivity in Soil Systems, Special Publication #11. Madison, WI: Soil Science Society of America. 49-64.
- Karickhoff, S. W. (1984). "Organic Pollutant Sorption in Aquatic Systems." Journal of Hydraulic Engineering, American Society of Civil Engineers 110(6): 707-735.
- Karickhoff, S. W., D. S. Brown and T. A. Scott. (1979). "Sorption of Hydrophobic Pollutants on Natural Sediments." Water Research 13: 241-248.
- Kay, B. D. and D. E. Elrick. (1967). "Adsorption and Movement of Lindane in Soils." Soil Science 104(5): 314-322.
- Kelley, R. D. (1985). "Synthetic Organic Compound Sampling Survey of Public Water Supplies." Iowa Department of Water, Air and Waste Management, Des Moines, IA, Technical Report.

- Kelley, R. D. and M. Wnuk. (1986). "Little Sioux River Synthetic Organic Compound Municipal Well Sampling Survey." Iowa Department of Water, Air and Waste Management, Des Moines, IA, Technical Report.
- Khan, S. and N. N. Khan. (1986). "The Mobility of Some Organophosphorous Pesticides in Soils as Affected by Some Soil Parameters." Soil Science 142(4): 214-222.
- Langmuir, I. (1918). "The Adsorption of Gases on Plane Surfaces of Glass, Mica and Platinum." Journal of American Chemistry Society 40: 1361.
- Lapidus, L. and N. R. Amundson. (1952). "Mathematics of Adsorption in Beds. VI. The Effect of Longitudinal Diffusion in Ion Exchange and Chromatographic Columns." Journal of Physical Chemistry 56: 984-988.
- Lee, L. S., P. S. C. Rao, M. L. Brusseau and R. A. Ogwada. (1988). "Nonequilibrium Sorption of Organic Contaminants During Flow through Columns of Aquifer Materials." Environmental Toxicology and Chemistry 7: 779-793.
- Leenher, J. A. and J. L. Alrichs. (1971). "A Kinetic and Equilibrium Study of the Adsorption of Carbaryl and Parathion upon Soil Organic Matter Surfaces." Proceedings of the Soil Science Society of America 35: 700-705.
- Leo, A., C. Hansch and D. Elkins. (1971). "Partition Coefficients and their Uses." Chemical Reviews 71(6): 525-555.
- Lindstrom, F. T., L. Boersma and D. Stockard. (1971). "A Theory on the Mass Transport of Previously Distributed Chemicals in a Water Saturated Sorbing Porous Medium: Isothermal Cases." Soil Science 112(5): 291-300.
- Lyman, W. J. (1982). "Octanol/Water Partition Coefficient." In Handbook of Chemical Property Estimation Methods: Environmental Behavior of Organic Compounds. Ed. W. J. Lyman, W. F. Reehl and D. H. Rosenblatt. New York: McGraw Hill. 1.1-54.
- Miller, C. T. (1984). "Modeling of Sorption and Desorption Phenomena for Hydrophobic Organic Contaminants in Saturated Soil Environments." Diss. U of Michigan, Ann Arbor.
- Mingelgrin, U. and Z. Gerstl. (1983). "Reevaluation of Partitioning as a Mechanism of Nonionic Chemicals Adsorption in Soils." Journal of Environmental Quality 12(1): 1-11.

- Mortland, M. M. (1970). "Clay-Organic Complexes and Interactions." Advances in Agronomy 22: 75-117.
- Murray, C. R. and E. B. Reeves. (1977). "Estimated Use of Water in the United States in 1975." United States Geologic Survey, Arlington Virginia, Circular 765.
- Nelson, D. W. and L. E. Sommers. (1982). "Total Carbon, Organic Carbon and Organic Matter." In Methods of Soil Analysis. Part 2 - Chemical and Microbiological Properties. Ed. A. L. Page, R. H. Miller and D. R. Kenney. 2nd ed. Madison, WI: American Society of Agronomy. 539-580.
- Nkedi-Kizza, P., J. W. Biggar, H. M. Selim, M. T. van Genuchten, P. J. Wierenga, P. J. Davidson and D. R. Nielsen. (1984). "On the Equivalence of Two Conceptual Models for Describing Ion Exchange During Transport Through an Aggregated Oxisol." Water Resources Research 20(8): 1123-1130.
- Nkedi-Kizza, P., P. S. C. Rao, R. E. Jessup and J. M. Davidson. (1982). "Ion Exchange and Diffusive Mass Transfer During Miscible Displacement Through an Aggregated Oxisol." Soil Science Society of America Journal 46: 471-476.
- Omoti, U. and A. Wild. (1979). "Use of Fluorescent Dyes to Mark the Pathways of Solute Movement through Soils under Leaching Conditions: 1. Laboratory Experiment." Soil Science 128(1): 28-33.
- Parker, J. C. and A. J. Valocchi. (1986). "Constraints on the Validity of Equilibrium and First-Order Kinetic Transport Models in Structured Soils." Water Resources Research 22(3): 399-407.
- Parker, J. C. and M. T. van Genuchten. (1984). "Determining Transport Parameters from Laboratory and Field Tracer Experiments." Virginia Agricultural Experiment Station, Bulletin 84-3.
- Perkins, T. K. and O. C. Johnston. (1963). "A Review of Diffusion and Dispersion in Porous Media." Society of Petroleum Engineers Journal 3: 70-84.
- Peter, C. J. and J. B. Weber. (1985). "Adsorption, Mobility and Efficacy of Alachlor and Metolachlor as Influenced by Soil Properties." Weed Science 33: 874-881.
- Rao, P. S. C. and J. M. Davidson. (1979). "Adsorption and Movement of Selected Pesticides at High Concentrations in Soil." Water Research 13: 375-380.

- Rao, P. S. C. and J. M. Davidson. (1980). "Estimation of Pesticide Retention and Transformation Parameters Required in Nonpoint Source Pollution Models." In Environmental Impact of Nonpoint Source Pollution. Ed. M. R. Overcash and J. M. Davidson. Ann Arbor, MI: Ann Arbor Science. 23-67.
- Rao, P. S. C., J. M. Davidson, R. E. Jessup and H. M. Selim. (1979). "Evaluation of Conceptual Models for Describing Nonequilibrium Adsorption-Desorption of Pesticides During Steady Flow in Soils." Soil Science Society of America Journal 43: 22-28.
- Rao, P. S. C., R. E. Green, L. R. Ahuja and J. M. Davidson. (1976). "Evaluation of a Capillary Bundle Model for Describing Solute Dispersion in Aggregated Soils." Soil Science Society of America Journal 40: 815-820.
- Rao, P. S. C. and R. E. Jessup. (1983). "Sorption and Movement of Pesticides and Other Toxic Organic Substance in Soils." In Chemical Mobility and Reactivity in Soil Systems, Special Publication #11. Madison, WI: Soil Science Society of America. 183-201.
- Rigby, M., E. B. Smith, W. A. Wakeham and G. C. Maitland. (1986). The Forces Between Molecules. Oxford: Clarendon Press.
- Rhoades, J. D. (1982). "Cation Exchange Capacity." Ed. A. L. Page, R. H. Miller and D. R. Keeney. Methods of Soil Analysis. Part 2 - Chemical and Microbiological Properties. 2nd ed. Madison, WI: American Society of Agronomy. 149-157.
- Roberts, P. V., M. N. Goltz, R. S. Summers, J. C. Crittenden and P. Nkedi-Kizza. (1987). "The Influence of Mass Transfer on Solute Transport in Column Experiments with an Aggregated Soil." Journal of Contaminant Hydrology 1: 375-393.
- Ruthven, D. M. (1984). Principles of Adsorption and Adsorption Processes. New York: John Wiley and Sons, Inc.
- Schwarzenbach, R. P. and J. Westall. (1981). "Transport of Nonpolar Organic Compounds from Surface Water to Groundwater: Laboratory Sorption Studies." Environmental Science and Technology 15: 1360-1367.
- Shuckrow, A. J., A. P. Pajak and C. J. Touhill. (1981). "Concentration Technologies for Hazardous Aqueous Waste Treatment." National Technical Information Service, USEPA 600/2-81-019, Springfield, VA.
- Skopp, J. (1986). "Analysis of Time-dependent Chemical Processes in Soils." Journal of Environmental Quality 15(3): 205-213.

- Skopp, J. and A. W. Warrick. (1974). "A Two-Phase Model for the Misable Displacement of Reactive Solutes in Soils." Soil Science Society of America Journal 38(4): 545-550.
- Smart, P. L. (1984). "A Review of the Toxicity of Twelve Fluorescent Dyes Used for Water Tracing." National Speleological Society Bulletin 46: 21-33.
- Smart, P. L. and I. M. S. Laidlaw. (1977). "An Evaluation of Some Fluorescent Dyes for Water Tracing." Water Resources Research 13(1): 15-33.
- Sposito, G. (1984). The Surface Chemistry of Soils. New York: Oxford Press.
- Sposito, G., R. E. White, P. R. Darrah and W. Jury. (1986). "A Transfer Function Model of Solute Transport Through Soil - 3. The Convection-Dispersion Equation." Water Resources Research 22(2): 255-262.
- Swanson, R. A. and G. R. Dutt. (1973). "Chemical and Physical Processes that Affect Atrazine and Distribution in Soil Systems." Proceedings of the Soil Science Society of America 37: 872-876.
- Tanford, C. (1980). The Hydrophobic Effect: Formation of Micelles and Biological Membranes. 2nd ed. New York: John Wiley and Sons, Inc.
- Thomas, R. G. (1982). "Volatilization from Water." In Handbook of Chemical Property Estimation Methods. Ed. W. J. Lyman, W. F. Reehl and D. H. Rosenblatt. New York: McGraw Hill. 15.1-34.
- Travis, C. C. and E. L. Etnier. (1981). "A Survey of Sorption Relationships for Reactive Solutes in Soil." Journal of Environmental Quality 10: 8-17.
- Trudgill, S. T. (1987). "Soil Water Dye Tracing with Special Reference to the use of Rhodamine WT, Lissamine FF and Amino G Acid." Hydrological Processes 1: 149-170.
- Tucker, W. A. and L. H. Nelken. (1982). "Diffusion Coefficients in Air and Water." In Handbook of Chemical Property Estimation Methods. Ed. W. J. Lyman, W. F. Reehl and D. H. Rosenblatt. New York: McGraw Hill. 17.1-25.
- United State Department of Agriculture. (1987). "Agricultural Resources: Inputs, Situation and Outlook Report." United States Department of Agriculture, Economic Research Service, Washington, DC, AR-5.

- United States Environmental Protection Agency. (1985). "Analysis of Certain Amine Pesticides and Lethane in Wastewater by Gas Chromatography - Method 645." United States Environmental Protection Agency, Environmental Monitoring and Support Laboratory, Physical and Chemical Methods Branch, Cincinnati, OH.
- United States Environmental Protection Agency. (1982). "The Determination of Triazine Pesticides in Industrial and Municipal Wastewater - Method 619." United States Environmental Protection Agency, Environmental Monitoring and Support Laboratory, Physical and Chemical Methods Branch, Cincinnati, OH.
- Valocchi, A. J. (1985). "Validity of the Local Equilibrium Assumption for Modeling Sorbing Solute Transport Through Homogeneous Soils." Water Resources Research 21(6): 808-820.
- van Genuchten, M. T. (1981). "Non-equilibrium Transport Parameters from Miscible Placement Experiments." United States Department of Agriculture, United States Salinity Lab, Riverside, CA, USDA-SEA-AR Research Report #119.
- van Genuchten, M. T. and W. J. Alves. (1982). "Analytical Solutions of the One-Dimensional Convective-Dispersive Solute Transport Equation." United States Department of Agriculture, Agricultural Research Service, Washington, DC, Technical Bulletin #1661.
- van Genuchten, M. T., J. M. Davidson and P. J. Wierenga (1974). "An Evaluation of Kinetic and Equilibrium Equations for the Prediction of Pesticide Movement through Porous Media." Soil Science Society of America Proceedings 38: 29-35.
- van Genuchten, M. T., D. H. Tang and R. Guennelon. (1984). "Some Exact Solutions for Solute Transport through Soils Containing Large Cylindrical Macropores." Water Resources Research 20(3): 335-346.
- van Genuchten, M. T. and P. J. Wierenga (1976). "Mass Transfer Studies in Sorbing Porous Media I. Analytical Solutions." Soil Science Society of America Journal 40(4): 473-480.
- van Genuchten, M. T., P. J. Wierenga and G. A. O'Connor. (1977). "Mass Transfer Studies in Sorbing Porous Media: III. Experimental Evaluation with 2, 4, 5-T." Soil Science Society of America Journal 41: 278-285.
- Veith, J. A. and G. Sposito. (1977). "On the Use of the Langmuir Equation in the Interpretation of 'Adsorption' Phenomena." Soil Science Society of America Journal 41: 697-702.

- Weber, J. B., P. J. Shea and H. J. Streck. (1980). "An Evaluation of Nonpoint Sources of Pesticide Pollution in Runoff." In Environmental Impact of Nonpoint Source Pollution. Ed. M. R. Overcash and J. M. Davidson. Ann Arbor: Ann Arbor Science. 69-98.
- Weber, W. J., Jr. (1972). Physiochemical Process for Water Quality Control. New York: John Wiley and Sons, Inc.
- Weber, W. J., T. C. Voice, M. Pirbazari, G. E. Hunt and D. M. Ulanoff. (1983). "Sorption of Hydrophobic Compounds by Sediments, Soils and Suspended Solids - II. Sorbent Evaluation Studies." Water Research 17(10): 1443-1452.
- Weed Science Society of America. (1983). Herbicide Handbook. Champaign, IL: Weed Science Society of America.
- Wilson, J. F., E. D. Cobb and F. A. Kilpatrick. (1986). "Fluorometric Procedures for Dye Tracing." United States Geological Survey, Techniques of Water-Resources Investigations, Book 3 (A12).
- Wintersteen, W. (1987). "Pesticides Used in Iowa Crop Production in 1985." Iowa State University, Cooperative Extension Service, Ames, IA, PM-1288.

ACKNOWLEDGEMENTS

The United States Department of Agriculture National Needs Fellowship Program, the Engineering Research Institute at Iowa State University, the Department of Civil and Construction Engineering at Iowa State University and the Iowa State Water Resources Research Institute provided financial support to make this program of study possible.

Sincere thanks are extended to Dr. T. Al Austin for his guidance, encouragement and friendship throughout my graduate work. His professional and personal influence will long be remembered. Gratitude is also extended to Dr. James L. Baker, Dr. John L. Cleasby, Dr. Robert A. Horton and Dr. Charles S. Oulman for their guidance and service on my graduate committee.

Thanks are extended to Dr. Neil Hutzler and Dr. John Crittenden of Michigan Technological University for making available the code for and assisting in the use of the physical nonequilibrium computer model.

My fellow students provided the advice, intellectual stimulus and camaraderie which made this effort more enjoyable. Without the loving support and endless prayers of my wife and family, this effort would not have been possible.

APPENDIX A: BATCH DATA¹Pesticide Batch Data² (see Table 6)

BATA - batch, atrazine, South Ames
BALA - batch, alachlor, South Ames

Dye Batch Data (see Tables 8 and 10)

BRA - batch, RWT, South Ames
BFA - batch, fluorescein, South Ames
BRH - batch, RWT, Halletts
BRACA - batch, RWT, South Ames, calcium chloride
Background ions

¹This appendix contains the data as plotted and manipulated in the text. The study abbreviations (e.g., BATA) are as utilized in the text. For experimental conditions, see summary Tables in the text.

²Pesticide data corrected for recovery efficiencies: 87.4% for atrazine and 84.3% for alachlor.

BATA

CO ($\mu\text{g/L}$)	Ce ($\mu\text{g/L}$)	q (g/g)
single solute		
25.0	21.2	7.6E-09
25.0	22.2	5.5E-09
50.0	36.2	2.8E-08
75.0	63.5	2.3E-08
75.0	54.7	4.1E-08
200.0	155.3	8.9E-08
500.0	400.7	2.0E-07
1000.0	752.9	4.9E-07
1000.0	934.1	1.3E-07
binary solute		
25.0	21.3	7.4E-09
50.0	40.6	1.9E-08
75.0	63.9	2.2E-08
200.0	166.3	6.7E-08
200.0	178.3	4.3E-08
1000.0	752.2	5.0E-07
1000.0	882.6	2.3E-07

BALA

CO ($\mu\text{g/L}$)	Ce ($\mu\text{g/L}$)	q (g/g)
single solute		
25.0	16.8	1.6E-08
25.0	20.2	9.5E-09
50.0	28.1	4.4E-08
75.0	48.6	5.3E-08
75.0	51.1	4.8E-08
200.0	124.7	1.5E-07
200.0	123.7	1.5E-07
500.0	352.0	3.0E-07
1000.0	603.7	7.9E-07
1000.0	666.7	6.7E-07
binary solute		
25.0	19.7	1.1E-08
25.0	17.6	1.5E-08
50.0	34.6	3.1E-08
75.0	56.2	3.8E-08
75.0	53.4	4.3E-08
200.0	126.6	1.5E-07
200.0	138.3	1.2E-07
1000.0	568.1	8.6E-07
1000.0	660.6	6.8E-07

BRA

CO ($\mu\text{g/L}$)	Ce ($\mu\text{g/L}$)	q (g/g)
25.0	7.0	3.60E-08
25.0	7.0	3.60E-08
100.0	26.0	1.50E-07
100.0	26.0	1.50E-07
400.0	126.0	5.50E-07
400.0	123.0	5.50E-07
2500.0	906.0	3.20E-06
2500.0	875.0	3.20E-06
9500.0	4200.0	1.10E-05
9500.0	4100.0	1.10E-05

BFA

CO ($\mu\text{g/L}$)	Ce ($\mu\text{g/L}$)	q (g/g)
50.0	46.0	8.0E-09
50.0	46.0	8.0E-09
150.0	132.0	3.6E-08
150.0	132.0	3.6E-08
400.0	350.0	1.0E-07
400.0	330.0	1.4E-07
1000.0	860.0	2.8E-07
1000.0	860.0	2.8E-07
2500.0	2330.0	3.4E-07
2500.0	2330.0	3.4E-07

BRH

CO ($\mu\text{g/L}$)	Ce ($\mu\text{g/L}$)	q (g/g)
50.0	20.0	6.0E-08
50.0	22.0	5.6E-08
150.0	66.0	1.7E-07
150.0	60.0	1.8E-07
400.0	168.0	4.6E-07
400.0	174.0	4.5E-07
1000.0	417.0	1.2E-06
1000.0	434.0	1.1E-06
2500.0	1220.0	2.6E-06
2500.0	1220.0	2.6E-06

BRACA

CO ($\mu\text{g/L}$)	Ce ($\mu\text{g/L}$)	q (g/g)
45.0	7.0	7.60E-08
45.0	6.0	7.80E-08
135.0	21.0	2.28E-07
135.0	22.0	2.26E-07
360.0	63.0	5.94E-07
900.0	191.0	1.42E-06
900.0	189.0	1.42E-06
2250.0	562.0	3.38E-06
2250.0	610.0	3.28E-06

Background Ions

Chemical added	Concentration added (M)	Ce ($\mu\text{g/L}$)
MgSO ₄	10 ⁻²	34.6
"	"	35.7
"	"	35.2
MgSO ₄	10 ⁻³	43.4
"	"	42.9
"	"	42.3
"	"	44.0
CaCl ₂	10 ⁻²	26.9
"	"	29.1
"	"	28.0
"	"	27.0
CaCl ₂	10 ⁻³	39.0
"	"	38.5
"	"	40.1
"	"	40.0
Blank	n/a	44.5
"	"	46.7
"	"	46.2
KCl	10 ⁻³	45.0
"	"	46.2
"	"	42.9
"	"	44.0
NaCl	10 ⁻³	49.5
"	"	50.0
"	"	48.9
"	"	49.0
CaSO ₄	10 ⁻³	43.4
"	"	41.7
"	"	41.7
"	"	41.0
KBr	10 ⁻³	45.0
NaCl	10 ⁻²	49.0
NaHCO ₃	10 ⁻³	48.0

APPENDIX B: COLUMN DATA¹Pesticide Column Data² (see Table 11)

CPA5 - column, pesticides, South Ames, 5 cm/h
CPA10 - column, pesticides, South Ames, 10 cm/h
CPA30 - column, pesticides, South Ames, 30 cm/h

Dye Column Data (see Tables 13 and 15)

CRA - column, RWT, South Ames
CFA - column, fluorescein, South Ames
CRACA - column, RWT, South Ames, calcium chloride
CRH - column, RWT, Halletts
CRAHP - column, RWT, South Ames, high PWV
GRAHC - column, RWT, South Ames, high CO
BW - column, RWT, South Ames, backwashed (> 75 μ m)
HT/850 - column, RWT, South Ames, heated @ 850 °C
BW-HT/550 - column, RWT, South Ames, backwashed and heated @ 550 °C
BW-HT/850 - column, RWT, South Ames, backwashed and heated @ 850 °C
GLBDS - column, RWT, glass beads
WS - column, RWT, South Ames, wet sieved (> 300 μ m)

¹This appendix contains the data as plotted and manipulated in the text. The study abbreviations (e.g., CPA5) are as utilized in the text. For experimental conditions, see summary Tables in the text.

²Pesticide data corrected for recovery efficiencies: 87.4% for atrazine and 84.3% for alachlor.

CPA5

V/V0	Atrazine		Alachlor	
	C ($\mu\text{g/L}$)	C/C0	C ($\mu\text{g/L}$)	C/C0
0.37	0.0	0.00	0.0	0.00
0.79	2.6	0.01	0.0	0.00
1.22	34.9	0.17	4.0	0.02
2.08	120.1	0.60	37.1	0.19
2.51	125.9	0.63	53.4	0.27
4.66	168.2	0.84	117.2	0.59
5.73	144.2	0.72	98.5	0.49
6.80	192.2	0.96	147.1	0.74
7.44	153.3	0.77	117.4	0.59
8.09	171.6	0.86	132.9	0.66
9.79	179.6	0.90	143.5	0.72
11.93	196.8	0.98	160.1	0.80
14.19	203.7	1.02	163.7	0.82
15.90	161.3	0.81	137.6	0.69
17.63	178.5	0.89	159.0	0.79
20.19	93.8	0.47	126.9	0.63
21.90	35.1	0.18	85.1	0.43
24.47	10.3	0.05	40.2	0.20
27.04	5.6	0.03	26.8	0.13
34.85	0.0	0.00	4.6	0.02

CPA10

V/V0	Atrazine		Alachlor	
	C ($\mu\text{g/L}$)	C/C0	C ($\mu\text{g/L}$)	C/C0
0.45	0.3	0.00	0.0	0.00
0.91	8.7	0.04	0.0	0.00
1.37	49.5	0.25	0.0	0.00
1.82	98.2	0.49	11.5	0.06
2.28	138.4	0.69	31.9	0.16
3.18	152.2	0.76	56.2	0.28
4.56	178.5	0.89	113.0	0.57
6.82	197.9	0.99	160.1	0.80
8.18	201.4	1.01	163.7	0.82
9.54	200.2	1.00	169.6	0.85
10.9	185.4	0.93	162.5	0.81
11.82	185.4	0.93	168.4	0.84
13.17	102.2	0.51	154.2	0.77
14.07	52.3	0.26	125.7	0.63
14.98	30.3	0.15	87.4	0.44
17.25	18.4	0.09	48.0	0.24
20.44	4.7	0.02	19.5	0.10
24.06	1.8	0.01	11.0	0.06
29.39	0.0	0.00	5.7	0.03

CPA30

V/VO	Atrazine		Alachlor	
	C($\mu\text{g/L}$)	C/CO	C($\mu\text{g/L}$)	C/CO
0.28	0.0	0.00	0.0	0.00
0.68	21.1	0.11	0.0	0.00
1.09	68.1	0.34	13.5	0.07
1.49	108.9	0.54	31.9	0.16
2.30	152.2	0.76	87.0	0.43
4.32	176.2	0.88	142.3	0.71
6.34	191.1	0.96	176.7	0.88
7.55	197.9	0.99	181.5	0.91
9.57	183.1	0.92	173.2	0.87
11.19	179.6	0.90	167.3	0.84
13.31	187.6	0.94	180.3	0.90
15.73	189.9	0.95	185.1	0.93
18.16	195.7	0.98	199.3	1.00
20.60	102.1	0.51	167.3	0.84
22.22	32.2	0.16	76.6	0.38
23.84	15.2	0.08	47.4	0.24
26.30	7.2	0.04	26.9	0.13
29.19	2.4	0.01	13.0	0.07
34.02	1.3	0.01	7.1	0.04

CRA

V/V0	C (µg/L)	C/C0	V/V0	C (µg/L)	C/C0
0.18	0	0.00	37.64	143	0.71
0.73	0	0.00	39.09	150	0.75
1.27	0	0.00	40.45	154	0.77
1.82	0	0.00	41.91	154	0.77
2.45	0	0.00	43.27	157	0.78
3.00	8	0.04	44.73	161	0.80
3.55	17	0.08	46.09	161	0.80
4.09	28	0.14	47.55	165	0.82
4.64	50	0.25	48.91	168	0.84
5.27	57	0.28	50.36	172	0.86
5.82	69	0.34	51.73	179	0.89
6.36	78	0.39	53.18	179	0.89
6.91	83	0.41	54.55	183	0.91
7.45	87	0.43	56.00	179	0.89
8.09	88	0.44	57.36	179	0.89
8.64	91	0.45	58.82	179	0.89
9.18	92	0.46	60.18	180	0.90
9.73	93	0.46	61.64	186	0.93
10.27	94	0.47	63.00	186	0.93
10.91	97	0.48	65.82	186	0.93
11.45	97	0.48	67.27	186	0.93
12.00	100	0.50	68.64	186	0.93
12.55	100	0.50	70.09	190	0.95
13.09	100	0.50	71.45	193	0.96
13.73	100	0.50	72.91	193	0.96
14.27	100	0.50	74.27	197	0.98
14.82	98	0.49	75.73	197	0.98
15.36	101	0.50	77.09	200	1.00
15.91	101	0.50	78.55	200	1.00
16.55	101	0.50	79.91	190	0.95
17.91	101	0.50	81.36	147	0.73
19.36	101	0.50	82.73	127	0.63
20.73	101	0.50	84.18	117	0.58
22.18	101	0.50	85.55	113	0.56
23.55	101	0.50	87.00	110	0.55
25.00	101	0.50	88.36	110	0.55
26.36	101	0.50	89.82	107	0.53
27.82	109	0.54	91.18	107	0.53
29.18	116	0.58	92.64	103	0.51
30.64	120	0.60	94.00	100	0.50
32.00	124	0.62	95.45	97	0.48
33.45	128	0.64	96.82	90	0.45
34.82	131	0.65	98.27	87	0.43
36.27	136	0.68	99.64	83	0.41

CRA - continued

V/V0	C ($\mu\text{g/L}$)	C/C0	V/V0	C ($\mu\text{g/L}$)	C/C0
101.09	77	0.38	144.73	23	0.11
102.64	73	0.36	146.18	22	0.11
103.91	70	0.35	147.55	22	0.11
105.27	67	0.33	149.00	20	0.10
106.73	63	0.31	150.36	19	0.09
108.09	60	0.30	151.82	17	0.08
109.55	58	0.29	153.18	16	0.08
110.91	56	0.28	154.64	15	0.07
112.36	55	0.27	156.00	15	0.07
113.73	54	0.27	157.45	15	0.07
115.18	53	0.26	158.82	15	0.07
116.55	51	0.25	160.27	15	0.07
118.00	49	0.24	161.64	14	0.07
119.36	46	0.23	163.09	13	0.06
120.82	44	0.22	164.45	14	0.07
122.18	43	0.21	165.91	13	0.06
123.64	42	0.21	167.27	12	0.06
125.00	41	0.20	168.73	12	0.06
126.45	40	0.20	170.09	12	0.06
127.82	38	0.19	171.55	11	0.05
129.27	37	0.18	172.91	11	0.05
130.64	35	0.17	174.36	11	0.05
132.09	31	0.15	175.73	11	0.05
133.45	30	0.15	177.18	11	0.05
134.91	29	0.14	180.00	11	0.05
136.27	28	0.14	182.82	11	0.05
137.73	27	0.13	185.64	10	0.05
139.09	27	0.13	188.45	10	0.05
140.55	26	0.13	191.27	10	0.05
141.91	24	0.12	194.09	9	0.04
143.36	23	0.11			

CFA

V/V0	C ($\mu\text{g}/\text{l}$)	C/C0
0.07	0	0.00
0.29	2	0.01
0.51	9	0.04
0.74	42	0.19
0.96	97	0.43
1.18	140	0.62
1.40	168	0.75
1.62	183	0.81
1.84	190	0.84
2.06	205	0.91
2.50	205	0.91
2.94	225	1.00
3.16	225	1.00
3.38	225	1.00
3.60	225	1.00
3.82	225	1.00
4.04	225	1.00
4.26	225	1.00
4.51	225	1.00
4.78	219	0.97
5.03	198	0.88
5.29	164	0.73
5.54	136	0.60
5.81	122	0.54
6.06	97	0.43
6.32	79	0.35
6.57	64	0.28
6.84	54	0.24
7.09	45	0.20
7.35	36	0.16
7.60	31	0.14
7.87	26	0.12
8.12	23	0.10
8.38	19	0.08
8.63	17	0.08
8.90	14	0.06
9.15	13	0.06
9.41	10	0.04

CRACA

V/V0	C ($\mu\text{g}/\text{l}$)	C/C0	V/V0	C ($\mu\text{g}/\text{l}$)	C/C0
0.09	0	0.00	89.91	140	0.72
0.66	0	0.00	92.83	147	0.75
2.17	0	0.00	95.75	150	0.77
3.58	1	0.01	98.68	147	0.75
5.09	8	0.04	101.60	147	0.75
6.51	19	0.10	104.53	147	0.75
8.02	30	0.15	107.45	153	0.78
9.43	41	0.21	110.38	153	0.78
10.94	47	0.24	113.30	157	0.81
12.36	56	0.29	116.23	157	0.81
13.87	62	0.32	119.15	164	0.84
15.28	68	0.35	122.08	164	0.84
16.79	72	0.37	125.00	164	0.84
18.21	75	0.38	127.92	171	0.88
19.72	78	0.40	130.85	167	0.86
21.13	79	0.41	133.77	170	0.87
22.64	80	0.41	136.70	177	0.91
24.06	81	0.42	139.62	174	0.89
25.57	80	0.41	142.55	177	0.91
26.98	82	0.42	145.47	175	0.90
28.49	83	0.43	148.40	179	0.92
29.91	87	0.45	151.32	182	0.93
31.42	93	0.48	154.25	182	0.93
32.83	93	0.48	157.17	180	0.92
34.34	97	0.50	160.09	180	0.92
35.75	100	0.51	162.92	184	0.94
37.26	100	0.51	165.85	167	0.86
40.19	103	0.53	168.77	136	0.70
43.11	103	0.53	171.70	126	0.65
46.04	103	0.53	174.62	119	0.61
48.96	103	0.53	177.55	112	0.57
51.89	103	0.53	180.47	109	0.56
54.81	107	0.55	183.40	106	0.54
57.74	107	0.55	186.32	99	0.51
60.66	117	0.60	192.17	92	0.47
63.58	123	0.63	195.09	89	0.46
66.51	127	0.65	200.94	82	0.42
69.43	133	0.68	206.79	75	0.38
72.36	133	0.68	212.64	65	0.33
75.28	133	0.68	221.42	58	0.30
78.21	133	0.68	224.34	53	0.27
81.13	136	0.70	227.26	49	0.25
84.06	140	0.72	230.19	47	0.24
86.98	140	0.72	233.11	43	0.22

CRACA - continued

V/V0	C ($\mu\text{g}/\text{l}$)	C/C0
236.04	41	0.21
247.74	41	0.21
256.51	33	0.17
265.28	30	0.15
274.06	31	0.16
279.91	30	0.15
285.75	28	0.14
291.60	28	0.14
297.45	26	0.13
303.30	24	0.12
309.15	24	0.12
315.00	21	0.11
320.85	20	0.10
326.70	19	0.10
332.55	19	0.10
338.40	18	0.09
344.25	17	0.09
350.09	17	0.09
355.94	17	0.09
361.79	16	0.08
367.64	16	0.08
373.49	15	0.08

CRH

V/V0	C ($\mu\text{g/L}$)	C/C0
0.46	0	0.00
1.23	0	0.00
2.00	0	0.00
2.77	0	0.00
3.54	4	0.02
4.31	13	0.07
5.08	24	0.12
5.85	34	0.17
6.62	47	0.24
8.15	64	0.32
9.69	77	0.39
11.23	84	0.42
12.77	90	0.45
15.08	96	0.48
17.38	94	0.47
19.69	97	0.49
22.38	97	0.49
25.08	98	0.49
28.15	105	0.53
30.46	112	0.56
32.77	116	0.58
35.08	125	0.63
37.38	132	0.66
39.69	140	0.70
42.00	144	0.72
44.31	144	0.72
46.62	152	0.76
48.92	160	0.80
51.23	160	0.80
53.54	168	0.84
55.85	168	0.84
58.15	176	0.88

CRAHP

V/V0	C ($\mu\text{g/L}$)	C/C0	V/V0	C ($\mu\text{g/L}$)	C/C0
0.13	0	0.00	72.88	163	0.82
0.78	0	0.00	73.88	150	0.76
1.41	0	0.00	74.84	140	0.71
2.06	1	0.01	76.47	132	0.67
2.38	4	0.02	79.75	112	0.57
2.69	11	0.06	83.00	87	0.44
5.00	64	0.32	86.28	72	0.36
5.66	77	0.39	89.56	63	0.32
6.31	81	0.41	92.84	50	0.25
6.97	86	0.43	96.13	43	0.22
7.63	86	0.43	99.41	38	0.19
8.94	89	0.45	102.69	32	0.16
10.25	93	0.47	105.97	29	0.15
12.22	96	0.48	112.53	23	0.12
13.53	96	0.48	125.66	18	0.09
14.84	96	0.48	132.22	16	0.08
16.16	96	0.48			
17.47	96	0.48			
19.09	94	0.47			
20.75	96	0.48			
22.38	99	0.50			
24.03	105	0.53			
25.66	114	0.58			
27.31	125	0.63			
28.94	134	0.68			
30.59	145	0.73			
32.22	155	0.78			
33.88	160	0.81			
35.50	163	0.82			
37.16	170	0.86			
38.78	175	0.88			
42.06	183	0.92			
45.34	187	0.94			
48.63	190	0.96			
51.91	193	0.97			
55.19	197	0.99			
58.47	195	0.98			
61.75	195	0.98			
65.03	197	0.99			
68.31	195	0.98			
69.94	197	0.99			
70.91	198	1.00			
71.91	198	1.00			

CRAHC

V/V0	C ($\mu\text{g/L}$)	C/C0
0.10	0	0.00
0.41	0	0.00
0.72	8	0.00
1.03	51	0.03
1.34	133	0.07
1.65	225	0.12
2.06	366	0.19
2.37	467	0.24
2.99	602	0.31
3.61	700	0.36
4.23	750	0.38
4.95	770	0.39
5.57	780	0.40
7.11	900	0.46
8.76	960	0.49
11.96	1130	0.58
15.15	1370	0.70
18.35	1570	0.81
21.55	1700	0.87
24.74	1750	0.90
27.94	1820	0.93
32.78	1880	0.96
34.43	1900	0.97
35.98	1900	0.97
37.63	1300	0.67
38.14	1000	0.51
41.34	730	0.37
44.54	530	0.27
47.73	420	0.22
50.93	370	0.19
54.12	300	0.15
57.32	240	0.12
60.52	190	0.10
63.71	165	0.08
66.91	152	0.08
70.10	142	0.07
73.30	125	0.06
76.49	112	0.06
79.69	97	0.05
82.89	85	0.04
86.08	77	0.04
89.28	68	0.03
92.47	65	0.03
95.67	61	0.03
98.87	58	0.03

BW

V/V0	C ($\mu\text{g/L}$)	C/C0	V/V0	C ($\mu\text{g/L}$)	C/C0
0.13	0	0.00	64.62	174	0.89
0.51	0	0.00	66.54	177	0.91
1.28	0	0.00	68.59	177	0.91
2.05	0	0.00	70.51	181	0.93
2.82	7	0.04	72.56	181	0.93
3.72	19	0.10	74.49	184	0.94
4.49	34	0.17	76.54	184	0.94
5.26	40	0.21	78.46	184	0.94
6.15	59	0.30	80.51	184	0.94
6.92	66	0.34	82.44	180	0.92
7.69	74	0.38	84.49	180	0.92
8.46	80	0.41	86.41	180	0.92
9.23	87	0.45	88.46	163	0.84
10.13	87	0.45	90.38	120	0.62
10.90	91	0.47	92.44	107	0.55
11.67	91	0.47	94.36	103	0.53
12.44	94	0.48	96.41	100	0.51
13.33	94	0.48	98.33	97	0.50
14.10	94	0.48	100.38	93	0.48
14.87	94	0.48	102.31	87	0.45
16.92	94	0.48	104.36	80	0.41
18.85	94	0.48	106.28	73	0.37
20.90	94	0.48	108.33	60	0.31
22.82	99	0.51	110.26	56	0.29
24.87	109	0.56	112.31	53	0.27
26.79	102	0.52	114.23	50	0.26
28.85	109	0.56	116.28	47	0.24
30.77	113	0.58	118.21	43	0.22
32.82	120	0.62	120.26	41	0.21
34.74	123	0.63	122.18	39	0.20
36.79	127	0.65	124.23	36	0.18
38.72	133	0.68	126.15	36	0.18
40.77	140	0.72	128.21	34	0.17
42.69	147	0.75	130.13	33	0.17
44.74	153	0.78	132.18	32	0.16
46.67	160	0.82	134.10	30	0.15
48.72	167	0.86	136.15	29	0.15
50.64	174	0.89	138.08	29	0.15
52.69	167	0.86	142.05	27	0.14
54.62	167	0.86	146.03	27	0.14
56.67	167	0.86	150.00	24	0.12
58.59	170	0.87	153.97	22	0.11
60.64	170	0.87	157.95	21	0.11
62.56	174	0.89	161.92	20	0.10

BW - continued

V/V0	C ($\mu\text{g/L}$)	C/C0
165.90	19	0.10
169.87	19	0.10
173.85	17	0.09
177.82	14	0.07
181.79	13	0.07
185.77	12	0.06
189.74	11	0.06
197.69	11	0.06

HT/850

V/V0	C ($\mu\text{g}/\text{l}$)	C/C0	V/V0	C ($\mu\text{g}/\text{l}$)	C/C0
0.10	0	0.00	33.88	65	0.33
0.41	4	0.02	35.51	44	0.22
0.71	12	0.06	37.04	33	0.17
1.02	32	0.16	38.67	27	0.14
1.33	48	0.24	40.20	19	0.10
1.63	59	0.30	41.84	14	0.07
2.04	67	0.34	43.37	13	0.07
2.35	70	0.36	45.00	9	0.05
2.65	75	0.38	46.53	7	0.04
2.96	79	0.40	48.16	7	0.04
3.27	82	0.42	49.69	6	0.03
3.57	86	0.44	51.33	5	0.03
3.88	93	0.47	52.86	5	0.03
4.18	100	0.51	54.49	4	0.02
4.49	107	0.55	56.02	3	0.02
4.80	110	0.56			
5.20	113	0.58			
5.51	117	0.60			
6.12	123	0.63			
6.73	130	0.66			
7.35	137	0.70			
7.96	143	0.73			
8.67	147	0.75			
9.29	150	0.77			
9.90	150	0.77			
10.51	157	0.80			
11.12	157	0.80			
11.84	160	0.82			
12.45	164	0.84			
13.06	171	0.87			
13.67	174	0.89			
14.29	178	0.91			
15.00	178	0.91			
16.53	181	0.92			
18.06	181	0.92			
19.69	181	0.92			
21.22	181	0.92			
22.86	181	0.92			
24.39	185	0.94			
26.02	188	0.96			
27.55	188	0.96			
29.18	181	0.92			
30.71	142	0.72			
32.35	104	0.53			

BW-HT/550

V/V0	C (µg/L)	C/C0	V/V0	C (µg/L)	C/C0
0.14	0	0.00	38.75	120	0.62
0.97	15	0.08	40.42	103	0.53
1.81	50	0.26	42.22	83	0.43
2.64	65	0.33	43.89	67	0.34
3.61	72	0.37	45.56	57	0.29
4.44	74	0.38	47.36	47	0.24
5.28	74	0.38	49.03	41	0.21
6.11	74	0.38	52.08	33	0.17
6.94	83	0.43	54.17	28	0.14
7.78	87	0.45	60.69	20	0.10
8.75	90	0.46	65.00	16	0.08
9.58	101	0.52	69.31	12	0.06
10.42	111	0.57	73.61	11	0.06
11.25	119	0.61	77.92	10	0.05
12.08	126	0.65			
13.06	129	0.66			
13.89	133	0.68			
14.72	130	0.67			
15.56	136	0.70			
16.39	140	0.72			
17.22	143	0.73			
18.06	147	0.75			
18.89	153	0.78			
19.72	153	0.78			
20.56	157	0.81			
21.53	157	0.81			
22.36	160	0.82			
23.19	164	0.84			
24.03	164	0.84			
25.00	167	0.86			
25.83	170	0.87			
26.67	174	0.89			
27.50	174	0.89			
28.33	174	0.89			
29.31	177	0.91			
30.14	177	0.91			
30.97	177	0.91			
31.81	181	0.93			
32.64	181	0.93			
33.61	184	0.94			
34.44	184	0.94			
35.28	167	0.86			
36.94	143	0.73			

BW-HT/850

V/V0	C ($\mu\text{g/L}$)	C/C0
0.10	0	0.00
0.72	5	0.03
1.03	26	0.13
1.34	63	0.32
1.65	109	0.55
2.37	130	0.66
2.99	143	0.72
3.61	167	0.84
4.23	181	0.91
4.85	194	0.98
6.49	198	1.00
8.35	198	1.00
10.31	167	0.84
11.24	55	0.28
12.16	32	0.16
13.09	16	0.08
14.02	11	0.06
14.95	9	0.05
18.14	6	0.03
21.44	3	0.02

GLBDS

V/V0	C ($\mu\text{g/L}$)	C/C0
0.26	6	0.03
0.66	67	0.35
1.05	140	0.72
1.45	163	0.84
1.84	173	0.89
2.24	183	0.94
2.76	180	0.93
3.16	187	0.96
3.55	193	0.99
4.08	194	1.00
4.47	194	1.00
4.87	185	0.95
5.26	109	0.56
5.66	57	0.29
6.05	40	0.21
6.45	30	0.15
6.84	23	0.12
7.37	20	0.10
7.76	16	0.08
8.16	13	0.07
8.55	11	0.06
8.95	10	0.05

WS

V/V0	C ($\mu\text{g/L}$)	C/C0
0.14	0	0.00
1.43	0	0.00
2.29	10	0.05
3.29	26	0.13
4.14	48	0.25
5.00	61	0.31
5.86	67	0.34
6.71	71	0.36
7.71	73	0.37
9.86	85	0.44
12.14	92	0.47
14.29	99	0.51
16.57	99	0.51
21.00	99	0.51
25.43	99	0.51
29.86	106	0.54
34.29	116	0.59
38.71	123	0.63
43.14	133	0.68
47.57	147	0.75
52.00	160	0.82
56.43	164	0.84
60.86	170	0.87
65.29	177	0.91